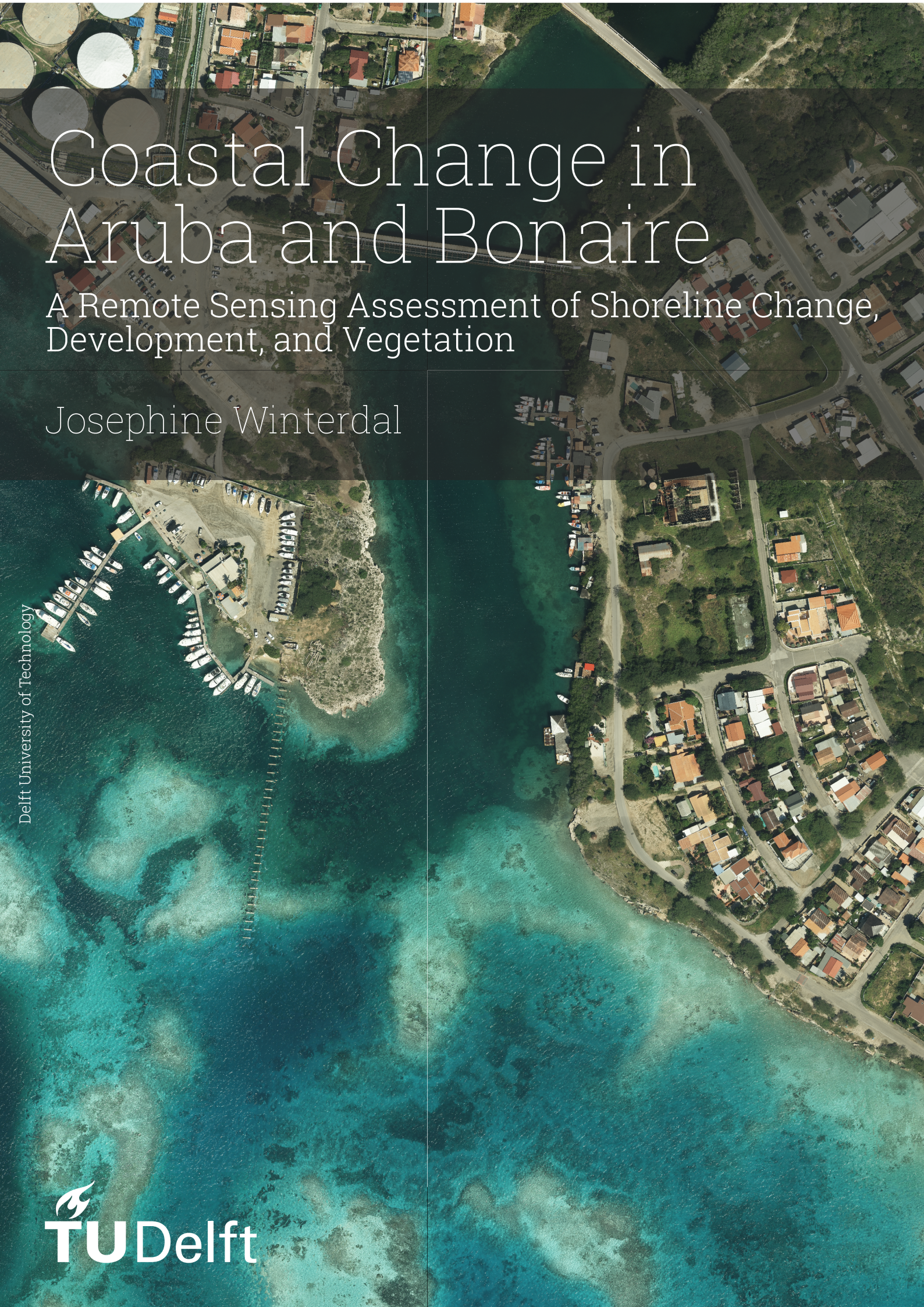


Coastal Change in Aruba and Bonaire

A Remote Sensing Assessment of Shoreline Change, Development, and Vegetation

Josephine Winterdal

Delft University of Technology

TU Delft

Coastal Change in Aruba and Bonaire

A Remote Sensing Assessment of Shoreline Change, Development, and Vegetation

by

Josephine Winterdal

1st Supervisor:	Dr. Roderik Lindenbergh
2nd Supervisor:	Dr. Azarakhsh Rafiee
Faculty:	Faculty of Architecture and the Built Environment

Cover: Derived from aerial imagery obtained from the Dienst Landmeetkunde en Vastgoedregistratie (DLV), Aruba (2018). Modified by the author.

TU Delft

Summary

The Dutch Caribbean islands are under increasing threat from climate change and anthropogenic activities. Specifically, coastal environments on these small islands are shaped by interacting natural and human processes, while development and ecosystems are often concentrated close to the shoreline. This thesis investigates how spatial patterns of coastal change vary in relation to coastal exposure, development, vegetation, and coastal characteristics in selected sections of Aruba and Bonaire. The study focuses on six coastal sections, three on each island, chosen to represent contrasting combinations of coastal type, development, vegetation, and exposure.

A remote-sensing and geospatial workflow was developed to analyse shoreline, building, and vegetation change. Shoreline position was extracted from approximately 3 m PlanetScope imagery using the Normalized Difference Water Index (NDWI), followed by automated water classification and transect-based change analysis. Summer (October to March) and winter (April-September) observations were analysed separately for the period 2016–2023. Detected building change was derived from the Google Open Buildings Temporal dataset, while vegetation was classified from PlanetScope imagery using the Normalized Difference Vegetation Index (NDVI) and image-specific thresholding. Island-wide patterns were assessed alongside detailed comparisons within the six coastal sections. The resulting shoreline, building, and vegetation layers were then combined spatially to identify contrasts and co-occurrences between different forms of coastal change rather than to produce a single vulnerability index.

The shoreline results show substantial spatial variability both between and within the study sections. In Aruba, Section 1 showed mean landward displacement in both seasonal datasets, Section 2 showed small mean seaward displacement, and Section 3 showed landward displacement, particularly in winter. Bonaire showed more mixed behaviour: Section 1 changed direction between summer and winter, Section 2 also differed in displacement direction between seasons, and Section 3 showed mean seaward displacement in both seasons. Local shoreline changes were often considerably larger than the section-wide means. Detailed examination showed that some of the larger localised deviations were associated with shoreline extraction errors, including cloud contamination and the incorrect detection of coastal features and built-up surfaces. However, the positional accuracy assessment showed that several mean displacement values are similar in magnitude to the shoreline extraction error, particularly on Aruba. Small shoreline changes should therefore be interpreted cautiously and not automatically as physical erosion or accretion.

Detected building change was concentrated mainly in already developed parts of both islands. Within the selected sections, Aruba Sections 1 and 2 showed increases of approximately 15,027 m^2 and 11,037 m^2 in detected building area, while Section 3 showed no net change. On Bonaire, Section 1 increased by approximately 20,072 m^2, Section 2 by 8,588 m^2, and Section 3 by only 31 m^2. Bonaire Section 1 showed the largest increase in detected building area among all six study sections. Building-detection accuracy was high for both islands, although false-positive detections remained present.

Remotely detected vegetation increased in all six coastal sections between 2016 and 2023, with the largest increases occurring in Aruba Section 2 and Bonaire Section 3. These vegetation results represent changes in detected vegetation extent rather than independently verified ecological improvement.

The integrated comparison shows that shoreline displacement, detected building change, and remotely detected vegetation change do not follow one common spatial pattern. Aruba and Bonaire show similarities in their rocky and exposed coastal sections, where limited development coincides with relatively consistent shoreline configurations. However, differences are also apparent. Aruba Section 1 combines substantial detected building growth with pronounced local shoreline variability along a sandy coast, while the developed limestone coastal sections of Bonaire generally show smaller shoreline variations along much of their length. More developed sections did not consistently show substantial shoreline variability. The occurrence of building growth and shoreline displacement within the same coastal section does not, however, establish a causal relationship between them. The results therefore

indicate that coastal change in Aruba and Bonaire varies across locally contrasting combinations of coastal setting, exposure, development, and vegetation. The study demonstrates the value of analysing several remotely sensed indicators within a shared spatial framework, while also showing that their interpretation depends strongly on spatial resolution, positional accuracy, temporal consistency, and image-acquisition conditions. The approach is therefore most useful as a comparative assessment of spatial patterns, contrasts, and co-occurrences rather than as a direct measure of coastal vulnerability or causality.

Contents

Summary **i**

1 Introduction **1**
1.1 Background and motivation . . . 1
1.2 Problem statement . . . 2
1.3 Research gap . . . 2
1.4 Research aim . . . 3
1.5 Research questions . . . 4
1.6 Scope and delimitation . . . 4
1.7 Scientific and practical contribution . . . 4
1.8 Thesis outline . . . 5

2 Theoretical background and related work **6**
2.1 Coastal systems and coastal morphodynamics . . . 6
2.2 Physical drivers of coastal change . . . 7
2.2.1 Waves and nearshore transformation . . . 7
2.2.2 Cross-shore sediment transport . . . 7
2.2.3 Longshore sediment transport . . . 8
2.2.4 Water-level variability . . . 8
2.3 Defining and measuring the shoreline . . . 8
2.4 Coastal typology and tropical reef-lined coasts . . . 9
2.4.1 Coastal typology . . . 9
2.4.2 Reef-lined coasts . . . 10
2.4.3 Coral-sand beaches . . . 10
2.5 Coastal remote sensing monitoring . . . 10
2.5.1 Advantages of satellite observation . . . 10
2.5.2 Optical remote sensing . . . 11
2.5.3 Satellite-derived shorelines . . . 11
2.5.4 Remote sensing of vegetation . . . 12
2.5.5 Remote sensing of buildings . . . 12
2.5.6 Data quality, spatial resolution, and uncertainty . . . 12
2.6 Vegetation and natural coastal buffering . . . 13
2.6.1 Coastal vegetation . . . 13
2.6.2 Vegetation and dune stability . . . 13
2.7 Coastal development and the built environment . . . 14
2.7.1 Development as coastal exposure . . . 14
2.7.2 Development as a morphodynamic influence . . . 14
2.8 External coastal exposure . . . 14
2.8.1 Coastal orientation . . . 14
2.8.2 Fetch . . . 15
2.8.3 Coral reefs as natural wave barriers . . . 15
2.9 Coastal vulnerability and multi-indicator assessment . . . 15
2.9.1 Coastal vulnerability as a multidimensional concept . . . 15
2.9.2 Multi-indicator coastal assessment . . . 16
2.10 Conceptual framework . . . 16

3 Study areas and data **18**
3.1 Regional context . . . 18
3.2 Aruba . . . 19
3.2.1 Physical geography and coastal morphology . . . 19

3.2.2 Coastal development . . . 20
3.2.3 Coastal environments and vegetation . . . 21
3.3 Bonaire . . . 21
3.3.1 Physical geography and coastal morphology . . . 21
3.3.2 Coastal development . . . 22
3.3.3 Coastal environments and vegetation . . . 22
3.4 Selected coastal study sections . . . 23
3.4.1 Selection criteria . . . 23
3.4.2 Aruba study sections . . . 23
3.4.3 Bonaire study sections . . . 25
3.5 Satellite and spatial data . . . 27
3.6 Initial data-quality assessment . . . 28

4 Methodology **30**
4.1 Shoreline extraction & change analysis . . . 31
4.1.1 NDWI calculation . . . 31
4.1.2 Automated water classification . . . 32
4.1.3 Main water body selection and shoreline vector extraction . . . 32
4.1.4 Transect-based shoreline-change analysis . . . 32
4.1.5 Seasonal shoreline comparison . . . 34
4.1.6 Positional accuracy assessment of the extracted shoreline . . . 34
4.2 Building detection and change analysis . . . 35
4.2.1 Google Open Buildings Temporal dataset . . . 35
4.2.2 Spatial preparation . . . 35
4.2.3 Island-wide building-area change . . . 36
4.2.4 Building polygons within the coastal sections . . . 36
4.2.5 Building-change classification . . . 36
4.2.6 Validation of building detection . . . 37
4.3 Vegetation detection and change analysis . . . 38
4.3.1 NDVI calculation . . . 38
4.3.2 Water exclusion and automated vegetation detection . . . 38
4.3.3 Raster-to-vector conversion . . . 38
4.3.4 Island-wide vegetation-area change . . . 38
4.3.5 Section-scale vegetation change . . . 39
4.4 Integrated spatial analysis . . . 39

5 Results **41**
5.1 Shoreline detection & change . . . 41
5.1.1 Aruba . . . 41
5.1.2 Bonaire . . . 46
5.1.3 Positional accuracy assessment of shoreline extraction . . . 51
5.2 Building detection & change . . . 54
5.2.1 Aruba . . . 54
5.2.2 Bonaire . . . 54
5.2.3 Validation of building detection . . . 55
5.3 Vegetation detection and change . . . 56
5.3.1 Aruba . . . 56
5.3.2 Bonaire . . . 57
5.4 Combined spatial results . . . 57
5.4.1 Aruba . . . 57
5.4.2 Bonaire . . . 59

6 Discussion **61**
6.1 Interpretation of the main findings . . . 61
6.1.1 Shoreline change and coastal characteristics . . . 61
6.1.2 Development, vegetation, and their spatial relationships . . . 62
6.2 Implications for coastal monitoring and management . . . 62
6.3 Limitations of the study . . . 63

6.3.1 Data availability, image quality, and spatial resolution 63
6.3.2 Shoreline extraction and temporal comparison 63
6.3.3 Building and vegetation indicators 64
6.3.4 Scope of the integrated analysis 65

7 Conclusion and recommendations **67**
7.1 Conclusion 67
7.2 Recommendations 68

References **70**

A Supplementary shoreline change results **73**

B Supplementary integrated spatial results. **80**

C Google Earth Engine building extraction script **82**

1

Introduction

1.1. Background and motivation

Within the Caribbean, the close relationship between development and the coastal environment further increases the importance of coastal monitoring. Coastal areas contain a large share of settlements, infrastructure, and tourism-related activities, while natural systems such as beaches, reefs, wetlands, and mangroves provide important environmental functions. Previous research in the Caribbean has shown that the combination of coastal development, tourism, environmental degradation, and climate-related pressures can increase the vulnerability of coastal infrastructure and ecosystems (Lewsey et al., 2004). Although Aruba and Bonaire differ from many of the Eastern Caribbean islands considered by Lewsey et al. (2004), these broader regional pressures provide relevant context for studying coastal change on the two islands.

The coastal zones are dynamic environments in which natural processes, ecosystems, human activities, and infrastructure are concentrated within a relatively narrow area. Their importance is therefore both environmental and socioeconomic. At the same time, coastal zones are exposed to pressures including erosion, flooding, sea-level rise, extreme weather, urbanisation, and increasing development. Human activities can further modify natural coastal systems, meaning that observed coastal change reflects the interaction between natural and anthropogenic influences rather than one isolated process (Xu et al., 2016).

As indicated, these issues are especially relevant for small islands with a high ratio of coastline to land area where coastal environments form an important part of the available space for settlement, infrastructure, economic activity, and ecosystems. Given that the Dutch Caribbean islands are also exposed to climate-related pressures such as sea-level rise, flooding, erosion, and extreme weather, vulnerability can vary considerably between different parts of the same island (Ng et al., 2019). Understanding this spatial variability is important because coastal change and the conditions influencing it are not distributed uniformly.

Aruba and Bonaire provide a useful comparative setting for investigating these processes. Both are relatively small Caribbean islands where human activity and natural environments are closely connected to the coast. The islands share a broadly similar regional setting, including persistent easterly trade winds and coastal environments shaped by carbonate reefs and historical sea-level changes (Schmutz et al., 2017). At the same time, their coastlines contain different combinations of developed areas, vegetation, reefs, beaches, rocky sections, and differently exposed coastal environments. Aruba contains extensive sandy beaches along its sheltered western coast and more exposed rocky shorelines to the east, while Bonaire is characterised by limestone coastal formations, reef-fringed shorelines, and mangrove environments (Gijsman et al., 2026; Schmutz et al., 2017). Their development patterns also differ, with intensive tourism-driven urbanisation on Aruba (Jurgens et al., 2024) and more spatially concentrated development on Bonaire (Frade et al., 2019). These contrasts provide an opportunity to investigate how observed coastal change is related to different combinations of human and natural coastal conditions.

Remote sensing provides an effective means of carrying out such an analysis across selected coastal areas and over multiple points in time. Satellite observations offer repeated and spatially extensive measurements that would be difficult to obtain through field observations alone. Remote sensing has consequently become an important tool for assessing changes in coastal resources and environments, particularly where consistent observations are required across relatively large areas (McCarthy et al., 2017). For Aruba and Bonaire, remotely sensed data make it possible to examine shoreline position alongside indicators of vegetation and development, while additional spatial information can be used to characterise differences in coastal type and external exposure.

The need for location-specific information on coastal change is also increasingly relevant for policy and adaptation. In January 2026, the District Court of The Hague ruled that the Dutch State had taken insufficient measures to protect Bonaire's inhabitants from the consequences of climate change and required the development of an adaptation plan (Rechtbank Den Haag, 2026). Although this ruling is not the primary motivation of the present research, it illustrates the growing practical importance of spatially detailed information on coastal change and exposure.

Against this background, this thesis examines coastal change in selected sections of Aruba and Bonaire using remote sensing and spatial analysis, with particular attention to shoreline movement, development, vegetation and differences in coastal setting.

1.2. Problem statement

For small Dutch Caribbean islands coastal conditions can vary considerably over relatively short distances. As such, geospatial differences in geomorphology, exposure, land use, vegetation, and development also causes variations between coastal sections and their vulnerability (Ng et al., 2019).

This creates a challenge for analysing the coastal changes of Aruba and Bonaire using remote-sensing. Observing shoreline change alone can only indicate where the land–water boundary has shifted, but not the drivers and pressures behind this change. A coastal section may simultaneously differ in development intensity, vegetation cover, coastal type, and external exposure.

Only a multi-indicator coastal assessments provides a way to address this issue by examining several dimensions of coastal condition together rather than in isolation. Pantusa et al. (2022), for example, combine indicators including shoreline erosion or accretion, geomorphology, hydrodynamic conditions, and vegetation within an integrated coastal assessment. However, no such analysis has been undertaken with remote sensing for the Dutch Caribbean islands of Aruba and Bonaire.

As such, the problem addressed in this research is a lack of understanding of how observed coastal change within selected areas of Aruba and Bonaire relates spatially to both human and natural coastal conditions. In response, shoreline change is examined with remote sensing together with development pressure, vegetation, coastal typology, and external exposure rather than treating these components as independent observations.

By analysing these indicators within a common spatial framework, the study seeks to identify where particular combinations of coastal change and coastal pressure occur and whether recurring spatial patterns and co-occurrences can be observed between the selected study areas. The intention is not to assign direct causality to individual indicators, but to provide a more comprehensive interpretation of coastal change within its environmental and anthropogenic context than would be possible from shoreline position alone.

1.3. Research gap

Coastal vulnerability assessment and remote sensing are both well-established approaches for analysing changing coastal environments. However, the way in which coastal vulnerability is assessed varies considerably between studies. Hamid et al. (2019) show that coastal vulnerability indices may combine physical, ecological, and socioeconomic variables, but that the number and type of variables used differ substantially between applications. They further emphasise that indicator selection should reflect the spatial scale and specific characteristics of the coastline being assessed.

This variation is important because the interpretation of coastal vulnerability is scale-dependent. Hamid

et al. (2019) describe studies in which vulnerability classifications differed depending on whether the assessment was conducted at national, regional, or local scales. A spatial framework that is too broad may therefore obscure local differences, while a more detailed assessment can distinguish contrasting coastal conditions more clearly.

At the same time, remote sensing provides an increasingly important source of information for coastal monitoring because it enables repeated and spatially extensive observation. McCarthy et al. (2017) show that satellite remote sensing is used across a wide range of coastal applications, including the monitoring of reefs, wetlands, water quality, and other coastal resources. These applications demonstrate the ability of remote sensing to observe different components of coastal environments, but such components are frequently studied for specific environmental or management purposes.

Integrated coastal assessment approaches attempt to bring several of these dimensions together. Ng et al. (2019), for example, combine external stressors, biophysical characteristics, and socioeconomic factors in a small-island vulnerability assessment, while Pantusa et al. (2022) integrate geomorphology, shoreline change, hydrodynamic variables, and vegetation. These studies demonstrate the value of multi-indicator approaches, while also showing that the composition of an assessment depends strongly on the objectives, scale, and physical characteristics of the study area.

The research gap addressed in this thesis therefore lies not in the absence of coastal vulnerability methods or remote-sensing techniques, but in the limited integrated comparison of shoreline change, development, vegetation, coastal typology, and external exposure within a common spatial framework for selected coastal environments on Aruba and Bonaire. These indicators represent different dimensions of coastal condition, but their spatial relationships are not necessarily captured when they are considered separately.

This thesis addresses that gap by analysing these indicators together within selected coastal study sections on both islands. The comparative approach makes it possible to examine whether similar or contrasting spatial patterns occur under different combinations of development, vegetation, coastal type, and exposure. Rather than applying a single composite index to the entirety of both islands, the study focuses on selected areas where these relationships can be examined in greater spatial detail.

1.4. Research aim

The aim of this thesis is to analyse spatial patterns of coastal change within selected coastal sections of Aruba and Bonaire and to investigate how these patterns vary in relation to both anthropogenic and natural coastal conditions.

To achieve this, the study combines remotely sensed and spatially derived indicators of shoreline change, built-up intensity, vegetation, coastal typology, and external coastal exposure. These indicators are examined within predefined coastal study areas selected to capture contrasting physical and development settings on both islands. This approach allows the analysis to focus on coastal sections where the relationships between shoreline change, human development, vegetation, and exposure can be investigated in greater detail.

By analysing these indicators together, the research seeks to identify where observed coastal change coincides with differences in development pressure, natural buffering, coastal characteristics, and exposure conditions. The comparison between Aruba and Bonaire further allows these relationships to be examined across two islands that share a broadly similar regional setting but differ in coastal morphology, vegetation, development patterns, and exposure.

The study does not aim to establish direct causal relationships between individual pressures and observed shoreline change. Instead, it focuses on identifying spatial associations and relative differences between the selected coastal sections. In doing so, the research aims to provide an integrated assessment of coastal change within its environmental and anthropogenic context.

Ultimately, the thesis aims to improve understanding of how coastal change varies across selected sections of Aruba and Bonaire and how these patterns relate to differences in human development, vegetation, coastal type, and external exposure.

1.5. Research questions

How do spatial patterns of coastal change vary in relation to external coastal exposure, development, vegetation, and coastal characteristics in selected coastal sections of Aruba and Bonaire?

Sub-questions:

- What coastal types and external exposure conditions characterise the selected coastal sections?
- How did shoreline position change within the selected coastal sections between 2016 and 2023, and how did this vary between seasonal observations?
- How did detected built-up area change within the selected coastal sections between 2016 and 2023?
- How did remotely detected vegetation extent change within the selected coastal sections between 2016 and 2023?
- How do patterns of shoreline change, development, and vegetation differ between coastal sections with contrasting coastal characteristics and exposure conditions?

1.6. Scope and delimitation

This study examines coastal change in selected areas of Aruba and Bonaire between 2016 and 2023. The detailed analysis is carried out within six predefined coastal study sections, with three sections selected on each island to represent contrasting combinations of coastal morphology, development, vegetation, and exposure. Island-wide analyses of building and vegetation change are additionally used to provide broader spatial context for the section-scale results.

The study focuses on four main components: shoreline position and displacement, detected building development, remotely detected vegetation extent, and contextual coastal characteristics such as coastal type and external exposure. These components are analysed within a common spatial framework to compare how different forms of coastal change occur across contrasting coastal settings.

Shoreline position is derived from optical satellite imagery and represents the instantaneous land–water boundary at the time of image acquisition. It should therefore not be interpreted as a fixed geomorphological coastline. Observed differences between shoreline positions may reflect both morphological change and shorter-term influences such as water-level variability, wave run-up, image conditions, and classification uncertainty.

The main temporal comparison covers 2016–2023. Summer and winter shoreline observations are analysed separately where suitable imagery is available in order to distinguish longer-term displacement from seasonal variability. Building change and section-scale vegetation change are also compared between 2016 and 2023. For the island-wide vegetation analysis of Bonaire, the comparison is limited to 2019–2023 because sufficiently clear full-island PlanetScope imagery was not available before 2019.

The study does not directly model the physical processes responsible for shoreline change. Hydrodynamic conditions, tides, waves, sediment transport, bathymetry, and sediment supply are discussed as relevant controls on coastal behaviour, but they are not reconstructed quantitatively for each study section. Similarly, detected building area is used as an indicator of development, while vegetation extent is used as an indicator of remotely observed vegetation presence and change; neither is interpreted as a complete measure of socioeconomic exposure or ecological functioning.

The integrated analysis is intended to identify spatial patterns, contrasts, and co-occurrences between the selected indicators rather than to establish direct causal relationships. The indicators are retained separately rather than combined into a single composite index. The findings should therefore be interpreted as a comparative remote-sensing assessment of coastal change within the selected study areas, rather than as a complete representation of all physical, ecological, or socioeconomic processes occurring on Aruba and Bonaire.

1.7. Scientific and practical contribution

The scientific contribution of this thesis is mainly in the combination of several indicators of coastal change within the same spatial framework. Shoreline displacement, building change, vegetation change,

coastal characteristics, and exposure are considered together for selected coastal sections on Aruba and Bonaire. This makes it possible to compare different types of change without reducing them to one single index.

A second contribution is the comparison between the two islands. Although Aruba and Bonaire are located in the same regional setting, the selected coastal sections differ in morphology, vegetation, development, and exposure. Looking at these differences at section scale helps show that coastal change is not uniform across either island and that local conditions are important when interpreting the results.

The thesis also provides a methodological contribution by showing what can and cannot be derived from the selected remote-sensing datasets. PlanetScope imagery, Google Open Buildings, and vegetation indices allow repeated observations over time, but they also have limitations related to spatial resolution, image quality, temporal availability, and classification uncertainty. These limitations form an important part of the interpretation of the results.

From a practical perspective, the combined analysis can help identify coastal sections where several types of change occur in the same area. These locations may be relevant for more detailed monitoring or field-based investigation. This is particularly relevant for Bonaire, where the need for location-specific information for climate adaptation has recently received greater attention. However, the results should be seen as a screening and comparison tool rather than a direct assessment of coastal risk.

1.8. Thesis outline

Chapter 2 presents the theoretical background and related work, including coastal morphodynamics, shoreline definition, remote sensing, vegetation, development, external exposure, and coastal vulnerability concepts. Chapter 3 describes the study areas and the datasets used for Aruba and Bonaire. Chapter 4 explains the methodology for shoreline extraction and change analysis, building detection, vegetation analysis, and the combined spatial comparison. Chapter 5 presents the results of these analyses for both islands. Chapter 6 discusses the main findings, methodological limitations, and the influence of data quality and spatial resolution. Finally, Chapter 7 summarises the main conclusions and provides recommendations for future research and coastal monitoring.

2

Theoretical background and related work

Coastal zones form the dynamic transition between terrestrial and marine environments. Their position and morphology are continuously influenced by hydrodynamic forcing, sediment transport, geomorphological characteristics, ecosystems, and human activities. Coastal change therefore cannot generally be interpreted as the result of a single process. Instead, an observed change in shoreline position represents the combined response of the coastal system to interacting processes operating over different spatial and temporal scales (Bosboom & Stive, 2023).

Remote sensing provides a means of observing several components of this system repeatedly over large spatial areas. However, satellite-derived indicators such as shoreline position, vegetation indices, or building presence do not directly measure the physical processes responsible for coastal change. They instead provide observable proxies from which patterns of coastal condition and change can be inferred. This distinction is important when such indicators are subsequently combined in an integrated spatial assessment of coastal change.

This section therefore first introduces the physical processes controlling coastal morphology and shoreline movement. It then discusses coastal typology and the characteristics of tropical reef-lined coasts before reviewing the use of remote sensing for shoreline, vegetation, and built-environment monitoring. Finally, external coastal exposure, multi-indicator coastal assessment, and the uncertainties associated with spatial Earth-observation datasets are considered.

2.1. Coastal systems and coastal morphodynamics

Coastal morphology develops through continuous interaction between hydrodynamics, sediment transport, and the shape of the coast itself. Bosboom and Stive (2023) describe coastal dynamics as the interaction between waves, flow, sediment transport, and the resulting morphodynamic response of coastal systems. These components are coupled: waves and currents transport sediment and thereby modify coastal morphology, while changes in morphology subsequently influence the propagation of waves and currents.

This feedback means that coastal morphology should not be viewed as a fixed boundary. A coastal system can adjust when its existing sediment distribution is no longer in balance with the prevailing forcing conditions. Sediment may be eroded from one part of the system, transported, and deposited elsewhere until a new morphological configuration develops (Bosboom & Stive, 2023).

The concept of equilibrium is useful in this context but does not imply that the shoreline or coastal morphology is motionless. Instead, equilibrium refers to a condition in which the morphology remains approximately stable at the scale and over the time period being considered. Short-term fluctuations may therefore occur within a coastal system that appears approximately stable over longer periods.

Temporal scale is particularly important when shoreline observations are interpreted. Beaches can respond to individual wave events, seasonal variations, and longer-term changes in sediment supply or forcing. Consequently, shoreline movement between two observations may reflect temporary variability rather than a persistent erosional or accretional trend. Maiti and Bhattacharya (2009) show that shoreline change can include both short-term variability and longer-term trends, making the temporal context of observations important when coastal change rates are calculated.

Spatial scale is similarly important. Local shoreline behaviour may differ from the broader behaviour of the coastal system because sediment can be redistributed between neighbouring sections. A locally eroding section may therefore be connected to accretion elsewhere through the same sediment-transport system.

Human intervention forms part of this morphodynamic system. Coastal structures can modify wave propagation or interrupt existing sediment-transport pathways. As a result, human modifications may cause morphological responses outside the immediate location of the intervention (Bosboom & Stive, 2023). This is particularly relevant when developed and undeveloped coastal sections are compared.

2.2. Physical drivers of coastal change

2.2.1. Waves and nearshore transformation

Waves represent an important mechanism through which offshore energy is transferred toward the coast. As waves move from deeper water into shallower coastal areas, they are transformed by the seabed and coastal geometry. Important transformation processes include shoaling, refraction, diffraction, and wave breaking (Bosboom & Stive, 2023).

Shoaling occurs when wave characteristics change as water depth decreases. Refraction occurs because different parts of a wave crest may propagate through different water depths, causing the direction of wave propagation to change. This process tends to modify the angle between incoming waves and the coastline and can concentrate wave energy in some areas while dispersing it in others.

Wave breaking occurs when waves become unstable in shallow water. Breaking dissipates part of the incoming wave energy and generates nearshore currents. These currents are important for coastal morphology because they contribute to the mobilisation and transport of sediment (Bosboom & Stive, 2023).

Nearshore wave conditions are therefore not determined solely by offshore wave height. Water depth, seabed morphology, wave direction, coastline orientation, reefs, and other nearshore features influence how much wave energy ultimately reaches the shoreline. A coastline exposed to the same regional offshore wave climate may consequently experience substantial spatial variation in nearshore forcing.

This relationship is important when simplified spatial indicators such as coastline orientation or fetch are used. These indicators can provide information about relative exposure, but they do not directly measure the amount of wave energy acting at the shoreline.

2.2.2. Cross-shore sediment transport

Cross-shore sediment transport refers to sediment movement approximately perpendicular to the coastline. It contributes strongly to changes in beach profile and shoreline position. Bosboom and Stive (2023) describe cross-shore transport as the result of interacting wave- and current-driven processes, including wave asymmetry, undertow, turbulence, and longer-period water motions.

During energetic conditions, sediment can be removed from the upper beach and transported toward the lower beach or submerged shoreface. This can produce a temporary landward movement of the visible shoreline. Under subsequent lower-energy conditions, part of this sediment may move landward again and contribute to beach recovery.

This behaviour demonstrates why shoreline retreat over a short period should not automatically be interpreted as permanent sediment loss. Sediment may remain within the broader beach system even when the instantaneous shoreline moves landward.

Cross-shore transport is also important when satellite-derived shorelines are interpreted, because each

image captures only one morphological state of the beach. If images are acquired before and after an energetic event, observed shoreline displacement may partly represent redistribution of sediment across the profile rather than a long-term change in the sediment budget.

2.2.3. Longshore sediment transport

Longshore sediment transport occurs approximately parallel to the coastline and is closely associated with waves approaching the coast at an angle. Oblique wave breaking generates longshore currents, while wave action mobilises sediment that can subsequently be transported alongshore (Bosboom & Stive, 2023).

Spatial differences in longshore transport are particularly important for shoreline change. Where more sediment leaves a coastal section than enters it, the local sediment budget becomes negative and erosion may occur. Where transport decreases and sediment accumulates, the shoreline may accrete.

Coastline orientation can influence these gradients. Because wave-incidence angle varies with shoreline orientation, differently oriented coastal sections may experience different longshore transport rates even when exposed to similar offshore wave conditions. Bosboom and Stive (2023) show that changes in shoreline orientation can therefore create zones of sediment-transport convergence and divergence.

Coastline orientation should nevertheless be interpreted only as an indicator of potential differences in sediment-transport conditions, rather than a direct measurement of sediment transport. Actual transport also depends on sediment availability, grain characteristics, wave conditions, bathymetry, and local coastal structures.

2.2.4. Water-level variability

The horizontal position of the land–water boundary changes when water level changes. Tides, storm surge, wave setup, and wave run-up can therefore alter the observed shoreline position even without a corresponding long-term change in coastal morphology.

This effect depends strongly on coastal slope. On a gently sloping beach, a relatively small vertical change in water level can produce a comparatively large horizontal displacement of the waterline. Consequently, the instantaneous shoreline detected in a satellite image may vary between acquisitions because the images were acquired under different hydrodynamic conditions.

García-Rubio et al. (2015) demonstrated that tidal level, surge, wave run-up, and beach slope contribute to uncertainty in satellite-derived shoreline position. Their comparison between remotely sensed and field-observed shorelines therefore shows why the instantaneous waterline should not automatically be interpreted as a fixed morphological reference.

Water-level variability is particularly relevant when shoreline changes are small. Where measured displacement is similar in magnitude to the expected positional uncertainty, interpretation of the change as erosion or accretion requires caution. This is particularly relevant for medium-resolution satellite imagery, where small horizontal shoreline differences may be of the same order of magnitude as positional and water-level uncertainty.

2.3. Defining and measuring the shoreline

Although the shoreline is commonly described as the boundary between land and water, this definition becomes more complicated when the boundary must be measured consistently. Coastal monitoring studies use different shoreline proxies depending on data availability, morphology, and research objective (Apostolopoulos & Nikolakopoulos, 2021). Figure 2.1 illustrates the main coastal zones and the distinction between high- and low-tide shoreline positions. This demonstrates how the location of the land–water boundary can vary with water level, even without changes in the underlying coastal morphology.

Possible proxies include the instantaneous waterline, vegetation line, wet–dry boundary, dune toe, cliff edge, or a contour corresponding to a particular elevation or tidal datum. These features do not necessarily occur at the same horizontal location.

For optical remote sensing, the instantaneous waterline is frequently used because water and land can

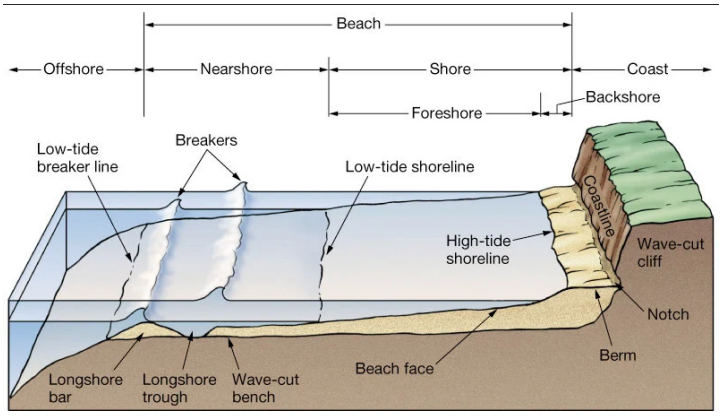


Figure 2.1: Schematic representation of coastal zones and morphological features, including the offshore, nearshore, foreshore, and backshore, and the distinction between high- and low-tide shoreline positions. Reproduced from The Coast: Beaches and Shoreline Processes, Figure 10.1.

often be distinguished spectrally. However, the detected boundary represents the location of water at the moment the satellite image was acquired. It is therefore influenced by tide, run-up, surge, and local topography.

The distinction between a geomorphological shoreline and a remotely sensed waterline is important. García-Rubio et al. (2015) found a systematic difference between satellite-derived shoreline positions and quasi-simultaneous field observations, despite the satellite-derived shoreline error being smaller than the nominal image pixel size in their study.

Consistency in shoreline definition is therefore essential in multitemporal analysis. If different proxies or extraction criteria are used between observations, methodological differences can appear as apparent coastal change.

The shoreline should consequently be interpreted as an observed indicator with associated positional uncertainty rather than as an exact, permanently fixed physical line. In this thesis, the extracted shoreline is therefore interpreted specifically as an instantaneous land–water boundary derived from optical satellite imagery, rather than as a fixed geomorphological coastline.

2.4. Coastal typology and tropical reef-lined coasts

2.4.1. Coastal typology

Coastlines differ substantially in morphology, material, vegetation, and degree of human modification. Rocky coasts, sedimentary beaches, dunes, wetlands, inlets, and engineered shorelines respond differently to hydrodynamic forcing and sediment transport.

Coastal typology provides a means of representing this heterogeneity systematically. Classification can be based on factors such as sediment characteristics, coastal morphology, ecological setting, or human modification. The usefulness of typology lies in the fact that the same environmental forcing does not necessarily produce the same response on different coastal types.

For example, an unconsolidated sandy shoreline can adjust through erosion and deposition relatively rapidly, whereas a rocky or heavily engineered shoreline is controlled by different physical processes. Dune systems additionally depend on interactions between wind, vegetation, and sediment supply.

Coastal type is also relevant to remote sensing. A clear sandy beach–water boundary may be relatively straightforward to identify spectrally, while reefs, wetlands, shallow water, rocky platforms, or engineered shorelines may produce more complex boundaries. Typology therefore provides important context when spatial differences in shoreline change, exposure, and shoreline-extraction uncertainty are interpreted.

2.4.2. Reef-lined coasts

Tropical reef-lined coasts represent a distinctive morphodynamic setting because coral reefs modify incoming waves before they reach the shoreline. The reef crest and reef flat act as shallow obstacles over which waves may break and dissipate energy.

Ruiz de Alegria-Arzaburu et al. (2013) compared two beaches in the Mexican Caribbean exposed to similar offshore wave conditions, one protected by a fringing reef and one without equivalent reef protection. The reef-fronted beach was considerably less morphodynamically active, and wave modelling indicated that the reef could reduce incident wave height by up to 85% during energetic shore-normal conditions.

The same study demonstrated that reef geometry is important. Reef-crest elevation controlled the amount of wave-energy dissipation, while reef-to-shore distance influenced the morphological response of the adjacent beach (Ruiz de Alegria-Arzaburu et al., 2013). Reef presence alone therefore does not completely describe the degree of protection.

Structural complexity provides an additional control. Harris et al. (2018) show that the three-dimensional complexity of coral reefs increases hydraulic roughness and frictional wave dissipation. Degradation that reduces reef structural complexity can therefore increase the wave energy transmitted into back-reef environments.

In a simplified spatial assessment, reef presence can therefore be used as an indicator of potential natural wave attenuation. However, it should be interpreted as a proxy rather than as a direct measurement of the actual protection provided at a particular location.

2.4.3. Coral-sand beaches

Tropical reef systems can also influence the composition of beach sediment because biological and reef-derived carbonate material contributes to beach formation. These sediments may differ physically from quartz-dominated beach sands.

Laboratory experiments by Yao et al. (2024) showed that equilibrium beach-profile relationships developed for quartz-sand beaches were not directly applicable to coral-sand beaches. Coral sand also produced different bar geometry under comparable experimental forcing.

This distinction is relevant when coastal theory developed mainly for quartz-sand beaches is applied to tropical reef-associated environments. The underlying sediment-transport concepts remain relevant, but sediment composition and grain characteristics can influence the magnitude and form of morphological response.

2.5. Coastal remote sensing monitoring

Satellite remote sensing provides a means of monitoring different components of coastal environments repeatedly and over large spatial areas. Through multispectral satellite imagery and derived spatial datasets, changes in shoreline position, vegetation, and the built environment can be observed and compared over time. However, the accuracy and interpretation of these observations depend on characteristics such as spatial and temporal resolution, image quality, and classification methods. This section introduces the remote-sensing approaches used for coastal monitoring, followed by the main limitations and uncertainties associated with the resulting indicators.

2.5.1. Advantages of satellite observation

Satellite remote sensing has become an important source of coastal observations because it provides repeated spatial coverage over areas that would be difficult to monitor continuously using field surveys alone.

Satellite imagery is particularly useful for historical analysis because long observational archives make it possible to reconstruct coastal behaviour over several decades. Vitousek et al. (2023) identify the ability of Earth-observing satellites to provide repeated observations over large spatial scales as one of their major advantages for coastal monitoring.

Traditional field methods such as GPS surveys, topographic surveys, and LiDAR can provide highly

accurate observations but generally cover smaller spatial areas and require repeated data-collection campaigns. Satellite observations involve lower positional accuracy but can provide much greater spatial and temporal coverage.

This trade-off makes satellite remote sensing particularly useful for comparative coastal studies where repeated observations are needed across large or spatially dispersed coastal areas.

2.5.2. Optical remote sensing

Optical satellite sensors measure reflected electromagnetic radiation in multiple wavelength bands. Differences in spectral behaviour between water, vegetation, bare ground, and constructed surfaces allow these surface types to be distinguished.

Water absorbs strongly in near-infrared and short-wave-infrared wavelengths, creating a strong contrast with many terrestrial surfaces. Vitousek et al. (2023) describe this spectral contrast as a central basis for automated shoreline detection from optical imagery.

Multispectral imagery can therefore support several indicators within the same coastal analysis. Water-sensitive spectral information can be used to distinguish land and water, while red and near-infrared bands can be used to assess vegetation.

Optical remote sensing nevertheless requires suitable atmospheric conditions. Clouds can obscure the surface, while shadows, sun glint, shallow water, suspended sediment, and bottom reflectance can complicate classification in coastal environments.

Spatial resolution introduces another limitation. Narrow beaches, small structures, and irregular coastal features may be represented by only a small number of pixels or by mixed pixels containing both land and water.

2.5.3. Satellite-derived shorelines

Satellite-derived shorelines are produced by identifying a spectral or classified boundary between land and water. Methods range from manual digitisation to automated spectral thresholding and more advanced classification approaches.

The ability to automate shoreline extraction is particularly important for long time series because manually digitising hundreds of images across long coastlines is highly time consuming. Vitousek et al. (2023) describe modern satellite shoreline methods as increasingly exploiting spectral differences between land and water to automate this process.

Pixel-based extraction methods can produce irregular or staircase-like boundaries because the shoreline follows individual raster cells. Sub-pixel approaches attempt to estimate the transition within or between neighbouring pixels and can therefore generate smoother shoreline positions.

Satellite-derived shoreline methods have also been adapted to monitor coastal features other than the instantaneous land–water boundary. Freund (2025), for example, developed CliffSat by modifying the CoastSat algorithm to detect coastal cliff lines using a combination of spectral indices and composite satellite imagery. Validation against in-situ observations along the Holderness Coast in England demonstrated the potential of this approach for monitoring cliff erosion. This distinction is relevant because the boundary identified through satellite imagery depends on the coastal feature being targeted. Consequently, an automatically extracted waterline should not necessarily be interpreted as representing changes in other geomorphological features, particularly along rocky or cliffed coastlines.

Regardless of the extraction method, validation remains important. Improvements in apparent spatial resolution do not automatically lead to equivalent improvements in shoreline accuracy because georeferencing, water level, run-up, and shoreline definition can remain important sources of error (Vitousek et al., 2023). For this reason, automated shoreline extraction should be evaluated against reference observations where possible, and the resulting positional uncertainty should be considered when interpreting small shoreline displacements.

2.5.4. Remote sensing of vegetation

In addition to shoreline monitoring, multispectral satellite imagery can be used to assess vegetation presence and change. Vegetation can be monitored remotely because healthy vegetation interacts strongly with red and near-infrared radiation. Chlorophyll absorbs much of the incoming red radiation, while internal leaf structure produces relatively high near-infrared reflectance.

The Normalized Difference Vegetation Index (NDVI) uses this contrast to provide a dimensionless spectral vegetation indicator:

$$NDVI = \frac{\rho_{\text{NIR}} - \rho_{\text{Red}}}{\rho_{\text{NIR}} + \rho_{\text{Red}}}, \tag{2.1}$$

where ρ_{NIR} and ρ_{Red} represent reflectance in the near-infrared and red bands, respectively.

NDVI has been applied successfully to coastal vegetation monitoring. Rodgers et al. (2009), for example, used Landsat NDVI to investigate coastal vegetation changes associated with Hurricane Katrina and subsequent environmental conditions.

Their results also demonstrate an important limitation. NDVI can change as a result of storm disturbance, salinity, drought, seasonal variation, and vegetation type. A decline in NDVI therefore cannot automatically be interpreted as permanent removal of vegetation.

For the purposes of coastal analysis, NDVI is most appropriately interpreted as a spectral indicator of vegetation presence or condition. It does not directly quantify the strength, width, root structure, sediment-trapping capacity, or wave-attenuation capacity of vegetation. Accordingly, changes detected in this thesis are interpreted as changes in remotely detected vegetation rather than as direct changes in coastal protection or ecological quality.

2.5.5. Remote sensing of buildings

In addition to monitoring natural coastal features, remote sensing can be used to assess changes in the built environment. Recent machine-learning methods have made it possible to derive building information over very large geographic areas from satellite imagery.

Sirko et al. (2023) developed a high-resolution building- and road-detection approach using Sentinel-2 imagery. This work underlies the Google Open Buildings temporal products and demonstrates that building information can be inferred at spatial detail finer than the original Sentinel-2 pixel grid through machine-learning-based processing.

However, changes in modelled building presence can result from genuine development but may also reflect differences in image quality, model confidence, or detection stability. Temporal building change should therefore be interpreted as change in the remotely detected built environment rather than as confirmed construction or demolition unless independently verified.

2.5.6. Data quality, spatial resolution, and uncertainty

The reliability of remotely sensed coastal indicators depends on several factors, including spatial resolution, georeferencing, temporal sampling, and classification uncertainty. These limitations are particularly relevant when changes are assessed over relatively short distances or between individual observation dates.

Spatial resolution constrains the minimum scale at which coastal features can be represented directly in raster data. Where a shoreline crosses a pixel, the recorded spectral value may contain contributions from both land and water. Such mixed pixels are particularly relevant for narrow beaches, complex rocky shorelines, shallow reefs, small coastal structures, and irregular land–water boundaries. Satellite-derived shoreline error is not necessarily equal to the nominal image pixel size. Sub-pixel extraction can estimate shoreline position more precisely than the raster spacing, while georeferencing and water-level effects can produce errors unrelated to pixel size. Vitousek et al. (2023) identify spatial resolution as an important limitation of satellite-derived shoreline observations but also emphasise that georeferencing and run-up can become limiting sources of error even when higher-resolution imagery is available.

Georeferencing and image co-registration are also important when comparing observations from different dates. Multitemporal shoreline analysis assumes that the images are spatially aligned, since a systematic offset between two images can otherwise appear as false shoreline movement. A consistent spatial reference reduces the likelihood of such errors but does not eliminate all positional uncertainty. This becomes particularly relevant when measured shoreline displacement is similar in magnitude to the positional uncertainty of the imagery.

Temporal resolution introduces another source of uncertainty. A denser observational record can help distinguish seasonal movement, short-term disturbance, and longer-term change that may be missed when only two dates are compared. Vitousek et al. (2023) emphasise that satellite imagery allows repeated observations of coastlines over several decades and across large geographic areas. However, observations acquired on different dates may correspond to different tides, wave conditions, vegetation seasons, or atmospheric conditions. Increasing the number of observations therefore improves temporal characterisation but does not necessarily make individual measurements directly comparable.

Uncertainty also affects vegetation and building indicators. NDVI can respond to differences in vegetation type, moisture, salinity, seasonal growth, and disturbance. Rodgers et al. (2009), for example, demonstrated that coastal NDVI changes following Hurricane Katrina were influenced by both the initial disturbance and subsequent environmental conditions. Similarly, building information derived through machine learning represents modelled detection rather than direct field observation. False positives, missed detections, and temporal variation in model performance can therefore influence apparent changes between years.

These uncertainties are not removed when multiple remotely sensed indicators are combined within an integrated assessment. Instead, the interpretation of spatial differences and co-occurrences must consider the limitations and validation results of the individual datasets. This is particularly important for the present study, where shoreline displacement, detected building change, and vegetation change are compared across coastal environments with different physical characteristics.

2.6. Vegetation and natural coastal buffering

2.6.1. Coastal vegetation

Coastal vegetation occurs in environments including dunes, beaches, marshes, estuaries, and rocky coastal areas. These environments impose stresses that include salinity, wind exposure, wave influence, sediment mobility, and periodic inundation. Asensi and Diez-Garretas (2017) describe coastal vegetation as developing under the combined influence of terrestrial and marine environmental conditions.

Vegetation distribution is therefore often spatially organised along environmental gradients. In dune systems, communities can change substantially between the active beach and more stable inland dunes as exposure, sand mobility, salinity, and organic-matter content change.

The relationship between vegetation and coastal morphology is bidirectional. Physical coastal conditions influence where plants can establish, while established plants can in turn modify sediment transport.

Vegetation loss can also affect adjacent coastal environments indirectly. Where terrestrial vegetation is reduced, increased erosion and surface runoff can enhance sediment delivery towards reefs, lagoons, and mangrove systems. In mangrove environments, vegetation condition can additionally be linked to tidal exchange, sediment accumulation, and salinity. Observed vegetation change can therefore reflect both direct land-cover change and changes in local environmental conditions (Gijsman et al., 2026; Zambrano Cortes, 2012).

2.6.2. Vegetation and dune stability

Vegetation can influence dune morphology by reducing sediment mobility. Stems and leaves modify near-surface airflow, while vegetation can trap moving sediment and contribute to dune development.

Acosta et al. (2007) describe an interdependence between dune morphology and coastal vegetation zonation. Their study shows that vegetation communities are related to local morphological and environmental gradients, while vegetation itself contributes to the stability and conservation of dune systems.

This function is relevant when interpreting coastal condition, because vegetated dunes can contribute to the natural buffering capacity of the coast. However, the effectiveness of vegetation depends on characteristics such as plant type, density, dune morphology, and disturbance.

Vegetation presence should therefore not be treated as automatically equivalent to coastal protection. Instead, vegetation should be treated as one coastal characteristic that may contribute to stability depending on the local setting.

2.7. Coastal development and the built environment

2.7.1. Development as coastal exposure

Human settlement is concentrated in many coastal areas, placing buildings and infrastructure close to environments that may experience erosion, flooding, or other forms of coastal change. The built environment can therefore represent one component of exposure, since a coastal section with a high concentration of buildings contains more constructed assets that may potentially be affected by shoreline retreat or other coastal hazards.

Coastal development can also be interpreted more broadly as a form of anthropogenic pressure. Urbanisation and tourism are associated with land-use and land-cover change, urban sprawl, and infrastructure development, which can alter the characteristics of coastal landscapes. These processes may involve the conversion of natural or less-developed land and an increasing concentration of human activity within the coastal zone (Petrişor et al., 2020).

The effects of urban pressure are not limited to the physical presence of buildings. Coastal urbanisation may also be associated with changes in vegetation, sediment conditions, water quality, biodiversity, and other environmental characteristics. These pressures can occur simultaneously, meaning that development should be understood as one component within a wider set of interacting human influences on the coastal system (Petrişor et al., 2020).

In this thesis, detected building area is therefore interpreted in two related ways. First, it represents the concentration of constructed assets that may be exposed to coastal change. Second, it provides a spatial proxy for development pressure and the degree of human occupation of the coastal zone. This does not imply that buildings themselves cause erosion, nor does detected building area directly measure processes such as runoff, pollution, sediment disruption, tourism pressure, or coastal engineering. Relationships between building development and shoreline change should therefore be interpreted as spatial associations rather than direct evidence of causation.

2.7.2. Development as a morphodynamic influence

Human development can also influence coastal processes when it includes coastal engineering. Structures such as groynes, jetties, breakwaters, and seawalls modify the natural interaction between waves, sediment transport, and shoreline morphology.

Bosboom and Stive (2023) describe how groynes and jetties can interrupt longshore sediment transport. Sediment may accumulate on the updrift side of the structure while reduced sediment supply contributes to downdrift erosion.

Built-up density and coastal engineering should therefore be conceptually separated. A high concentration of buildings indicates development and potential exposure, but it does not necessarily indicate that the shoreline has been physically modified by coastal structures.

A spatial relationship between building development and shoreline change should therefore be interpreted as an association rather than as evidence that development caused the observed shoreline behaviour.

2.8. External coastal exposure

2.8.1. Coastal orientation

The orientation of the coastline relative to incoming wave and wind directions influences coastal exposure. Because wave-incidence angle affects refraction and longshore currents, coastal sections

facing different directions can experience different morphodynamic conditions under the same regional wave climate (Bosboom & Stive, 2023).

Coastal orientation can therefore be used as an indicator of relative exposure where the predominant wave or wind direction is known or relatively persistent.

However, coastline orientation does not directly represent wave energy. Nearshore bathymetry, reefs, islands, headlands, and other coastal features can substantially modify wave propagation before waves reach the shoreline.

2.8.2. Fetch

Fetch describes the distance over water across which wind can transfer energy to the sea surface. Longer unobstructed water distances can permit the development of larger locally generated waves when wind conditions are otherwise suitable.

Fetch can therefore be used as an additional indicator of relative exposure, particularly when comparing coastal sections with different degrees of shelter from surrounding land or islands. In general, a longer unobstructed fetch indicates greater potential for locally generated wave development under suitable wind conditions.

As with orientation, fetch simplifies a more complex process. Actual wave conditions depend on wind speed, wind duration, water depth, offshore wave conditions, and nearshore transformation. Fetch should consequently be interpreted as a proxy rather than a direct measure of wave forcing.

2.8.3. Coral reefs as natural wave barriers

Coral reefs can substantially modify external coastal exposure because wave breaking and friction dissipate energy across the reef platform.

The Caribbean comparison by Ruiz de Alegria-Arzaburu et al. (2013) provides direct evidence that a fringing reef can reduce wave energy and produce a less morphodynamically active beach than an adjacent coast exposed to similar offshore forcing.

Reef protection is nevertheless spatially variable. Reef-crest height and reef-to-shore distance influence the amount of energy transmitted toward the beach (Ruiz de Alegria-Arzaburu et al., 2013).

Reef condition introduces further variability. Harris et al. (2018) show that structural complexity is important for frictional wave dissipation, meaning that a degraded reef may provide less protection than a structurally complex reef.

Reef presence can therefore indicate the potential for reduced wave exposure, but it should not be interpreted as a direct measurement of wave attenuation at a specific location.

Orientation, fetch, and reef setting therefore provide complementary information on coastal exposure. None of these indicators represents wave forcing directly, but together they can help distinguish relatively sheltered and exposed coastal settings. In this thesis, these indicators are used to support the comparison of the selected coastal sections, while their calculation and application are described in the methodology.

2.9. Coastal vulnerability and multi-indicator assessment

2.9.1. Coastal vulnerability as a multidimensional concept

Vulnerability is a multidimensional concept and does not have one universally applicable definition. Its meaning depends partly on whether the assessment focuses on physical susceptibility, human exposure, socioeconomic conditions, adaptive capacity, or a combination of these components. Roukounis and Tsihrintzis (2022) show that coastal vulnerability studies vary considerably in both the indicators that are included and the way vulnerability is defined.

This distinction is important when remotely sensed indicators are used. Variables such as shoreline change, vegetation, coastal morphology, and building presence can provide information on physical and environmental conditions, but they do not represent all dimensions of vulnerability. In particular, they do not directly measure factors such as socioeconomic sensitivity, adaptive capacity, or the ability

of communities to respond to coastal hazards. A study based mainly on physical and remotely sensed indicators should therefore not automatically be interpreted as a complete assessment of societal vulnerability.

2.9.2. Multi-indicator coastal assessment

Coastal vulnerability studies often combine several indicators because coastal condition cannot be described by one variable alone. Common indicators include geomorphology, coastal slope, shoreline change, tidal range, wave conditions, sea-level change, coastal protection, vegetation, land use, infrastructure, and the built environment (Roukounis & Tsihrintzis, 2022). The choice of indicators depends on the purpose, spatial scale, and definition of vulnerability adopted in the study.

Combining these variables into a single index can make spatial comparison easier, but it also introduces additional assumptions. Indicators with different units generally need to be normalised or classified before they can be combined, while decisions also have to be made about weighting and aggregation. Torresan et al. (2012), for example, used normalisation to compare indicators on a common scale. The resulting values represented relative vulnerability within the study area rather than an absolute measure that could be transferred directly to another location.

These choices can strongly influence the final result. A high index value is therefore dependent on the variables that were selected, the way they were scaled, and the spatial extent of the assessment. Weighting introduces another assumption about the relative importance of the indicators, while equal weighting also assumes that each variable contributes equally.

For this reason, the present study does not combine the selected indicators into a single vulnerability index. Shoreline change, detected building development, remotely detected vegetation, coastal type, and external exposure are instead analysed separately and compared within the same spatial framework. This allows patterns and co-occurrences between the indicators to be examined without assigning an assumed weight or level of importance to each one. The analysis therefore uses ideas from multi-indicator vulnerability assessment, but the final output is interpreted as a comparative assessment of coastal change rather than as a numerical measure of vulnerability.

2.10. Conceptual framework

The conceptual framework used in this thesis is based on the idea that coastal change should be interpreted in relation to both the physical coastal setting and changes in the human and natural environment. Remote-sensing data are used to derive the main observed indicators, including shoreline position, building development, and vegetation change. As illustrated in Figure 2.2, shoreline displacement forms the main indicator of observed coastal change, while coastal type, orientation, fetch, and reef setting describe differences in the physical setting and external exposure of the selected sections. Building development and vegetation change provide additional information on changes occurring in the surrounding coastal environment.

The different indicators are first analysed separately and are then brought together in the integrated spatial comparison. The purpose of this comparison is to identify spatial patterns, contrasts, and co-occurrences between the selected sections of Aruba and Bonaire. The framework does not assume that development, vegetation, or exposure directly causes the observed shoreline changes. Instead, these indicators provide context for interpreting differences in coastal change between locations.

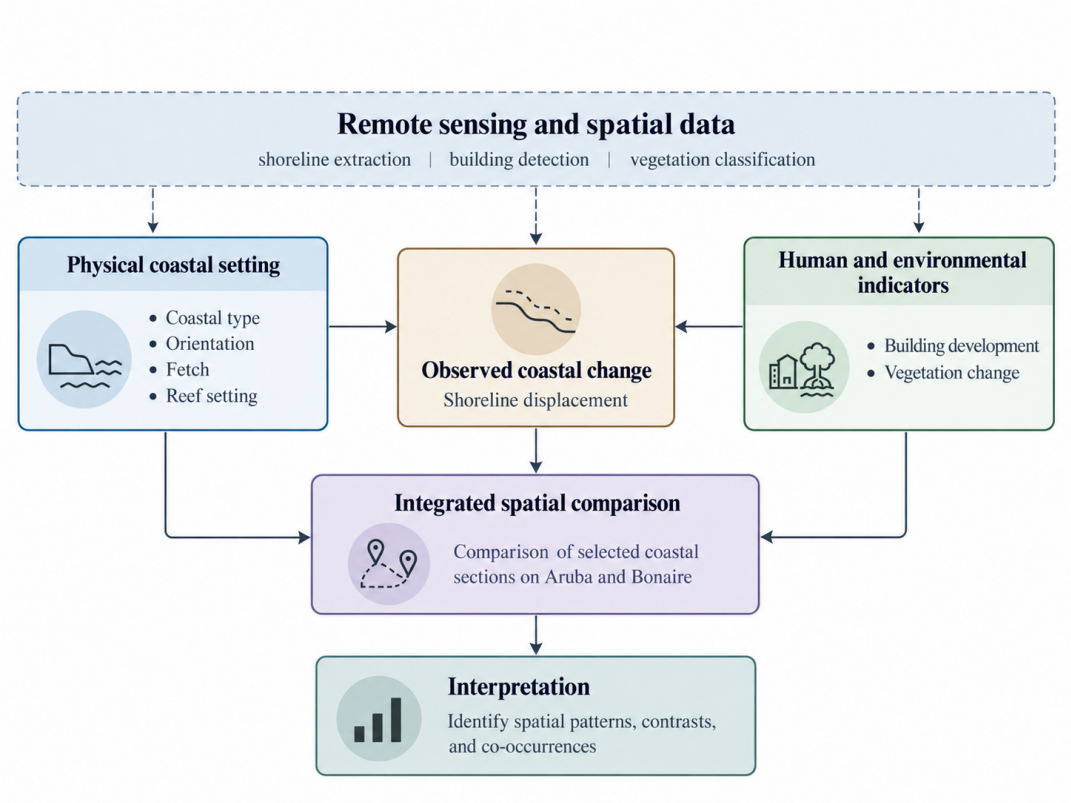


Figure 2.2: Conceptual framework used to compare coastal change, physical coastal setting, development, and vegetation across the selected coastal sections of Aruba and Bonaire.

3

Study areas and data

3.1. Regional context

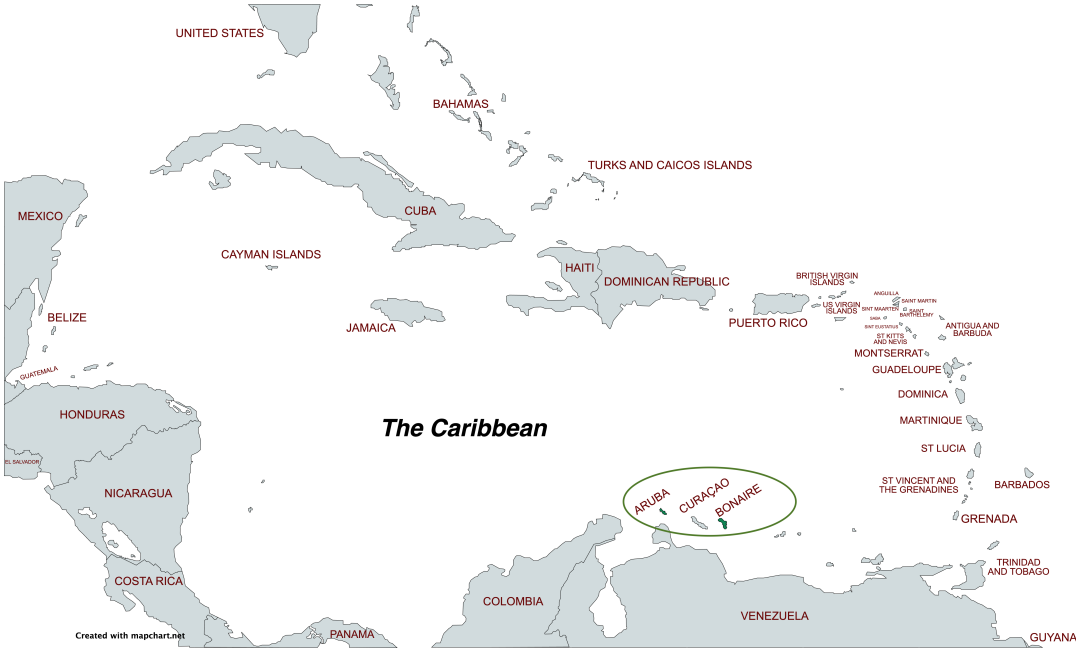


Figure 3.1: Location of Aruba and Bonaire within the Caribbean. The two islands are highlighted in green. Source: mapchart.net, edited by the author.

Aruba and Bonaire are located in southern Caribbean, north of the Venezuelan coast, and form part of the Leeward Antilles together with Curaçao. The islands share a broadly comparable regional geological and climatic setting, while differing considerably in coastal morphology, land use, and intensity of human development. Aruba has a land area of approximately 179 km^2, whereas Bonaire covers approximately 287–288 km^2 (Schmutz et al., 2017).

The geological development of the islands is associated with the Leeward Antilles ridge and the interaction between the Caribbean and South American plates. Their geological cores consist predominantly of Cretaceous and Paleogene volcanic, intrusive, and sedimentary rocks, partly overlain by younger limestone deposits and Quaternary marine terraces (Hippolyte & Mann, 2011). These coastal terraces reflect the combined influence of tectonic uplift, marine erosion, and Quaternary sea-level fluctuations. Early geomorphological mapping identified multiple terrace levels on both Aruba and Bonaire and showed that their elevation, width, and preservation vary spatially around each island (Alexander, 1961).

Recent research on Aruba has further demonstrated that the morphology of emerged fossil coral-reef terraces is strongly spatially variable. Although a slight north–south tectonic tilt may contribute to differences in terrace elevation, local basement slope and wave exposure appear to exert the strongest control on terrace geometry (Chauveau et al., 2026). This illustrates the importance of local exposure and morphology when coastal sections are compared.

Both islands occur within the southern Caribbean dry zone. Bonaire has a steppe climate with an annual precipitation of approximately 463 mm, a relatively dry season from February to June, and a wetter season from September to January (Royal Netherlands Meteorological Institute, 2017). Aruba has a similarly dry climate, with low rainfall, high evaporation, and persistent trade-wind conditions (Departamento Meteorologico Aruba, n.d.).

A defining atmospheric characteristic of the region is the persistent easterly trade-wind regime. On Aruba, easterly winds dominate throughout most of the year and form an important control on nearshore wave conditions (Departamento Meteorologico Aruba, n.d.). Bonaire experiences a comparable trade-wind regime, although wind strength varies seasonally (Royal Netherlands Meteorological Institute, 2024). The orientation of the islands relative to these prevailing winds creates an important contrast between exposed eastern and northeastern coastlines and comparatively sheltered western and southwestern coasts.

This windward–leeward contrast is clearly reflected in coastal morphology. Windward shorelines generally experience greater wave energy and commonly consist of rocky limestone coasts, erosional terraces, cliffs, and coarse deposits, whereas the more sheltered leeward coasts contain a larger proportion of sandy beaches, reef-fringed shorelines, and protected embayments (Schmutz et al., 2017). Marine terraces are correspondingly better expressed along exposed coastal sections, where platforms and erosional scarps tend to be more pronounced (Alexander, 1961).

Although Aruba and Bonaire lie near the southern margin of the main Atlantic hurricane belt and direct hurricane impacts are relatively uncommon, tropical cyclones passing elsewhere in the Caribbean can still generate energetic swell. For Bonaire, KNMI estimates that a hurricane passes within approximately 150 km only on the order of once per decade, substantially less frequently than for the Windward Caribbean Netherlands (Royal Netherlands Meteorological Institute, n.d.). Nevertheless, offshore hurricanes can still produce strong coastal wave conditions.

The geological record also indicates exposure to rarer extreme marine events. Large coastal boulders occur on emerged fossil reef surfaces along the windward sides of Aruba, Bonaire, and Curaçao. Recent geomorphological mapping, radiocarbon dating, and hydrodynamic modelling suggest that several major Holocene boulder-emplacement events were most consistent with tsunami forcing (Scardino et al., 2025). These deposits are concentrated particularly along exposed coastal sections and provide additional evidence of strong spatial variability in external coastal exposure.

The shared regional climate and geological setting therefore provides a common environmental framework for Aruba and Bonaire. At the same time, differences in orientation, morphology, reef configuration, vegetation, and development result in substantial local variations in coastal behaviour. These differences provide the physical basis for comparing shoreline position, vegetation change, building development, and external coastal exposure in this study.

3.2. Aruba

3.2.1. Physical geography and coastal morphology

Aruba is the westernmost of the ABC islands and covers approximately 179 km^2. The island is relatively low in elevation and elongated in a northwest–southeast direction (Schmutz et al., 2017). Together with the prevailing easterly trade winds, this orientation creates a pronounced contrast between the exposed northern and northeastern coasts and the more sheltered western and southwestern coast.

The geological basement of Aruba consists primarily of Cretaceous volcanic and sedimentary rocks affected by later intrusive and tectonic activity. Younger limestone deposits occur around substantial parts of the island and form a sequence of emerged marine and fossil coral-reef terraces (Hippolyte & Mann, 2011). Alexander (1961) distinguished three principal marine-terrace levels on Aruba, although

their elevation, width, and preservation vary considerably around the island.

Recent high-resolution research confirms that the geometry of Aruba's emerged fossil reef terraces is strongly influenced by local coastal conditions. Chauveau et al. (2026) found that antecedent basement slope and wave exposure are the main controls on reef-terrace morphology, while a possible north–south tectonic tilt contributes additional spatial variation. This is relevant to the present study because it shows that coastal morphology and exposure vary considerably around the island.

The windward coast is generally rocky and exposed to persistent wave attack. In contrast, the sheltered western coast contains Aruba's most extensive sandy beach environments, including Palm Beach, Eagle Beach, and Manchebo Beach (Schmutz et al., 2017). The contrast between these coastal environments is illustrated in Figure 3.2.



(a) Sheltered leeward coastline.

(b) Exposed windward coastline.

Figure 3.2: Contrasting coastal environments of Aruba, illustrating differences between the sheltered leeward coast and the more exposed windward coast.

The western sandy coastline is characterised by active longshore sediment transport. Under normal trade-wind conditions, refracted waves generate longshore currents that transport sediment along Eagle Beach and Pelican Beach towards a convergence area near Manchebo (Kohsiek et al., 1987). Episodic swell events can temporarily alter this pattern and cause substantial beach erosion. Reef configuration also varies around the island and can modify local wave exposure, adding to the contrast between sheltered and exposed coastal sections (Chauveau et al., 2026).

3.2.2. Coastal development

Aruba has undergone substantial urban and tourism development during the twentieth and early twenty-first centuries. Much of this development has occurred along the sheltered western coastline, where the island's major sandy beaches and tourism infrastructure are concentrated (Schmutz et al., 2017).

The magnitude of this transformation is demonstrated by recent land-use analysis. Jurgens et al. (2024) estimated that Aruba's built environment increased from approximately 29 km^2 in 1986 to approximately 60 km^2 in 2020. This means that developed land expanded to approximately one-third of the island. Earlier development was characterised primarily by outward urban sprawl, whereas more recent expansion increasingly occurred through infilling.

Tourism has been a major driver of this land-use transformation. Aruba is among the more tourism-intensive destinations in the Caribbean, and continued tourism development has created increasing competition for limited land resources (Jurgens et al., 2024). Historical tourism-planning documents already identified concern that further expansion could place additional pressure on highly developed areas and remaining natural landscapes (Cole & Razak, 2003).

The concentration of tourism and infrastructure close to the shoreline increases the practical importance of coastal change. Beachfront hotels, recreational infrastructure, and other economically important assets are concentrated in low-lying coastal areas (Massetti, 2025). Consequently, relatively small changes in shoreline position may occur immediately adjacent to highly valuable developed areas.

Human intervention has also altered natural coastal processes. Kohsiek et al. (1987) linked the deepening

of Aruba's harbour entrance in the early 1950s to disruption of the natural sediment supply along the western coast. Sediment derived from coral reefs was increasingly trapped in the harbour channel rather than reaching the adjacent beaches. Subsequent hotel construction therefore occurred along beaches already affected by reduced natural sediment supply.

3.2.3. Coastal environments and vegetation

Aruba's coastline contains a heterogeneous combination of rocky shores, limestone and fossil-reef terraces, sandy beaches, reef environments, and strongly developed urban and tourism coastlines. The broad distinction between an exposed rocky windward coast and a sheltered sandy leeward coast is one of the most prominent characteristics of the island (Schmutz et al., 2017).

The terrestrial environment is adapted to semi-arid conditions. Low rainfall and high evaporation result in relatively sparse drought-adapted vegetation compared with wetter Caribbean islands. Consequently, vegetation detected close to the coast may occur in discontinuous patches and can vary according to local water availability, land use, and disturbance.

This climatic setting is important when interpreting NDVI. Low NDVI values should not automatically be interpreted as vegetation degradation because sparse vegetation is a natural feature of Aruba's dry environment. Temporal changes in NDVI are therefore more informative when considered relative to the local baseline and in combination with other variables such as detected building development and shoreline change.

Aruba's coastal ecosystems are also affected by pressures from human development. Recent coral-reef assessments identify local stressors including water-quality deterioration, eutrophication, and coral disease (Eicher, 2023). A recent regional investigation of nearshore waters around the ABC islands also found spatial differences in biological indicators of nutrient enrichment, particularly near more densely populated and urbanised areas (van Duyl et al., 2024).

The combination of heterogeneous coastal morphology, intensive development, sparse semi-arid vegetation, and reef-mediated wave conditions means that shoreline change, vegetation, development, and exposure are likely to vary considerably between different parts of Aruba.

3.3. Bonaire

3.3.1. Physical geography and coastal morphology

Bonaire covers approximately 288 km^2 and forms part of the Caribbean Netherlands (Gijsman et al., 2026). The island has greater local topographic variability than Aruba. Its northern region is comparatively elevated and rugged, whereas much of southern Bonaire is low lying and contains extensive salt flats and saline water bodies.

As on Aruba, Bonaire's geology includes older volcanic and sedimentary rocks overlain by younger limestone formations. Marine terraces form a prominent component of the coastal landscape. Alexander (1961) identified three principal terrace levels on Bonaire, with the lowest terrace extending around a substantial proportion of the island. Higher terrace surfaces and erosional scarps are particularly well developed in several northern areas.

The morphology of Bonaire's coastline reflects a pronounced windward–leeward contrast. The eastern and northeastern coast is directly exposed to prevailing trade winds and associated waves and is generally rocky and high-energy. In contrast, the western coast is more sheltered and is bordered by extensive fringing reef systems (Frade et al., 2019). Sandy beaches occur on Bonaire but are generally less extensive than the long sandy beach systems of western Aruba.

Evidence of extreme marine events is particularly prominent along Bonaire's windward coast. Large coastal boulders and associated deposits occur on emerged reef terraces and rocky shoreline surfaces. Recent hydrodynamic modelling indicates that both hurricanes and tsunamis can generate energetic coastal conditions, although the largest prehistoric boulder-emplacement events investigated by Scardino et al. (2025) are more consistent with tsunami forcing.

The sheltered leeward coast is strongly influenced by coral reefs. Bonaire's reefs extend along much of the western coast and descend rapidly into deeper water (Frade et al., 2019). These reef systems modify

incoming waves and are therefore an important control on local nearshore exposure.

3.3.2. Coastal development

Bonaire has experienced increasing urban and tourism development, although the scale and spatial configuration differ substantially from Aruba. Population centres and much of the tourism-related development are concentrated along the central and southwestern-facing leeward side of the island (Frade et al., 2019). Tourism is strongly associated with the marine environment, particularly diving and other nature-based recreational activities.

Historical land-use change has considerably affected Bonaire's terrestrial ecosystems. Grazing, wood harvesting, agriculture, and subsequent urban and tourism development have contributed to degradation and fragmentation of the island's dry vegetation (Zambrano Cortes, 2012).

Bonaire's spatial development therefore involves an important tension between economic expansion and ecosystem conservation. Earlier land-use planning included the construction of housing, roads, and tourism facilities while simultaneously emphasising the need to conserve natural and cultural landscapes (Zambrano Cortes, 2012). More recent research similarly identifies land use, infrastructure, economic priorities, and governance as important factors influencing the implementation of more nature-inclusive development on Bonaire (Hermans et al., 2026).

At the same time, Bonaire contains an extensive system of protected coastal and marine environments. The Bonaire National Marine Park extends around the island and provides protection to substantial areas of reef habitat (Frade et al., 2019). This contributes to a coastal development pattern that differs from Aruba's more densely developed western tourism corridor.

Detected building area is therefore useful as a comparative indicator because the spatial pattern of development differs between the two islands. On Bonaire, built-up areas are more geographically concentrated, allowing coastal change to be compared between developed and less-developed coastal environments.

3.3.3. Coastal environments and vegetation

Bonaire contains a diverse range of coastal environments, including rocky limestone terraces, coral reefs, small beaches, salt ponds, hypersaline lakes, lagoons, and mangrove forests. This diversity is particularly important for the interpretation of remotely sensed shoreline and vegetation indicators.

Lac Bay, situated on southeastern Bonaire, represents one of the island's most distinctive coastal ecosystems. The system consists of an open bay, reef structures, and an extensive mangrove forest and is designated as a Ramsar wetland of international importance (Gijsman et al., 2026). The mangrove forest consists predominantly of *Rhizophora mangle* and *Avicennia germinans*, together with a smaller area likely dominated by *Laguncularia racemosa*. Recent estimates indicate approximately 136 ha of *Rhizophora mangle*, 77 ha of *Avicennia germinans*, and less than 9 ha of the third vegetation type (Gijsman et al., 2026).

Lac Bay is characterised by a microtidal regime with a tidal range below approximately 0.5 m. Tidal exchange between the open bay, tidal creeks, and interior mangrove lagoons is sensitive to relatively small changes in water level (Gijsman et al., 2026). Mangrove vegetation creates additional resistance to water flow, while the configuration of individual tidal creeks influences the direction and magnitude of water and sediment exchange.

The northern Awa di Lodo area of the mangrove forest has experienced ecosystem degradation during recent decades. Excess terrestrial sediment and infilling of tidal creeks have been associated with reduced tidal flushing and salinity stress, while sediment accumulation has been associated with mangrove expansion in other parts of Lac Bay (Gijsman et al., 2026).

Terrestrial vegetation elsewhere on Bonaire is also strongly influenced by dry climatic conditions and land-use pressure. Historical grazing and land clearance have reduced and degraded substantial areas of dry forest (Zambrano Cortes, 2012).

These conditions are important when interpreting NDVI change. Variations in vegetation near Bonaire's coast may reflect urban development, grazing pressure, rainfall variability, mangrove degradation, mangrove expansion, or local hydrological changes. NDVI should therefore be interpreted together with

shoreline position, detected building development, and coastal setting rather than as an independent measure of coastal condition.

3.4. Selected coastal study sections

3.4.1. Selection criteria

The detailed coastal analysis was carried out within six predefined study sections, with three sections selected on Aruba and three on Bonaire. The sections were chosen to represent contrasting coastal settings rather than to provide continuous coverage of the entire coastline. This made it possible to compare areas that differ in morphology, development, vegetation, and external exposure while keeping the analysis at a spatial scale suitable for shoreline, building, and vegetation comparison. The selection also considered the availability and quality of the satellite imagery required for the multi-temporal analysis. Each section needed sufficient PlanetScope coverage for shoreline and vegetation extraction over the study period, while the same spatial boundaries were used for the building and integrated analyses. Processing the sections separately also reduced interference from unrelated land–water boundaries elsewhere in the satellite scenes.

The selected sections are therefore not intended to represent every coastal environment present on Aruba and Bonaire. Instead, they provide a set of contrasting case-study areas in which shoreline change can be examined together with detected building development, remotely detected vegetation change, and differences in coastal setting. The same section boundaries are retained throughout the analysis so that the different indicators can be compared within a common spatial framework.

3.4.2. Aruba study sections

Figure 3.3 shows the locations of the three selected coastal study sections on Aruba, while Figures **??** to 3.7 provide a closer view of the individual analysis areas. Sections 1 and 2 are located on the more sheltered western and southwestern side of the island, whereas Section 3 is situated on the more exposed eastern side. Aruba is dominated by easterly trade winds, and the associated wind waves approach primarily from the east. Along the western coast, these waves are refracted around the northern and southern ends of the island before reaching the shoreline, resulting in substantially lower-energy conditions than on the directly exposed windward coast.



Figure 3.3: Location of the three selected coastal study sections on Aruba. Red boxes indicate the analysis areas used for the detailed coastal assessment.



Figure 3.4: Aruba Section 1, a developed sandy hotel and tourism coast on the sheltered western side.

Aruba Section 1

Aruba Section 1 is located on the western leeward side of the island and represents a strongly developed sandy coastal setting. The surrounding area contains a high concentration of hotels and tourism-related infrastructure close to the shoreline. This part of Aruba forms part of the island's main tourism coast, where hotels and resorts are situated directly adjacent to white coral-sand beaches (Giardino et al., 2018). The coastline is broadly west-facing and is relatively sheltered from the prevailing easterly trade-wind wave regime. Rather than receiving the dominant waves directly, wave energy reaching this coast is strongly influenced by refraction around the island (Giardino et al., 2018; Kohsiek et al., 1987).

Aruba Section 2



Figure 3.5: Aruba Section 2, a sheltered mangrove-influenced coast with residential development.

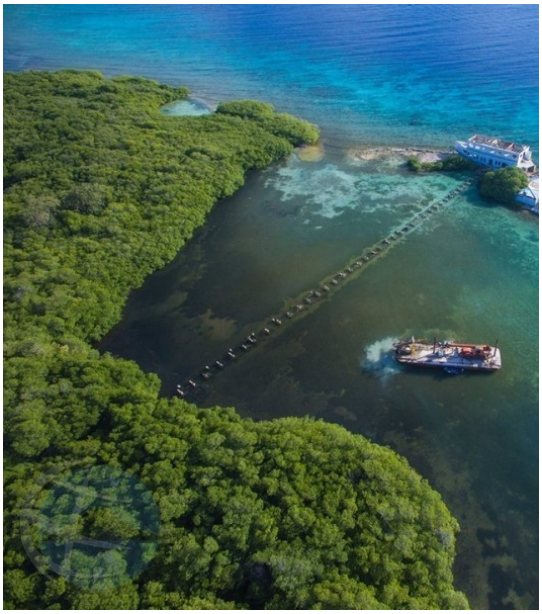


Figure 3.6: Mangrove-influenced coastal environment within Aruba Section 2.

Aruba Section 2 is also situated on the sheltered southwestern side of the island but differs from Section 1 in its coastal environment. The section contains residential development together with substantial coastal vegetation, particularly mangroves that can be seen in Figure 3.6. Mangrove communities occur along parts of Aruba's southwestern coast and are associated with sheltered coastal environments where fine sediments can accumulate (Giardino et al., 2018). The coastline is generally oriented toward the west to southwest and is therefore located on the leeward side relative to the dominant easterly trade winds. As with Section 1, the normal wind-wave regime reaches this coast mainly after refraction around the island rather than through direct exposure to incoming easterly waves (Kohsiek et al., 1987)).

Aruba Section 3

Aruba Section 3 is located on the eastern windward side of the island and represents a markedly different coastal setting. The section contains vegetation but very limited or no building development. The eastern and northeastern coasts of Aruba are directly exposed to the prevailing easterly trade-wind regime and are largely characterised by eroding Pleistocene reef-complex and rocky coastal formations, in contrast to the coral-sand-dominated western coast (Kohsiek et al., 1987). Its east-facing orientation means that the coastline is much more directly aligned with the dominant incoming wind and wave direction.



Figure 3.7: Aruba Section 3, a more exposed and largely undeveloped coastal section on the eastern side of the island.

3.4.3. Bonaire study sections

Figure 3.8 shows the locations of the three selected coastal study sections on Bonaire, while Figures 3.9 to 3.11 provide a closer view of the individual analysis areas. Sections 1 and 2 are located on the western and southwestern leeward coast, whereas Section 3 is situated on the eastern windward side of the island. Bonaire experiences persistent easterly trade winds, and Engel et al. (2012) describes the eastern shore as continuously exposed to high wave energy, while the western coast is comparatively calmer and more sheltered.



Figure 3.8: Location of the three selected coastal study sections on Bonaire. Red boxes indicate the analysis areas used for the detailed coastal assessment.



Figure 3.9: Bonaire Section 1, a developed rocky residential coast on the sheltered southwestern side.

Bonaire Section 1

Bonaire Section 1 is located on the southwestern leeward coast and represents a developed residential coastal setting. The immediate shoreline is predominantly rocky rather than characterised by an extensive sandy beach, with residential development occurring relatively close to the coast. Its west- to

southwest-facing position places it on the sheltered side of the island relative to the dominant easterly trade-wind regime. Engel et al. (2012) identifies the western coast of Bonaire as the calmer leeward side, in contrast to the more energetic eastern coast.



Figure 3.10: Bonaire Section 2, a developed rocky limestone coast in the Hato area on the sheltered western side.

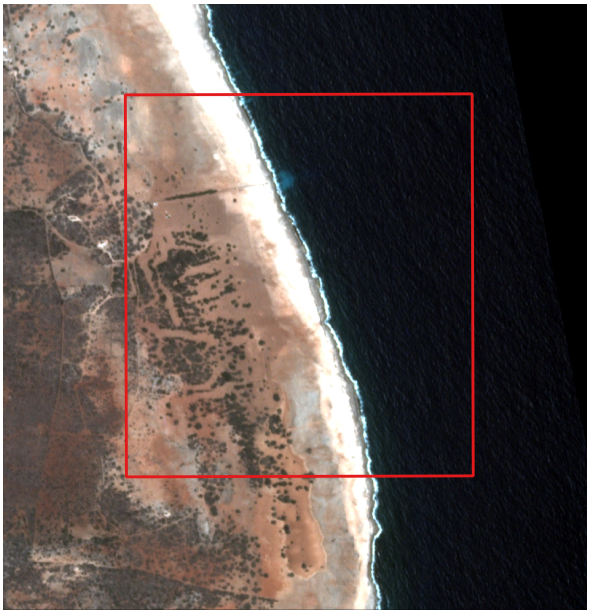


Figure 3.11: Bonaire Section 3, a more exposed and largely undeveloped coastal section on the eastern side of the island.

Bonaire Section 2

Bonaire Section 2 is located in the Hato area on the western leeward coast. The section contains residential and resort development together with some vegetation, while the shoreline is mainly formed by a low rocky limestone edge rather than a broad sandy beach. Its generally west-facing orientation places it in the lee of the prevailing easterly trade winds. Under normal conditions, this results in substantially lower wave exposure than on the eastern side of the island, although extreme storm events can still affect the leeward coast. Engel et al. (2012) notes that the western coast is normally calmer but can experience significant morphological impacts during unusual tropical-cyclone events.

Bonaire Section 3

Bonaire Section 3 is located on the eastern windward side of the island and represents a largely undeveloped coastal environment. Vegetation is present within the section, while building development is very limited or absent. Its east-facing position means that the coastline is more directly exposed to the prevailing easterly trade-wind and wave regime than Sections 1 and 2. Engel et al. (2012) specifically describes Bonaire's eastern shore as being continuously exposed to high wave energy, making Section 3 the most exposed of the three selected Bonaire sections.

Table 3.1: Overview of coastal characteristics across the six study sections in Aruba and Bonaire.

Section	Coastal setting	General orientation	Development	Vegetation	Relative exposure
Aruba 1	Sandy beach coast	West-facing	High; hotel and tourism development	Limited to moderate	Sheltered / leeward
Aruba 2	Mangrove-influenced coast	West to southwest-facing	Residential development	Substantial mangrove vegetation	Sheltered / leeward
Aruba 3	Rocky exposed coast	East-facing	Very limited or absent	Present	Exposed / windward
Bonaire 1	Rocky limestone coast	West to southwest-facing	Residential development	Some vegetation	Sheltered / leeward
Bonaire 2	Rocky limestone coast	West-facing	Residential and resort development	Some vegetation	Sheltered / leeward
Bonaire 3	Rocky exposed coast	East-facing	Very limited or absent	Present	Exposed / windward

Table 3.1 summarises the main contrasts represented by the six study sections. These characteristics are used as contextual descriptors in the later comparison of shoreline, building, and vegetation change.

3.5. Satellite and spatial data

Several remote-sensing and geospatial datasets with different spatial and temporal characteristics were used for Aruba and Bonaire. The availability and temporal coverage of these datasets differed between the two islands. As a result, the study combined several data sources rather than relying on a single uniform dataset for all analyses.

The main source of multi-temporal optical satellite imagery for both Aruba and Bonaire was PlanetScope. PlanetScope imagery was available for several years, with at least one suitable image acquired for most years included in the analysis. For the shoreline analysis, the image selection aimed to include two observations per year, one from the summer period (October–March) and one from the winter period (April–September), depending on image availability and quality. The imagery has an approximate spatial resolution of 3 m and provided the most consistent temporal coverage of the optical datasets used in this study. The relatively frequent temporal coverage of PlanetScope made it the main dataset for the multi-temporal analysis of shoreline position and remotely detected vegetation. The multispectral imagery contains blue, green, red, and near-infrared bands, allowing both water and vegetation indices to be derived from the same imagery.

For Bonaire, additional very-high-resolution optical imagery was available through Dutch geospatial data sources. Images were obtained through the Netherlands Space Agency (NLSA) at an approximate spatial resolution of 30 cm. However, the temporal coverage of this imagery was limited, with only a small number of suitable acquisitions available. The imagery was therefore used primarily as a high-resolution reference rather than as the main input for temporal change analysis.

For Aruba, high-resolution aerial imagery from 2018 was obtained from the Dienst Landmeetkunde en Vastgoedregistratie (DLV). The imagery had a spatial resolution of approximately 5 cm and provided considerably greater spatial detail than the satellite imagery used for the multi-temporal analysis. However, only one acquisition was available, meaning that it could not be used for temporal change detection. Instead, the aerial imagery was used as a high-resolution reference for examining coastal features that could not be distinguished clearly in the lower-resolution satellite imagery.

Pléiades Neo very-high-resolution satellite imagery was also made available for educational use under specific conditions. Although this imagery could have provided additional spatial detail, the available acquisitions did not offer suitable temporal coverage for the 2016–2023 comparison used in this study. Furthermore, the imagery covered coastal areas selected during an earlier stage of the research, which did not fully correspond to the final study sections. For these reasons, the Pléiades Neo imagery was not included in the analysis.

Building development was analysed using the Google Open Buildings Temporal dataset, accessed through Google Earth Engine. The dataset provides annual modelled estimates of building presence and associated building characteristics. For this study, the building-presence layer was used as the primary input for identifying detected building area between 2016 and 2023. The building-related raster data have an effective spatial resolution of approximately 4 m. Because the dataset consists of modelled detections rather than cadastral building records, the resulting building areas are interpreted as detected building development rather than confirmed construction or demolition.

Overall, the available datasets involved a trade-off between spatial resolution and temporal coverage. PlanetScope provided the most consistent multi-year imagery for both islands but at a coarser spatial resolution than the available reference imagery. In contrast, the very-high-resolution aerial and satellite datasets provided considerably greater spatial detail but were available for only one or a limited number of dates. The primary datasets were therefore selected according to their suitability for repeated observations through time, while the higher-resolution imagery was used mainly to support interpretation and reference checks.

Table 3.2: Overview of datasets used for Aruba and Bonaire

Dataset	Aruba	Bonaire	Spatial resolution	Temporal availability	Main use
PlanetScope imagery	✓	✓	~3 m	Multiple years	Shoreline and vegetation change
NSLA imagery	×	✓	~30 cm	Very limited	High-resolution reference
DLV aerial imagery	✓	×	~5 cm	2018 only	High-resolution reference
Google Open Buildings Temporal	✓	✓	4 m effective	Annual, 2016–2023	Built-up development

3.6. Initial data-quality assessment

The datasets used in this study differ in spatial resolution, temporal availability, and level of spatial detail. These differences were considered before the analyses were carried out because they influence which coastal features can be distinguished and how confidently changes between dates can be interpreted.

PlanetScope imagery has an approximate spatial resolution of 3 m. At this resolution, narrow beaches, irregular rocky shorelines, small vegetation patches, foam, and other fine coastal features may occupy only one or a few pixels. Pixels near the land–water boundary may therefore contain mixed spectral information from water, sand, rock, vegetation, or white water. This is particularly relevant for shoreline extraction, where small apparent displacements may approach the spatial scale of the source imagery.

Image quality also varied between acquisition dates. Differences in cloud cover, haze, water conditions, sun illumination, wave activity, and image contrast affected the visibility of the coastline and vegetation. Images with substantial cloud contamination or insufficient coastal visibility were excluded where possible, while the remaining variability was taken into account during image selection and interpretation.

Temporal availability was not uniform across all datasets. PlanetScope provided the most consistent

multi-year coverage and was therefore used for the main shoreline and vegetation analyses. However, suitable cloud-free imagery was not available for every desired date or season. This was especially relevant for the island-wide vegetation analysis of Bonaire, for which the comparison begins in 2019 rather than 2016 because suitable complete-island imagery was not available for the earlier period.

The high-resolution reference imagery available for Aruba and Bonaire provided substantially greater spatial detail than PlanetScope but was available for only one or a limited number of dates. These datasets were therefore useful for inspecting coastal features and supporting interpretation, but they could not provide an equivalent multi-temporal record.

The Google Open Buildings Temporal dataset introduces a different type of uncertainty. It represents modelled estimates of building presence rather than cadastral observations. Differences between years may therefore reflect actual building development, but they may also result from changes in source imagery, model confidence, or detection geometry. For this reason, the building results are interpreted as changes in detected building area rather than confirmed construction or demolition.

These initial data-quality considerations informed the methodological choices described in Chapter 4. More detailed validation and uncertainty assessment are presented alongside the individual shoreline, building, and vegetation analyses.

4

Methodology

This study used a combination of remote sensing, image classification, and geospatial analysis to investigate shoreline change, building development, and vegetation change on Aruba and Bonaire. The overall methodological framework was developed specifically for this study rather than adopted from an existing methodology. It combines established remote-sensing and geospatial techniques within a workflow designed to address the research objectives. The methodology was designed to analyse these indicators at two spatial scales. First, island-wide analyses were used to identify broader patterns in building and vegetation change. Second, three predefined coastal sections on each island were analysed in greater detail to compare shoreline displacement with local changes in buildings and vegetation. Figure 4.1 provides an overview of the methodological framework and summarises the three main analytical components of the study: shoreline change, building development, and vegetation change.

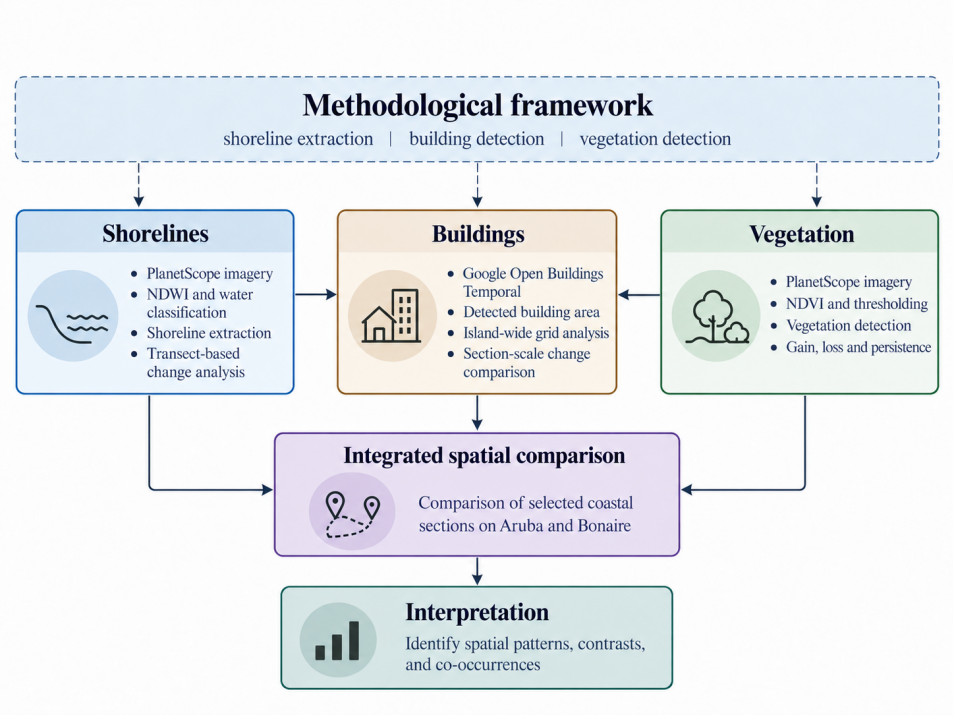


Figure 4.1: Overview of the methodological framework used in this study. Shoreline change, detected building development, and remotely detected vegetation change were analysed separately using remote-sensing and geospatial data, and were subsequently compared within the selected coastal study sections on Aruba and Bonaire.

PlanetScope imagery formed the main input for the shoreline and vegetation analyses because it

provided repeated observations at approximately 3 m spatial resolution. Building development was analysed using polygon data derived from the Google Open Buildings Temporal dataset. The main temporal comparison covered the period from 2016 to 2023, although the available time span for the island-wide vegetation analysis of Bonaire was shorter because suitable cloud-free imagery covering the complete island was not available before 2019.

The shoreline workflow consisted of shoreline extraction from the Normalized Difference Water Index (NDWI), automated separation of water and non-water pixels, vector shoreline generation, transect-based change analysis, seasonal comparison, and positional validation. Summer and winter observations were processed separately.

The building workflow consisted of two complementary analyses. Island-wide building growth was quantified using a regular 500 m grid, while the coastal-section analysis compared the geometry of buildings detected in 2016 and 2023 and classified areas as new, removed, or unchanged. The building-detection data were additionally evaluated against manually identified reference buildings.

Vegetation was extracted from the PlanetScope imagery using the Normalized Difference Vegetation Index (NDVI). Water pixels were excluded before an image-specific vegetation threshold was calculated using Otsu's method. The classified vegetation masks were cleaned, converted into vector polygons, and used to calculate both island-scale vegetation-area change and section-scale vegetation gain, loss, and stability.

The outputs of the shoreline, building, and vegetation analyses were finally combined within the same coastal study sections. This integrated analysis was used to examine where different types of environmental and anthropogenic change occurred spatially in relation to one another. The analysis was designed to identify spatial associations rather than direct causal relationships.

4.1. Shoreline extraction & change analysis

Shoreline position was extracted from PlanetScope multispectral imagery with an approximate spatial resolution of 3 m. The imagery contains blue, green, red, and near-infrared bands. For the shoreline analysis, band 2 was used as the green band and band 4 as the near-infrared band.

Rather than extracting the shoreline from the complete satellite scene at once, the imagery was processed within predefined coastal study sections. Three sections were selected on Aruba and three on Bonaire. A polygon representing each study section was used to crop the corresponding satellite image before further processing. This reduced interference from unrelated land–water boundaries elsewhere in the satellite scene and allowed each section to be processed under its own local coastal conditions.

The shoreline analysis covered the period from 2016 to 2023. Summer and winter observations were processed as separate time series so that longer-term shoreline displacement could be evaluated together with seasonal variability.

4.1.1. NDWI calculation

Water was identified using the Normalized Difference Water Index (NDWI). NDWI enhances the spectral contrast between water and non-water surfaces because open water generally reflects more strongly in the green wavelength while absorbing strongly in the near-infrared wavelength.

For each valid raster pixel, NDWI was calculated as:

$$NDWI = \frac{G - NIR}{G + NIR}, \tag{4.1}$$

where G represents the reflectance value in the green band and NIR represents the corresponding reflectance value in the near-infrared band.

For the PlanetScope imagery used in this study, band 2 was assigned as the green band and band 4 as the near-infrared band. Pixels for which the denominator was zero or for which no valid data were available were excluded from the threshold calculation.

4.1.2. Automated water classification

The continuous NDWI raster was converted into a binary water mask using an image-specific threshold. Rather than applying one fixed NDWI value to all images, Otsu's thresholding method was used independently for each image. This allowed the water threshold to adapt to differences in image-specific radiometric and environmental conditions. Otsu's method determines a threshold from the distribution of image values by separating them into two classes while minimising within-class variance (Xu et al., 2011). Pixels with NDWI values above the calculated threshold were initially classified as water, while pixels below the threshold were classified as non-water.

An additional correction was applied to improve the classification of deep water. In some images, both green and near-infrared reflectance over deeper water were low, which could result in unstable NDWI values. This could cause the extracted boundary to follow the transition between shallow and deeper water rather than the actual land–water boundary. To reduce this effect, a second Otsu threshold was calculated from the near-infrared band. Pixels with sufficiently low near-infrared reflectance were also classified as water.

The resulting binary water mask was cleaned using morphological opening and closing. Two iterations of each operation were applied. This level of filtering was selected to remove small isolated classification artefacts and fill minor gaps without excessively altering the position of the main land–water boundary. Morphological opening removed small isolated groups of incorrectly classified pixels, while morphological closing filled small gaps within larger connected regions.

4.1.3. Main water body selection and shoreline vector extraction

Following the spectral classification, connected-component analysis was used to identify the principal water and land regions within each coastal section. Small isolated water bodies and disconnected classification artefacts were excluded by retaining the main connected regions.

The boundary between the resulting land and water classes was then converted to a vector line. Contours located directly adjacent to no-data regions or image boundaries were removed because these were considered raster-edge artefacts rather than real shoreline features.

Where several shoreline fragments remained after the filtering process, the longest continuous shoreline component was retained, as this was assumed to represent the principal coastal boundary within the study section. The final shoreline was saved as a vector GeoJSON feature together with information on the corresponding year, season, image, and classification threshold. The resulting GeoJSON shorelines were subsequently used for visualisation and change analysis in QGIS and Python.

The shoreline extracted using this procedure represents an instantaneous land–water boundary at the time of satellite acquisition. It should therefore not be interpreted as a fixed geomorphological coastline. Consequently, differences between extracted shoreline positions may reflect both morphological shoreline change and short-term effects such as water level, wave run-up, foam, and image conditions. These effects are considered during the validation and interpretation of the results.

4.1.4. Transect-based shoreline-change analysis

Shoreline displacement was quantified using a transect-based analysis implemented in Python. Summer and winter shoreline datasets were analysed separately. For each coastal section and season, the oldest available shoreline was used as the baseline. Where the shoreline consisted of multiple connected components, the longest continuous component was selected. Using a common baseline ensured that shoreline positions from different years were measured at consistent locations within each section.

Before transects were constructed, the baseline was smoothed using a moving-average window of 300 m. The purpose of this smoothing was to follow the general coastal orientation rather than individual pixel-scale steps, small protrusions, or sharp irregularities in the extracted shoreline. A 300 m window provided sufficient smoothing to generate stable transect orientations while retaining the larger-scale curvature of the coastline.

Transects were generated at intervals of 50 m along the smoothed baseline. This spacing provided repeated measurements along each coastal section without producing an unnecessarily dense set of highly overlapping observations. Each transect extended 200 m to either side of the baseline, providing

sufficient length to intersect the shoreline positions observed during the study period on both the landward and seaward sides of the reference position.

A representative point near the centre of each island was used only to determine the sign and seaward direction of each transect. The side pointing away from the island centre was defined as seaward, while the opposite direction was defined as landward.

For each transect, the position of every available yearly shoreline was measured relative to the baseline. In locations where a transect intersected the shoreline more than once, for example around small bays, coastal hooks, or irregular shoreline geometry, the outermost seaward intersection was selected. This approach reduced the possibility that the analysis would switch between different shoreline segments from one year to another. Figure 4.2 illustrates the transect-based measurement for an example comparison between the summer 2022 and summer 2023 shoreline positions. The displacement value recorded at each transect represents the difference in shoreline position along that transect.

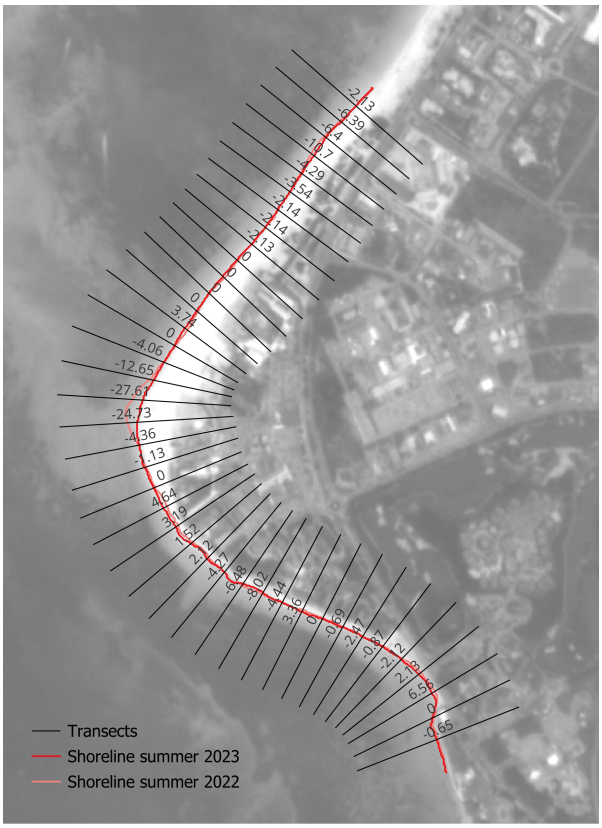


Figure 4.2: Example of the transect-based shoreline-change analysis between the summer 2022 and summer 2023 shoreline positions. Negative values represent landward displacement, while positive values represent seaward displacement.

Shoreline displacement, ΔS between two observations was calculated as:

$$\Delta S = P_{t_2} - P_{t_1}, \tag{4.2}$$

where P_{t_1} and P_{t_2} represent shoreline position along the transect for the earlier and later observation, respectively.

A positive value indicates that the later shoreline was positioned farther seaward, whereas a negative value indicates that the later shoreline was located farther landward.

Net shoreline displacement between the first and final year was calculated as:

$$\Delta S_{\text{net}} = P_{2023} - P_{2016}. \tag{4.3}$$

Where both observations were available, this represented the detected net shoreline displacement between 2016 and 2023.

The analysis also calculated shoreline displacement between consecutive available observations. For each comparison period, summary statistics were calculated to describe the magnitude and direction of shoreline change across the transects. These included mean and median shoreline displacement, together with the maximum landward and seaward displacement.

The shoreline-change graphs presented in Chapter 5 show the individual changes between successive observations, while the thicker black line represents the net displacement between the first and final shoreline positions.

4.1.5. Seasonal shoreline comparison

Summer and winter shorelines from the same year were additionally compared where both observations were available. The same transect geometry was used for both seasonal datasets so that shoreline positions were measured at equivalent locations along each coastal section.

Seasonal displacement was defined as:

$$\Delta S_{\text{seasonal}} = P_{\text{summer}} - P_{\text{winter}}. \tag{4.4}$$

A positive value therefore indicates that the summer shoreline was located farther seaward than the winter shoreline, while a negative value indicates that the summer shoreline was positioned farther landward. The seasonal comparison was used to assess the magnitude and spatial pattern of within-year shoreline variability and to provide context for interpreting the longer-term 2016–2023 displacement.

4.1.6. Positional accuracy assessment of the extracted shoreline

The automatically extracted shorelines were evaluated using manually interpreted shoreline reference points. The reference points were digitised directly from the same PlanetScope TIFF imagery used for the automated NDWI-based shoreline extraction. For Aruba, the reference points were created from the summer 2023 image, while for Bonaire the winter 2023 image was used. Points were placed manually along the visually interpreted land–water boundary within each of the three coastal sections on both islands. For Aruba, the manual reference dataset contained 99 points in Section 1, 105 in Section 2, and 106 in Section 3. For Bonaire, 126 points were used in Section 1, 80 in Section 2, and 85 in Section 3, resulting in 601 reference points in total.

Because the manual reference points were derived from the same source imagery as the automated shoreline, this procedure does not constitute an independent validation against a separate dataset. Instead, it provides a measure of how closely the automated extraction corresponds to a manually interpreted shoreline boundary within the PlanetScope imagery.

For each reference point, the shortest distance to the automatically extracted shoreline was calculated in a projected coordinate reference system. The positional error for reference point i was defined as:

$$e_i = d(P_i, L), \tag{4.5}$$

where P_i represents reference point i and L represents the automatically extracted shoreline.

Several descriptive statistics were calculated from the resulting positional errors. These included the mean error, median error, standard deviation, minimum error, maximum error, and the 90th and 95th percentile errors.

The root mean square error (RMSE) was calculated as:

$$RMSE = \sqrt{\frac{1}{n}\sum_{i=1}^{n} e_i^2}, \tag{4.6}$$

where e_i represents the positional error of reference point i and n represents the number of reference points.

In addition to these descriptive statistics, accuracy was evaluated using a set of distance thresholds related to the approximate 3 m spatial resolution of the PlanetScope imagery. The selected thresholds were 1.5, 3, 6, 9, and 15 m, corresponding approximately to 0.5, 1, 2, 3, and 5 image pixels.

For each distance threshold, the percentage of manually interpreted reference points located within the specified distance of the automatically extracted shoreline was calculated.

The spatial distribution of positional error was also visualised by plotting the reference points together with the extracted shoreline and assigning each point a colour based on its calculated distance error. The resulting error statistics were used as a positional-uncertainty reference when interpreting the magnitude of the detected shoreline displacement.

4.2. Building detection and change analysis

4.2.1. Google Open Buildings Temporal dataset

Detected building development was analysed using the Google Open Buildings Temporal dataset accessed through Google Earth Engine (see Chapter 2.5.5). The dataset provides repeated modelled estimates of building presence through time and was used to derive yearly building polygons for Aruba and Bonaire.

A Google Earth Engine script was created to process the temporal Open Buildings imagery for each island. The analysis started from 2016, which corresponded to the beginning of the study period. For each available year, the `building_presence` band was extracted and a confidence threshold of 0.5 was applied. Pixels with a building-presence value greater than 0.5 were therefore classified as detected building area. The 0.5 threshold was used as the decision boundary between lower- and higher-confidence building-presence estimates and was applied consistently across all years and both islands.

The resulting binary building mask was converted from raster data to polygon features at a spatial scale of 4 m using the `reduceToVectors` function in Google Earth Engine. Each exported polygon additionally contained its observation year and calculated area in square metres.

Separate areas of interest were defined for Aruba and Bonaire using island-scale bounding boxes. The available years within the Open Buildings Temporal ImageCollection were identified automatically, after which yearly building datasets were exported to Google Drive in GeoJSON format. The complete Google Earth Engine script used for this extraction and export procedure is provided in Appendix C.

For the building-change analysis presented in this thesis, the final temporal change analysis used the exported building datasets for 2016 and 2023 for both Aruba and Bonaire. These datasets were treated as modelled building detections rather than cadastral building records. Consequently, differences between the 2016 and 2023 datasets may represent actual construction, removal, or modification of buildings, but may also reflect differences in model detection or extracted polygon geometry between years.

4.2.2. Spatial preparation

The building polygon datasets were processed using Python and GeoPandas. All geometries were transformed to `EPSG:32619` (UTM Zone 19N) so that distance and area calculations could be expressed in metres.

Invalid geometries were repaired before analysis, and only polygon and multipolygon features were retained.

Two complementary spatial analyses were conducted. First, a regular grid covering each complete island was used to quantify broad spatial patterns in detected building-area change. Second, building polygons within the predefined coastal study sections were compared directly to classify changes in detected building geometry. The island-wide and section-scale analyses were therefore based on the same underlying building detections but addressed different spatial scales of change.

4.2.3. Island-wide building-area change

Island-wide building change was quantified using a square grid with a cell size of 500 m by 500 m. The grid was aligned to the projected coordinate system and clipped to the outline of each island. For each grid cell, the detected building polygons were intersected with the grid geometry. The total building area was calculated separately for 2016 and 2023.

Absolute building-area change was calculated as:

$$\Delta B = B_{\text{end}} - B_{\text{start}}, \tag{4.7}$$

where B_{start} represents the detected building area in 2016 and B_{end} represents the detected building area in 2023.

Positive values indicate an increase in detected building area between 2016 and 2023, while negative values indicate a decrease. The resulting grid values were used to map the spatial distribution of detected building-area change across each island. The same absolute area calculation was also applied to the predefined coastal study sections so that section-scale building change could be compared with shoreline and vegetation change.

4.2.4. Building polygons within the coastal sections

For the detailed coastal analysis, the 2016 and 2023 building datasets were clipped to each of the predefined coastal sections.

All detected building polygons occurring within the same section and year were combined before the two years were compared. This generated one 2016 building geometry and one 2023 building geometry for each coastal section.

The resulting geometries formed the input for the section-scale building-change classification, in which areas of newly detected, no longer detected, and persistent building geometry were identified.

4.2.5. Building-change classification

Building change between 2016 and 2023 was assessed by spatially comparing the Open Buildings polygon datasets from the two years within each coastal study section.

Because the Open Buildings data have an effective spatial resolution of approximately 4 m, small differences in building position or outline between years were not automatically interpreted as real change. A positional tolerance of 4 m was therefore applied around the 2016 and 2023 building geometries. This tolerance corresponds approximately to the effective spatial resolution of the Open Buildings data and was used to reduce false change caused by small positional differences between yearly model outputs. Differences falling within this tolerance were treated as variation in modelled building geometry rather than actual building change.

To further reduce small geometric artefacts, change polygons narrower than 4 m were removed. Features narrower than approximately one raster cell were considered more likely to represent boundary shifts in modelled geometry than meaningful building-area change. Remaining change polygons smaller than 50 m^2 were also excluded from the final dataset. This minimum-area filter was used to suppress very small isolated differences that were more likely to represent model noise or minor geometric inconsistencies than substantial building change.

The comparison produced three building-change classes:

- **New**: building area present in 2023 but not within the tolerance distance of the 2016 building geometry. This class also includes extensions of buildings that were already present in 2016.
- **Removed**: building area present in 2016 but not within the tolerance distance of the 2023 building geometry. This class also includes portions of buildings that became smaller between the two observations.
- **Unchanged**: building area considered present in both years after accounting for the positional tolerance.

The classes were derived using geometric difference operations. Areas appearing outside the buffered 2016 building geometry were classified as new. Areas disappearing outside the buffered 2023 building geometry were classified as removed. The remaining 2023 building geometry was classified as unchanged.

For each coastal section, the area of every resulting change polygon was calculated in square metres. The classified polygons were exported as a GeoJSON layer for spatial visualisation, while the summed area associated with the new, removed, and unchanged classes was exported as a section-level summary table.

Because the input data represent modelled building detections rather than cadastral observations, the classes *new* and *removed* describe differences in modelled building geometry between 2016 and 2023. They should not be interpreted automatically as confirmed construction or demolition.

4.2.6. Validation of building detection

Building-detection performance was evaluated for both Aruba and Bonaire using manually identified reference buildings derived from high-resolution reference imagery and the corresponding Google Open Buildings polygons.

For Aruba, reference buildings were manually identified from the high-resolution 2018 DLV aerial imagery, and these were compared with the 2018 Open Buildings detections. For Bonaire, reference buildings were identified from high-resolution optical imagery obtained from the Netherlands Space Agency (NLSA), acquired in winter 2023, and compared with the 2023 Open Buildings detections.

One manually interpreted point was placed on each visually identified building within the selected validation areas, with each point representing one reference building. A reference building was classified as detected when the corresponding point fell inside an Open Buildings polygon or within a maximum positional tolerance of 3 m from a polygon. The tolerance accounted for small positional differences between the manually interpreted reference data and the modelled building polygons.

The validation used the following classes:

- **True positive (TP)**: a reference building matched to an Open Buildings detection.
- **False negative (FN)**: a manually identified reference building for which no Open Buildings detection was found.
- **False positive (FP)**: an Open Buildings polygon that did not correspond to a manually identified reference building.

A true-negative count was not calculated because the non-building background does not represent a finite collection of countable objects.

Recall was calculated as:

$$Recall = \frac{TP}{TP + FN}, \tag{4.8}$$

while precision was calculated as:

$$Precision = \frac{TP}{TP + FP}. \tag{4.9}$$

The F1-score was used to summarise precision and recall in a single metric:

$$F1 = 2\frac{Precision \times Recall}{Precision + Recall}. \tag{4.10}$$

The assessment also identified cases in which several manually interpreted buildings corresponded to a single Open Buildings polygon. This can occur when neighbouring structures are represented by the model as one connected building object.

The accuracy assessment was conducted separately for Aruba and Bonaire because different high-resolution reference datasets were available for the two islands. The resulting precision, recall, and F1-scores were therefore reported separately for each island.

4.3. Vegetation detection and change analysis

4.3.1. NDVI calculation

Remotely detected vegetation was identified from PlanetScope imagery using the Normalized Difference Vegetation Index (NDVI), as introduced in Chapter 2.5.4 and defined in Equation 2.1. For the PlanetScope imagery used in this study, band 3 was assigned as the red band and band 4 as the near-infrared band.

4.3.2. Water exclusion and automated vegetation detection

Before vegetation detection, water pixels were identified using NDWI, as defined in Equation 4.1. Pixels with NDWI values greater than zero were excluded from the vegetation-threshold calculation. The NDVI distribution of the remaining valid land pixels was then used to calculate an image-specific threshold using Otsu's method.

Vegetation classification was expressed as:

$$V(x) = \begin{cases} 1, & NDVI(x) > T_{\text{NDVI}}, \\ 0, & NDVI(x) \leq T_{\text{NDVI}}, \end{cases} \tag{4.11}$$

where T_{NDVI} represents the Otsu threshold calculated independently for each image.

A fixed NDVI threshold was therefore not applied across all observations. The use of an image-specific threshold allowed the classification to respond to differences in image-specific radiometric conditions and spectral vegetation response. One iteration was used to remove small isolated classification artefacts and fill minor gaps without substantially altering larger vegetation patches. Connected vegetation regions smaller than 20 pixels were removed from the final detection to reduce isolated classification artefacts and mixed-pixel effects.

4.3.3. Raster-to-vector conversion

After classification and raster cleaning, the vegetation mask was converted into vector polygons. Only pixels classified as vegetation were included in the conversion.

Adjacent vegetation pixels were grouped into connected polygon features while retaining the spatial reference of the original PlanetScope imagery. The resulting geometries were transformed to a projected coordinate reference system so that vegetation area could be calculated in square metres.

The resulting vegetation polygon datasets were used as the input for both the island-wide vegetation-change analysis and the detailed comparison within the predefined coastal study sections.

4.3.4. Island-wide vegetation-area change

Island-wide vegetation change was evaluated using the same 500 m by 500 m grid structure used for the island-wide building analysis. The grid was clipped to the island boundary so that area and cover calculations were based only on the land portion of each cell.

Vegetation polygons from the start and end observations were intersected with every grid cell, and total detected vegetation area was calculated for each date.

Absolute vegetation-area change was calculated as:

$$\Delta V = V_{\text{end}} - V_{\text{start}}, \tag{4.12}$$

where V_{start} and V_{end} represent detected vegetation area at the beginning and end of the comparison period, respectively.

Positive values indicate an increase in detected vegetation area, while negative values indicate a decrease. The resulting grid values were used to map the spatial distribution of vegetation change across each island.

For Aruba, suitable full-island imagery was available for 2016 and 2023, allowing the island-wide analysis to cover the complete study period. For Bonaire, no sufficiently clear full-island PlanetScope image was available before 2019. The island-wide Bonaire vegetation comparison was therefore conducted between 2019 and 2023. This difference in temporal coverage reflects image availability rather than a difference in the vegetation-processing method.

4.3.5. Section-scale vegetation change

The smaller spatial extent of the coastal study sections allowed suitable imagery to be obtained for an earlier period than was possible for the complete island of Bonaire. The section-scale vegetation analysis was therefore conducted from 2016 to 2023 for both Aruba and Bonaire.

For each coastal section, the vegetation geometries from the start and end dates were clipped to the section boundary and combined into year-specific geometries.

Three vegetation-change classes were then calculated.

Stable vegetation was defined as the spatial intersection between vegetation present in both observations:

$$V_{\text{stable}} = V_{\text{start}} \cap V_{\text{end}}. \tag{4.13}$$

Vegetation gain was defined as:

$$V_{\text{gain}} = V_{\text{end}} - V_{\text{start}}, \tag{4.14}$$

and vegetation loss was calculated as:

$$V_{\text{loss}} = V_{\text{start}} - V_{\text{end}}. \tag{4.15}$$

Small gain and loss polygons below 20 m² were removed to reduce the influence of very small overlay artefacts and minor geometric differences between the two classified vegetation layers.

For each coastal section, the total areas of vegetation gain, vegetation loss, and stable vegetation were calculated in square metres. Net change in detected vegetation area was additionally calculated from the difference between the start- and end-year vegetation areas.

No independent reference dataset was available for validation of the vegetation classification. Consequently, the results are interpreted as changes in remotely detected vegetation rather than confirmed ecological vegetation gain or loss.

4.4. Integrated spatial analysis

The final stage of the methodology combined the shoreline, building, and vegetation outputs within each coastal study section.

The integrated analysis was based on the same spatial boundaries used during the individual analyses so that the different indicators could be examined within a common geographic framework. For each coastal section, the combined map included the shoreline position at the start and end of the comparison period, building areas classified as newly detected, no longer detected, or persistent, and vegetation classified as detected gain, detected loss, or stable vegetation.

The different indicators were overlaid rather than combined into a single numerical index. This allowed the spatial patterns of shoreline displacement, detected building change, and remotely detected vegetation change to be compared directly while retaining the original information represented by each dataset.

Locations where different forms of change occurred close to one another were identified as spatial co-occurrences. For example, landward shoreline displacement occurring near newly detected building area or detected vegetation loss could be highlighted as a location where several indicators changed within the same coastal section. Such spatial co-occurrences were not interpreted as evidence that one observed change caused another.

The resulting spatial patterns were interpreted in relation to the contextual characteristics of each section, including coastal type, exposure setting, development, and vegetation. Exposure was treated as a contextual descriptor based on coastal orientation and published information on prevailing wind and wave conditions rather than as a separately quantified index.

The integrated analysis therefore focused on identifying spatial patterns, contrasts, and co-occurrences between the six coastal study sections and between Aruba and Bonaire. These outputs formed the basis for the comparative interpretation presented in the Chapters 5 and 6.

The scripts developed for the shoreline extraction, building detection, vegetation analysis, and integrated spatial analysis are available in a GitHub repository at https://github.com/jcmwinterdal/Coastal_change_detection_aruba_bonaire.git. The repository contains the codes used to process the remote-sensing and geospatial datasets presented in this study.

5

Results

This chapter presents the results of the remote-sensing and spatial analyses for Aruba and Bonaire. The results are organised into four main components: shoreline detection and change, detected building change, vegetation detection and change, and the combined spatial patterns of these indicators. For the shoreline analysis, positive values indicate seaward displacement of the detected shoreline, whereas negative values indicate landward displacement. Building change represents differences in remotely detected building geometry rather than confirmed construction or demolition. Vegetation change represents differences in remotely detected vegetation between the selected observation dates.

5.1. Shoreline detection & change

The extracted shorelines show considerable spatial and temporal variability within the analysed coastal sections. Although the annual shoreline positions generally follow the same overall coastal geometry, the degree of separation between observations differs substantially both between sections and along individual sections.

The transect-based analysis was used to describe spatial variation in shoreline displacement and the net displacement between the first and final observations.

5.1.1. Aruba

The three selected coastal sections in Aruba show different patterns of shoreline change between 2016 and 2023. While the extracted shorelines generally follow a consistent coastal configuration, the magnitude and spatial distribution of displacement vary between sections. Sections 1 and 2 show relatively limited changes along much of the coastline, with more pronounced deviations concentrated at specific locations. In contrast, Section 3 shows smaller, more distributed fluctuations, without a single dominant area of change. These differences are examined in more detail below, using the extracted summer shoreline positions and corresponding displacement profiles, supported by additional winter results in Appendix A.

Section 1

Figure 5.1 presents the extracted summer shoreline positions for Aruba Section 1 between 2016 and 2023. Overall, the shoreline follows a relatively consistent configuration throughout the study period, with the extracted positions closely overlapping along most of the coastline. However, two locations show more pronounced variation. The first, indicated as Area A, is located around the curved central part of the section, while the second, Area B, is situated towards the end of the coastline. At these locations, the greater separation between the extracted shoreline positions indicates that shoreline displacement is not distributed uniformly along the section, but is concentrated in specific areas. A similar spatial pattern is observed in the winter dataset, with the largest shoreline variations occurring at approximately the same locations. The corresponding winter shoreline positions and displacement profiles are presented in Figures A.1 and A.2 in Appendix A.

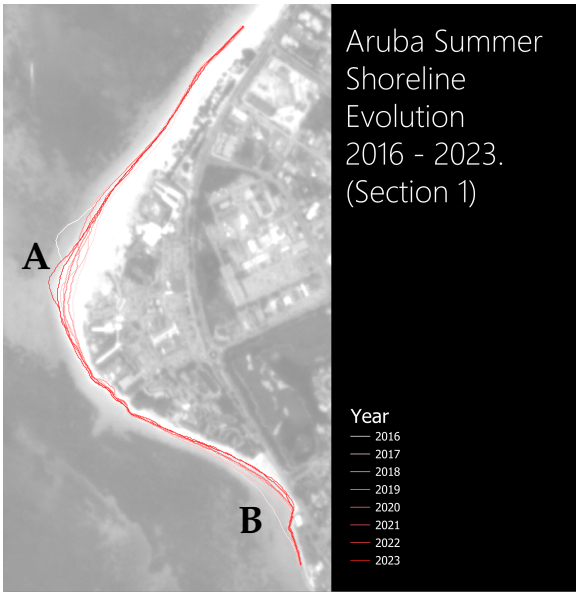


Figure 5.1: Extracted summer shoreline positions for Aruba Section 1 between 2016 and 2023.

The spatial variation becomes more apparent in Figure 5.2, which shows the shoreline displacement between consecutive summer observations, together with the net displacement between 2016 and 2023. Along much of the approximately 2 km coastline, the annual changes remain relatively limited, with displacement values fluctuating around zero. However, substantially larger deviations occur at certain locations, particularly during the 2016–2017 period. Around 750–800 m along the coastline, a pronounced landward displacement of approximately 100 m is observed, corresponding to Area A. In contrast, around 1850–1900 m, corresponding to Area B, the shoreline shows a seaward displacement of approximately 50 m. These differences indicate that considerable local shoreline changes can occur even where the overall coastal configuration remains relatively consistent.

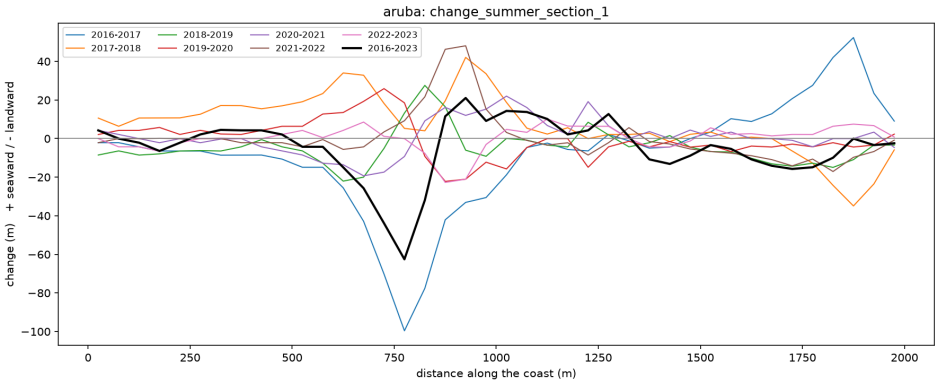


Figure 5.2: Summer shoreline change along Aruba Section 1. Coloured lines represent change between successive available observations and the black line represents net change between 2016 and 2023. Positive values indicate seaward displacement and negative values indicate landward displacement.

The changes between 2016 and 2017 are examined in greater detail in Figures 5.3 and 5.4, which presents close-up comparisons of Areas A and B. In Area A, the 2017 shoreline is positioned considerably further landward than in 2016, particularly around the curved section where the beach previously extended further into the water. This indicates a substantial reduction in the detected beach extent between the two observations. Area B shows the opposite pattern, with the 2017 shoreline extending further seaward than the 2016 position. Here, the change is most pronounced along the curved part of the beach, where an increase in the detected beach extent is visible. The comparison therefore illustrates

two contrasting forms of local shoreline change within the same coastal section, with apparent beach loss in one location and beach expansion in another.

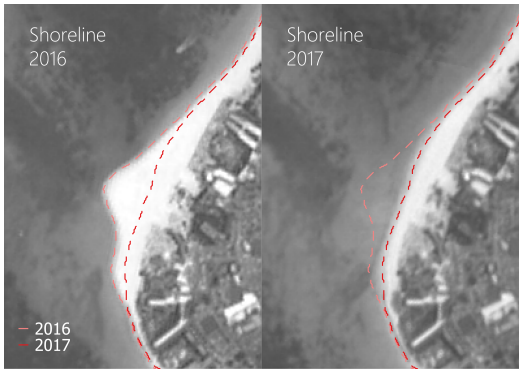


Figure 5.3: Detailed comparison of the extracted summer shoreline positions in 2016 and 2017 at Area A.

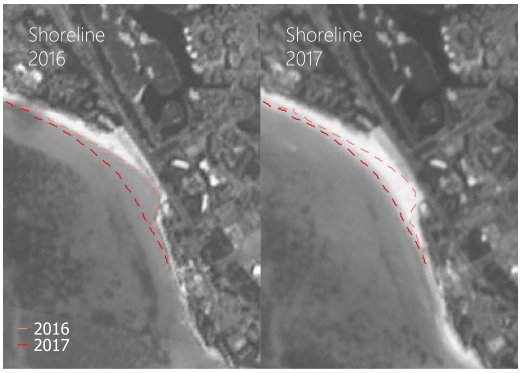


Figure 5.4: Detailed comparison of the extracted summer shoreline positions in 2016 and 2017 at Area B.

Despite these pronounced local variations, the mean net shoreline displacement between 2016 and 2023 was relatively small, at -4.72 m for summer and -8.36 m for winter. Both values indicate an overall landward displacement of the detected shoreline, with a greater negative mean observed in the winter dataset. However, the detailed spatial results show that these section-wide averages do not fully represent the differences occurring along the coastline. Aruba Section 1 is therefore characterised by relatively limited displacement along much of its length, combined with substantially larger localised changes, particularly around Areas A and B.

Section 2

Figure 5.5 presents the extracted summer shoreline positions for Aruba Section 2 between 2016 and 2023. Similar to Section 1, the shorelines remain relatively consistent throughout most of the study period, with the extracted positions closely overlapping along the majority of the coastline. However, a more pronounced variation is visible around the middle of the section, indicated as Area C. At this location, the shoreline forms a curved, protruding feature, where the separation between the extracted shoreline positions is noticeably greater than along the surrounding coast. The winter dataset shows a similar spatial pattern, with the largest variations occurring around the same location. The corresponding winter shoreline map and displacement profile are provided in Figures A.3 and A.4 in Appendix A.

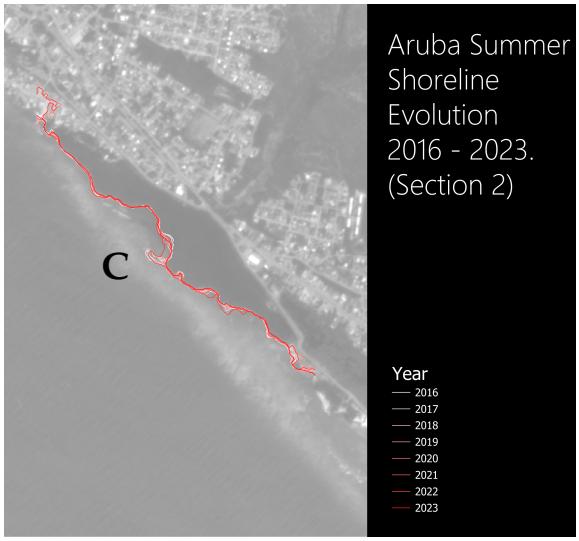


Figure 5.5: Extracted summer shoreline positions for Aruba Section 2 between 2016 and 2023.

The shoreline displacement profile in Figure 5.6 further highlights this localised variation. Along most of the approximately 1.7 km coastline, the annual displacement values remain relatively small, generally fluctuating around zero. However, around 800–850 m, several consecutive-year comparisons show pronounced deviations, with both landward and seaward displacements approaching or exceeding 100 m. In contrast, the net displacement between 2016 and 2023 is strongly negative at this location, reaching approximately -95 m. This indicates that the large changes are concentrated within a relatively short part of the coastline rather than being representative of the entire section.

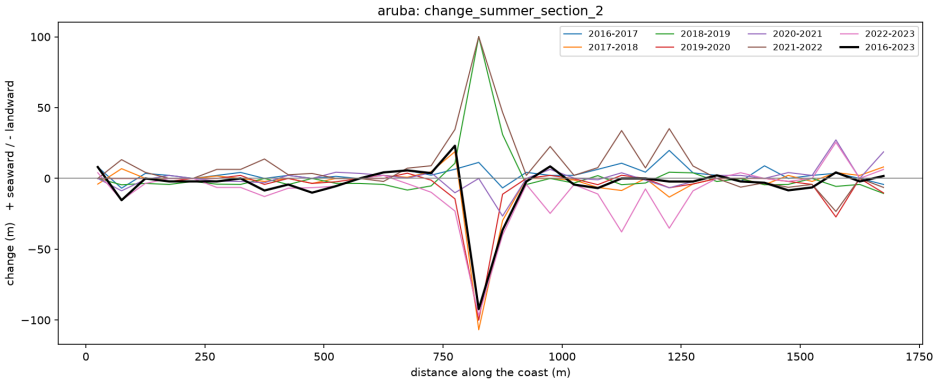


Figure 5.6: Summer shoreline change along Aruba Section 2. Coloured lines represent change between successive available observations and the black line represents net change between 2016 and 2023. Positive values indicate seaward displacement and negative values indicate landward displacement.

To examine this variation more closely, Figure 5.7 compares the extracted shoreline positions for 2018 and 2019 in Area C. The satellite imagery shows a small island-like feature adjacent to the coastline, which is visible in both observations. However, while the feature is included in the extracted shoreline in 2019, it is not detected in the same way in 2018. This difference in shoreline extraction provides an explanation for the pronounced displacement values observed around this location. Rather than necessarily indicating the physical appearance or disappearance of the feature, the large differences may result from changes in how the automated classification identifies and represents the land–water boundary.

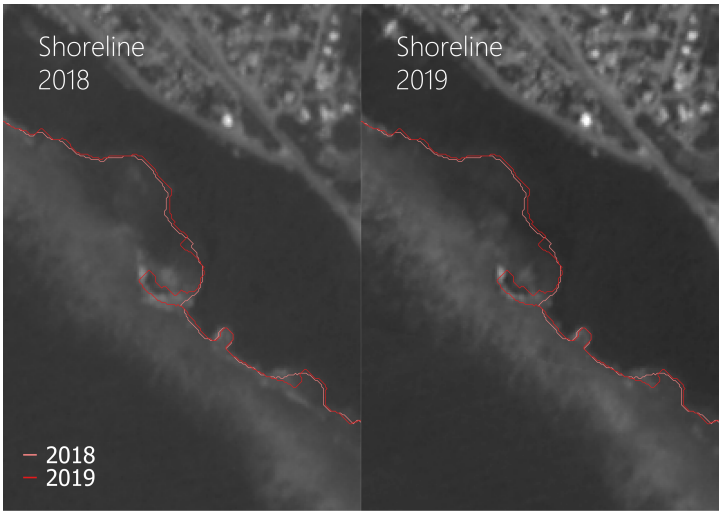


Figure 5.7: Detailed comparison of the extracted summer shoreline positions in 2018 and 2019 at Area C.

Despite these localised variations, the mean net shoreline displacement between 2016 and 2023 was -4.63 m in summer and -1.79 m in winter, indicating a relatively small overall landward displacement in both datasets. The close agreement between shoreline positions along most of the section is

consistent with these relatively small mean values. However, the pronounced deviations around Area C demonstrate how individual coastal features and differences in their detection can strongly influence local shoreline-change measurements.

Section 3

Figure 5.8 presents the extracted summer shoreline positions for Aruba Section 3 between 2016 and 2023. Compared with Sections 1 and 2, the shoreline positions show relatively limited separation throughout the study period, with the extracted shorelines closely following the same overall coastal configuration. Small variations are visible along different parts of the coastline, particularly around bends and protruding features, but no single location shows the pronounced and concentrated changes observed in the previous two sections. A similar pattern is observed in the winter dataset, with the corresponding shoreline map and displacement profile provided in Figures A.5 and A.6 in Appendix A.

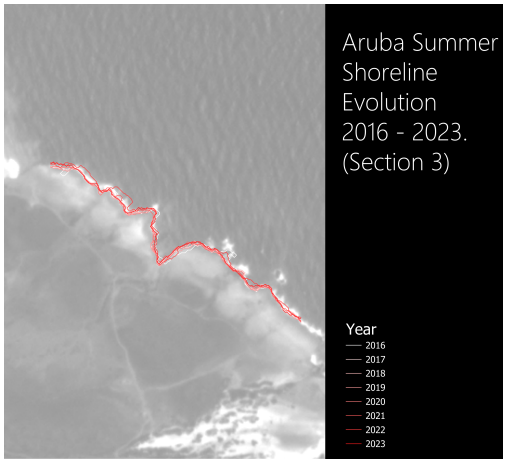


Figure 5.8: Extracted summer shoreline positions for Aruba Section 3 between 2016 and 2023.



Figure 5.9: Example of the rocky coastline characteristic of Aruba Section 3, showing exposed rock formations and steep coastal edges.

The shoreline displacement profile in Figure 5.10 confirms this pattern. Annual changes alternate between positive and negative values along the approximately 900 m coastline, with most displacements remaining within a relatively limited range. Some larger localised fluctuations are visible, particularly around 250–300 m, 400–450 m, and 550–700 m. However, these deviations do not form one consistently dominant zone of landward or seaward displacement. The net shoreline change between 2016 and 2023 also varies along the coastline, with an overall mean displacement of -1.19 m in summer and -12.34 m in winter. Although both seasonal datasets indicate a negative mean displacement, the winter observations show a more pronounced overall landward shift.

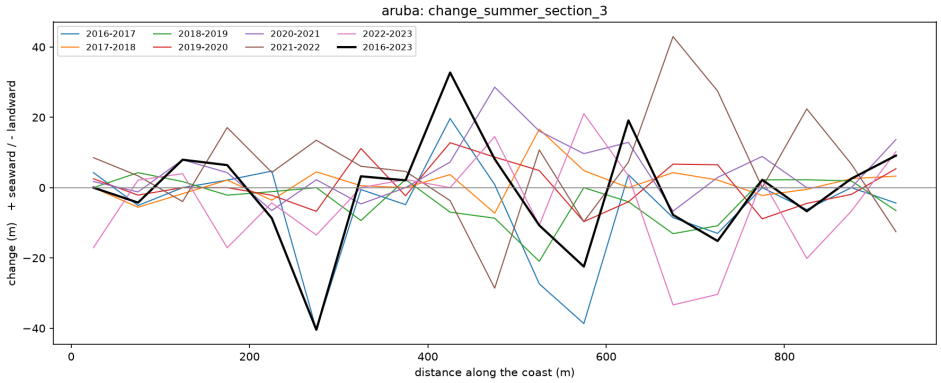


Figure 5.10: Summer shoreline change along Aruba Section 3. Coloured lines represent change between successive available observations and the black line represents net change between 2016 and 2023. Positive values indicate seaward displacement and negative values indicate landward displacement.

The relatively limited variation in shoreline position is consistent with the rocky coastal characteristics of Section 3, as illustrated in Figure 5.9. Unlike the sandy beaches in Section 1 and mangrove covered beach in Section 2, this section is characterised by a rocky coastline with steep coastal edges and exposed rock formations. Such coastlines are generally less susceptible to rapid changes in shoreline geometry through sediment erosion and deposition than unconsolidated sandy beaches.

Overall, Aruba Section 3 shows relatively limited changes in its detected shoreline configuration between 2016 and 2023, with smaller fluctuations distributed along the coast rather than concentrated at a single location. This contrasts with Sections 1 and 2, where much larger localised deviations are observed. The results suggest that the rocky character of Section 3 is associated with a more consistent shoreline geometry.

5.1.2. Bonaire

The three selected coastal sections in Bonaire also show spatial variation in detected shoreline displacement between 2016 and 2023. Overall, the extracted shoreline positions remain relatively consistent along most of the analysed coastlines, although localised deviations occur in Sections 1 and 2. In contrast, Section 3 shows a more uniform shoreline configuration, with smaller variations distributed along the coastline. As observed in Aruba, the largest local deviations do not necessarily correspond to physical shoreline change, but may also reflect differences in shoreline extraction. The following sections present the summer shoreline results in greater detail, while the corresponding winter figures are provided in Appendix A.

Section 1

Figure 5.11 presents the extracted summer shoreline positions for Bonaire Section 1 between 2016 and 2023. Overall, the shoreline positions remain relatively consistent throughout the study period, with the extracted shorelines closely overlapping along most of the approximately 1.4 km coastline. However, a more pronounced deviation is visible towards the end of the section, indicated as Area D. At this location, the shoreline position differs considerably between certain observations, whereas the remaining coastline shows relatively limited variation. A similar spatial pattern is observed in the winter dataset, for which the corresponding shoreline map and displacement profile are provided in Figures A.7 and A.8 in Appendix A.

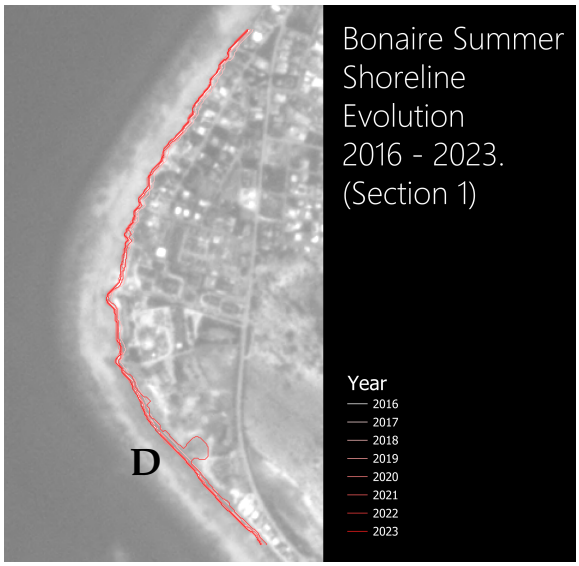


Figure 5.11: Extracted summer shoreline positions for Bonaire Section 1 between 2016 and 2023.

The shoreline displacement profile in Figure 5.12 further illustrates this pattern. Along most of the coastline, the annual displacement values remain relatively small, generally fluctuating within approximately 10 m of zero. However, around 1150–1200 m, a pronounced positive peak is visible, reaching approximately 65 m in both the 2022–2023 comparison and the net displacement between 2016

and 2023. This indicates that the large displacement is concentrated within a very short part of the section rather than representing a general seaward movement of the coastline.

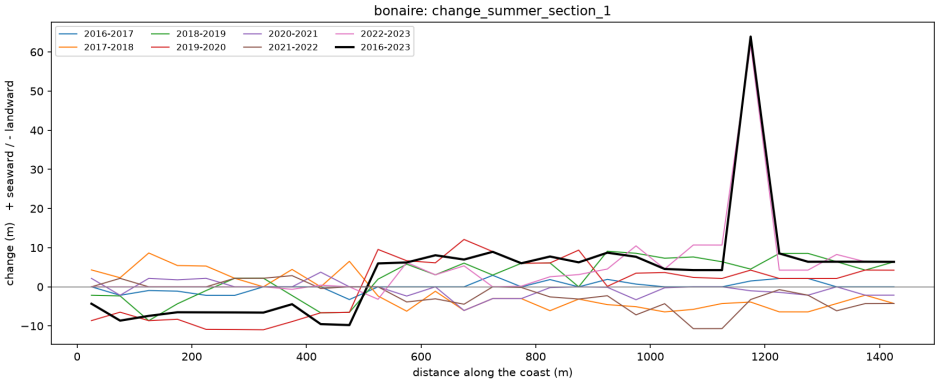


Figure 5.12: Summer shoreline change along Bonaire Section 1. Coloured lines represent change between successive available observations and the black line represents net change between 2016 and 2023. Positive values indicate seaward displacement and negative values indicate landward displacement.

To investigate this deviation, Figure 5.13 presents a detailed comparison of the extracted shoreline positions in Area D for 2022 and 2023. The satellite imagery shows a small coastal basin connected to the sea through a narrow opening. In 2022, the extracted shoreline follows the inner boundary of the basin, whereas in 2023, the detected boundary largely follows the outer coastline without including the basin. Closer inspection of the imagery suggests that the opening to the basin appears slightly narrower or more enclosed in 2023. This difference may have influenced how the automated water classification identified the connection between the basin and the surrounding sea, resulting in the basin being excluded from the extracted shoreline. The pronounced displacement in the profile therefore appears to be associated with a difference in shoreline detection rather than a substantial physical advance of the coastline.

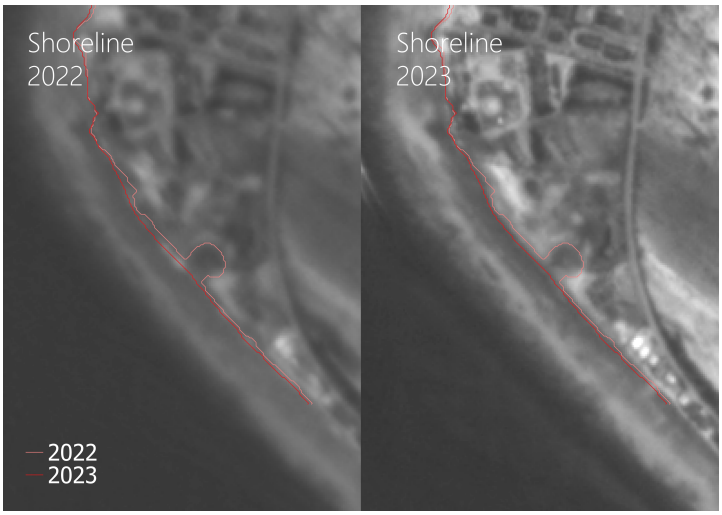


Figure 5.13: Detailed comparison of the extracted summer shoreline positions in 2022 and 2023 at Area D.

The mean net shoreline displacement between 2016 and 2023 was +3.91 m in summer and -4.48 m in winter, indicating a small overall seaward shift in the summer dataset and a landward shift in the winter dataset. Although the seasonal means differ in direction, both datasets show relatively limited shoreline variation along much of the section. The large localised deviation around Area D demonstrates how the detection of individual coastal features can strongly influence the calculated shoreline displacement.

As in Aruba Section 2, this highlights the importance of inspecting local shoreline geometry when interpreting unusually large changes in the displacement profiles.

Section 2

Figure 5.14 presents the extracted summer shoreline positions for Bonaire Section 2 between 2016 and 2023. Overall, the shorelines follow a relatively consistent configuration, with the extracted positions closely overlapping along most of the approximately 1.4 km coastline. However, two locations show substantially greater variation, indicated as Areas E and F. Area E is situated in the first part of the section, while Area F is located around the middle of the coastline. At both locations, individual shoreline positions deviate considerably from the general coastal alignment. The winter dataset shows a broadly similar spatial pattern, with the corresponding shoreline map and displacement profile provided in Figures A.9 and A.10 in Appendix A.

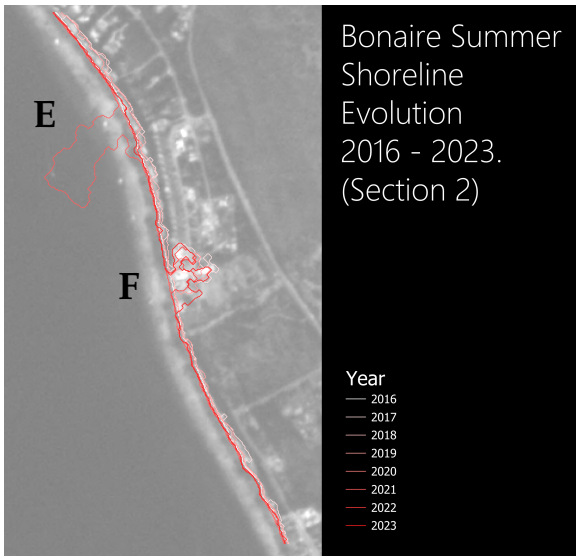


Figure 5.14: Extracted summer shoreline positions for Bonaire Section 2 between 2016 and 2023.

The shoreline displacement profile in Figure 5.15 further highlights these localised deviations. Along most of the section, annual displacement values remain relatively small, generally fluctuating around zero. However, Area E, located around 250–300 m along the coastline, shows particularly large opposing displacement values between 2020–2021 and 2021–2022, reaching approximately +135 m and -140 m, respectively. These fluctuations suggest that the detected shoreline temporarily deviated from its usual position before returning to approximately the previous alignment. Around Area F, at approximately 650–750 m, several annual comparisons show similarly large variations in both directions, with values exceeding 100 m in some years. The net 2016–2023 displacement is also strongly negative at this location, despite the relatively limited changes observed along the remainder of the coastline.

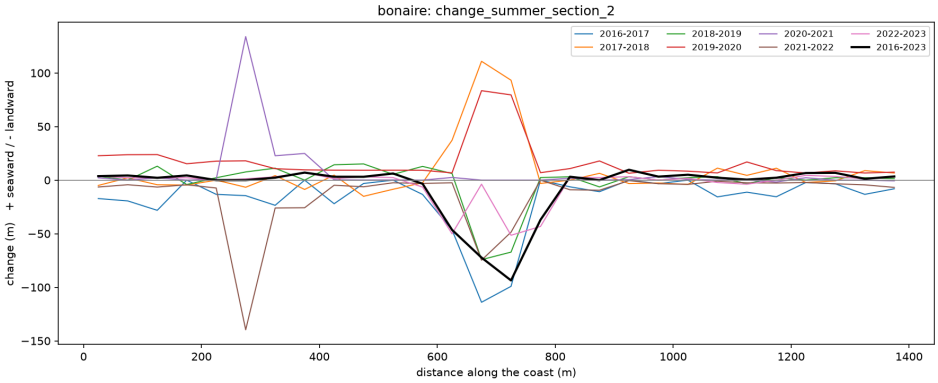


Figure 5.15: Summer shoreline change along Bonaire Section 2. Coloured lines represent change between successive available observations and the black line represents net change between 2016 and 2023. Positive values indicate seaward displacement and negative values indicate landward displacement.

To investigate these deviations, Figures 5.16 and 5.17 present detailed comparisons of Areas E and F. In Area E, the comparison between 2020 and 2021 shows that a bright cloud-like feature is present over the coastal water in the 2021 imagery. The extracted shoreline follows the boundary of this feature rather than the actual land–water boundary, resulting in a substantial apparent seaward displacement. This indicates that the large change recorded at this location is caused by cloud contamination affecting the automated shoreline extraction rather than a physical change in shoreline position.

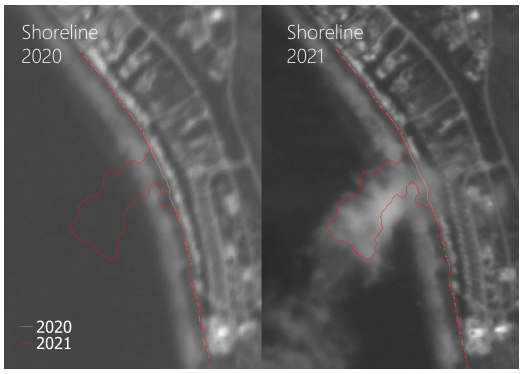


Figure 5.16: Detailed comparison of the extracted summer shoreline positions in Area E for 2020 and 2021. A bright feature over the coastal water in the 2021 imagery affects the extracted boundary, producing an apparent seaward shoreline displacement.

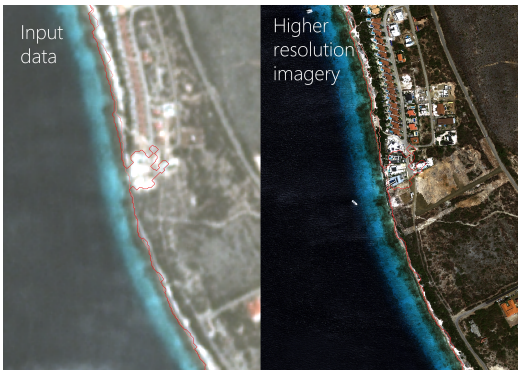


Figure 5.17: Comparison of the 2023 shoreline extraction in Area F using the original PlanetScope input imagery and higher-resolution reference imagery. The detected boundary extends inland around existing buildings rather than following the physical coastline, illustrating a misclassification in the automated shoreline extraction.

Area F presents a different type of detection error. Here, the extracted shoreline extends inland around a group of buildings, with the extent of this deviation varying between observations. To investigate this further, the 2023 shoreline extraction was compared with higher-resolution imagery of the same location, as shown in Figure 5.17. The comparison reveals that the irregular inland boundary corresponds to existing buildings and other built-up surfaces rather than the coastline. These surfaces were therefore incorrectly included in the extracted shoreline geometry. The comparison demonstrates that the large displacement values in this area are associated with misclassification of the land–water boundary rather than actual shoreline retreat or advance.

Despite these pronounced localised deviations, the mean net shoreline displacement between 2016 and 2023 was +1.21 m in summer and +1.94 m in winter, indicating relatively limited overall seaward displacement in both datasets. The close agreement between shoreline positions along most of the section is consistent with these small mean values. However, the substantial deviations observed in Areas E and F demonstrate that individual classification errors can produce large apparent shoreline changes

within an otherwise relatively consistent coastline. The results therefore highlight the importance of inspecting anomalous shoreline positions alongside the original satellite imagery and, where available, higher-resolution reference imagery.

Section 3

Figure 5.18 presents the extracted summer shoreline positions for Bonaire Section 3 between 2016 and 2023. Overall, the shoreline positions remain relatively consistent throughout the study period, with the extracted shorelines closely overlapping along most of the approximately 2 km coastline. Unlike Sections 1 and 2, no single location shows a particularly pronounced deviation from the general shoreline alignment. Instead, small variations occur along the entire section, particularly around bends and irregularities in the coastline. A similar spatial pattern is observed in the winter dataset, with the corresponding shoreline map and displacement profile provided in Figures A.11 and A.12 in Appendix A.

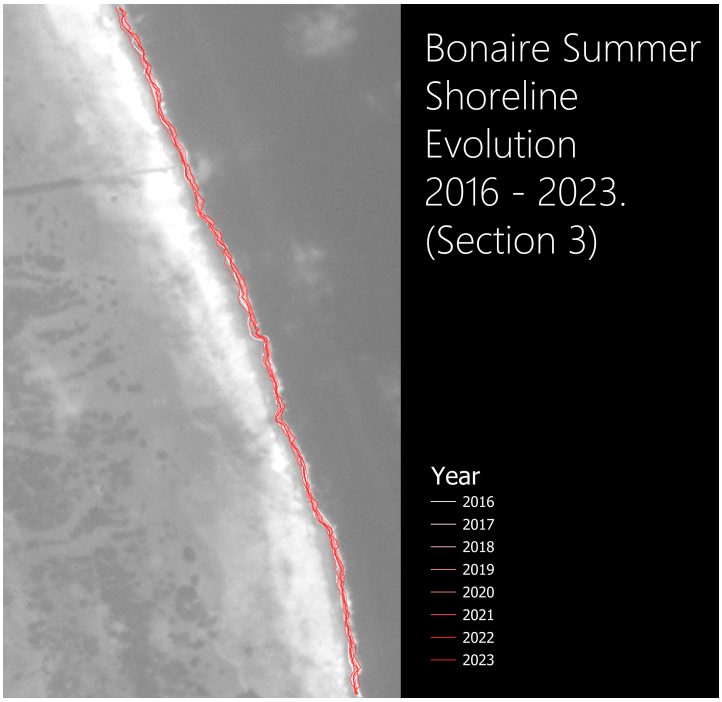


Figure 5.18: Extracted summer shoreline positions for Bonaire Section 3 between 2016 and 2023.

The shoreline displacement profile in Figure 5.19 provides a more detailed view of these variations. Annual displacement values alternate between positive and negative along the coastline, with most changes remaining within approximately 20 m of zero. Some larger fluctuations are visible, particularly around 950–1100 m, where individual annual comparisons show both landward and seaward displacement. However, these changes do not form a consistently dominant zone of retreat or advance. The net displacement between 2016 and 2023 is also relatively moderate, with a mean of +4.96 m in summer and +6.12 m in winter, indicating a small overall seaward shift in both seasonal datasets.

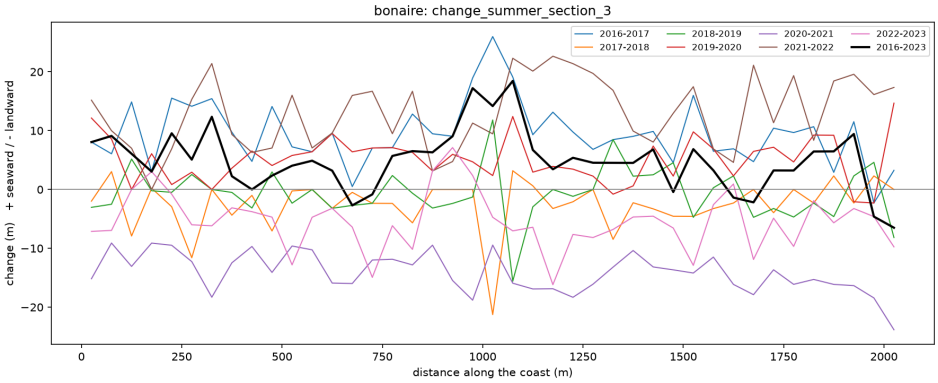


Figure 5.19: Summer shoreline change along Bonaire Section 3. Coloured lines represent change between successive available observations and the black line represents net change between 2016 and 2023. Positive values indicate seaward displacement and negative values indicate landward displacement.

The relatively consistent shoreline configuration is comparable to that observed in Aruba Section 3. Both sections are characterised by predominantly rocky coastlines, where the shoreline geometry is more strongly constrained by resistant geological material than along sandy beaches. The limited separation between the extracted shoreline positions is therefore consistent with the coastal characteristics of these areas. Nevertheless, the fluctuations observed in the displacement profile indicate that the detected land–water boundary is not identical between observations, particularly around irregular coastal features.

5.1.3. Positional accuracy assessment of shoreline extraction

The positional agreement between the automatically extracted shoreline and the manually interpreted reference points was assessed for all six coastal sections. For Aruba, the reference points were derived from the summer 2023 PlanetScope imagery, while for Bonaire the winter 2023 imagery was used. In total, 601 manually interpreted reference points were included in the assessment.

The percentage of reference points falling within distance thresholds of 1.5, 3, 6, 9, and 15 m from the extracted shoreline was calculated. These thresholds correspond approximately to 0.5, 1, 2, 3, and 5 PlanetScope pixels. These thresholds were selected in relation to the approximately 3 m spatial resolution of the PlanetScope imagery.

Table 5.1: Percentage of shoreline reference points within different positional error thresholds (1.5, 3, 6, 9, and 15 m) for each section of Aruba and Bonaire.

Island	Section	1.5 m	3 m	6 m	9 m	15 m
Aruba	Section 1	8.1%	15.2%	54.6%	88.9%	100.0%
Aruba	Section 2	4.7%	10.3%	28.0%	51.4%	83.2%
Aruba	Section 3	15.1%	33.0%	58.5%	78.3%	93.4%
Bonaire	Section 1	23.0%	55.6%	81.0%	92.1%	96.8%
Bonaire	Section 2	26.3%	56.3%	86.3%	93.8%	100.0%
Bonaire	Section 3	16.5%	36.5%	76.5%	96.5%	100.0%

The threshold-based results show clear differences in positional agreement between the study sections. For Aruba, Section 3 showed the strongest agreement at the 6 m threshold, with 58.5% of the reference points located within this distance of the extracted shoreline, compared with 54.6% in Section 1 and 28.0% in Section 2. At the 15 m threshold, these values increased to 93.4%, 100.0%, and 83.2%, respectively.

Positional agreement was generally higher for Bonaire. At the 6 m threshold, 81.0% of the reference points in Section 1, 86.3% in Section 2, and 76.5% in Section 3 were located within this distance of the extracted shoreline. At 9 m, the corresponding values increased to 92.1%, 93.8%, and 96.5%. Nearly all Bonaire reference points were located within 15 m of the extracted shoreline.

The descriptive statistics show the same general difference between the two islands. For Aruba, mean

Table 5.2: Positional error statistics for the automatically extracted shoreline relative to the manually interpreted reference points. All error values are expressed in metres.

Island	Section	n	Mean	Median	RMSE	P90	P95
Aruba	Section 1	99	5.75	5.73	6.29	9.02	9.35
Aruba	Section 2	107	9.50	8.88	10.79	16.62	17.55
Aruba	Section 3	106	6.04	5.33	7.60	13.29	16.27
Bonaire	Section 1	126	4.05	2.81	6.22	8.08	11.64
Bonaire	Section 2	80	3.50	2.61	4.62	6.92	9.84
Bonaire	Section 3	85	4.12	3.77	4.84	7.31	8.53

positional errors ranged from 5.75 to 9.50 m, with RMSE values between 6.29 and 10.79 m. Section 1 had the lowest mean error and RMSE, while Section 2 showed the highest values. For Bonaire, mean positional errors ranged from 3.50 to 4.12 m, while RMSE values ranged from 4.62 to 6.22 m. Bonaire Section 2 had the lowest RMSE of all six sections. The P90 and P95 values were also generally lower for Bonaire, indicating that larger positional discrepancies were less frequent than in the Aruba sections.

The spatial distribution of these errors is presented in Figures 5.20 and 5.22 for Aruba and Bonaire, respectively. Point colours represent the shortest distance between each manually interpreted reference point and the automatically extracted shoreline. For both islands, the errors are not distributed uniformly along the coastlines, with sections of relatively close agreement interrupted by locations with larger positional differences.

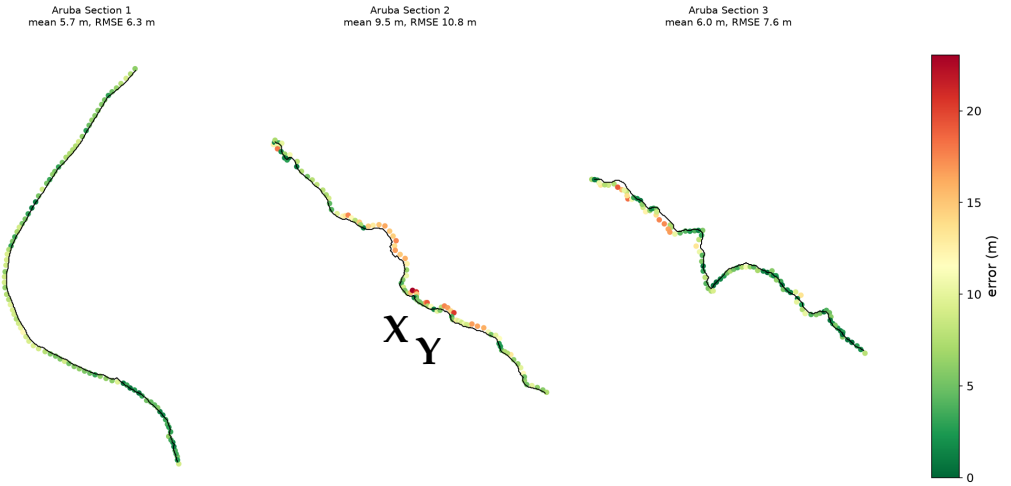


Figure 5.20: Spatial distribution of positional error between manually interpreted reference points and the automatically extracted shoreline for the three Aruba sections. Point colours indicate the shortest distance to the extracted shoreline, with the mean error and RMSE reported for each section.

In Aruba, the largest positional errors were observed in Section 2, although localised differences are also visible in Sections 1 and 3. A closer examination of Section 2, shown in Figure 5.21, reveals that the manually interpreted reference points were generally placed along the coastal mangrove boundary, whereas the automatically extracted shoreline was positioned slightly further towards the water. This results in a relatively consistent separation between the reference points and the detected shoreline along parts of the section. Two locations, indicated as X and Y, show more pronounced differences. At both locations, the imagery suggests the presence of shallow coastal features, possibly including exposed or submerged sand. Around X, the detected shoreline appears to partially follow this feature, whereas around Y, the boundary is not represented in the same way. These differences suggest that the spectral characteristics of shallow water, sand, and the surrounding coastal environment may influence the detected land–water boundary.

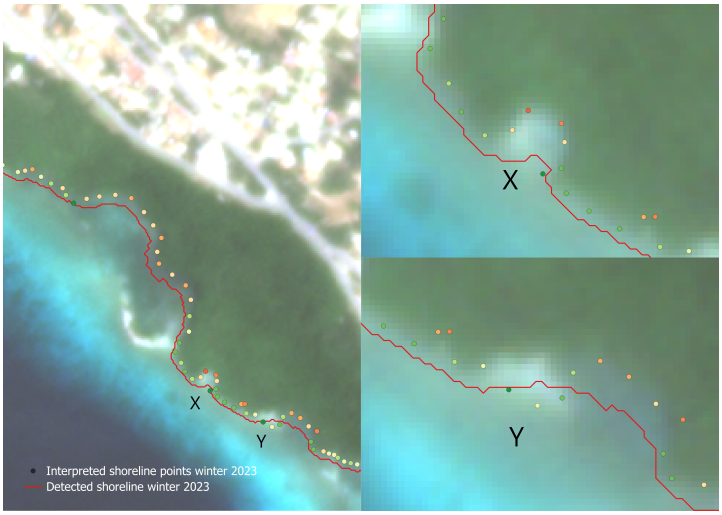


Figure 5.21: Detailed view of shoreline extraction accuracy in Aruba Section 2. The manually interpreted reference points are compared with the automatically extracted shoreline, with Areas X and Y highlighting local differences in the detection of the coastal boundary

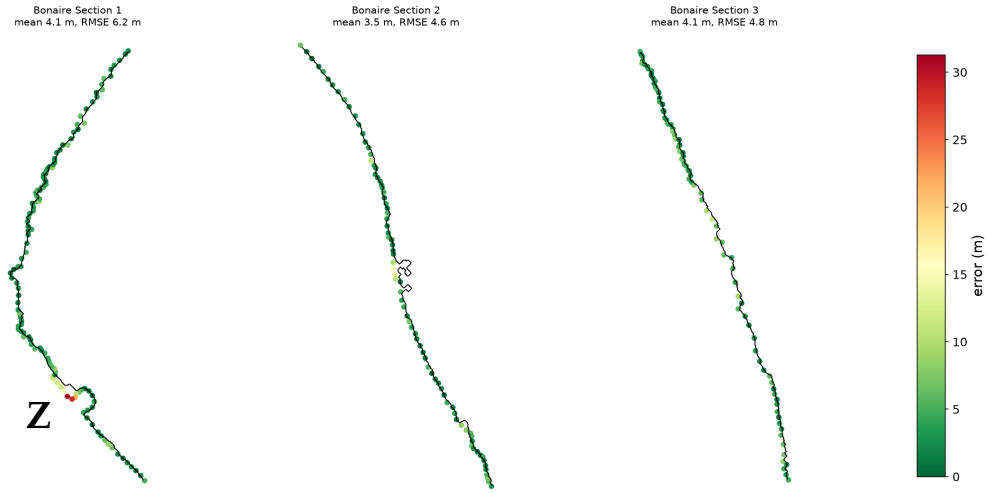


Figure 5.22: Spatial distribution of positional error between manually interpreted reference points and the automatically extracted shoreline for the three Bonaire sections. Point colours indicate the shortest distance to the extracted shoreline, with the mean error and RMSE reported for each section.

For Bonaire, the spatial error maps show generally smaller positional differences, with most reference points located close to the extracted shoreline. However, a localised deviation is visible in Section 1, indicated as Area Z. As shown in Figure 5.23, the automatically extracted shoreline does not fully follow a small coastal indentation identified by the manually interpreted reference points. Comparison with higher-resolution imagery confirms that this feature forms part of the coastal boundary. Although sufficiently clear higher-resolution imagery from 2023 was not available, imagery from 2025 provides additional spatial detail of the location. The feature is included in the extracted shoreline in some observations but not in others, indicating inconsistent detection of this local coastal geometry. In the 2023 observation used for validation, the feature was not fully captured, resulting in larger positional errors around Area Z.

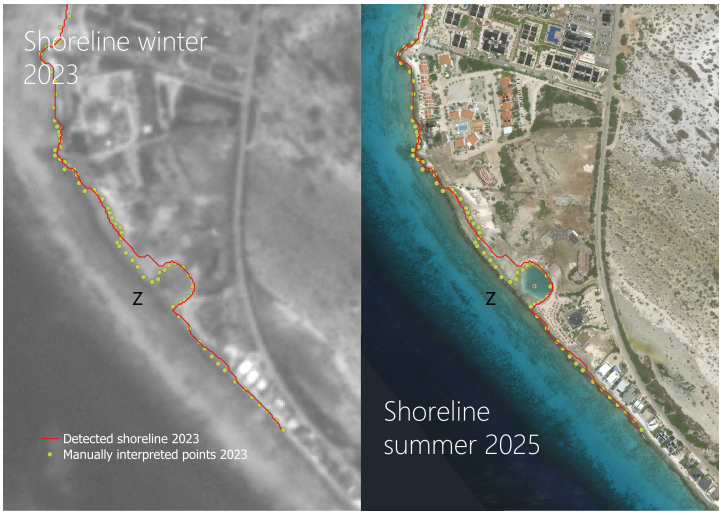


Figure 5.23: Detailed comparison of shoreline extraction in Area Z of Bonaire Section 1. The 2023 PlanetScope imagery and automatically extracted shoreline are compared with manually interpreted reference points and higher-resolution imagery from 2025, illustrating a coastal feature that was not fully captured by the automated extraction.

Because the reference points were interpreted from the same PlanetScope images used for the automated extraction, these results represent a positional accuracy assessment within the source imagery rather than an independent validation against a separate dataset. The reported errors are therefore used as an uncertainty reference when interpreting the magnitude of detected shoreline displacement.

5.2. Building detection & change

The building-change analysis shows spatially uneven patterns of detected building-area change across both islands between 2016 and 2023. Positive values indicate an increase in detected building area, while negative values indicate a decrease in detected building area between the two observations.

5.2.1. Aruba

Detected building area change across Aruba between 2016 and 2023 is spatially heterogeneous. The strongest positive changes are concentrated mainly in the western and central parts of the island, where several 500 m grid cells show increases of several thousand square metres. The largest mapped increase is approximately 15,159 m². The eastern and northeastern parts of Aruba show comparatively limited detected change. A smaller number of grid cells contain negative values, indicating that less building area was detected in 2023 than in 2016. Overall, the island-wide pattern shows that increases in detected building area are concentrated mainly in the more developed western and central parts of Aruba, while large parts of the eastern side show relatively little change.

5.2.2. Bonaire

Detected building area change across Bonaire between 2016 and 2023 is also spatially uneven. The strongest positive changes are concentrated mainly in the central and south-central settled parts of the island. The largest mapped increase is approximately 19,921 m² within a single 500 m grid cell. Much of northern Bonaire shows comparatively little detected building-area change. Smaller positive and negative values occur elsewhere across the island, indicating more limited differences between the 2016 and 2023 building detections. Overall, the island-wide pattern shows that the largest increases in detected building area are concentrated mainly within existing developed parts of Bonaire, while less developed areas show relatively little change.

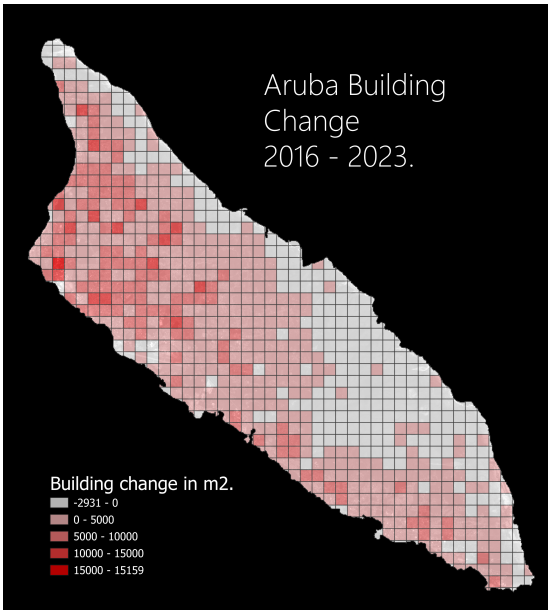


Figure 5.24: Change in detected building area across Aruba between 2016 and 2023, aggregated to a 500 m grid. Positive values indicate an increase in detected building area and negative values indicate a decrease.

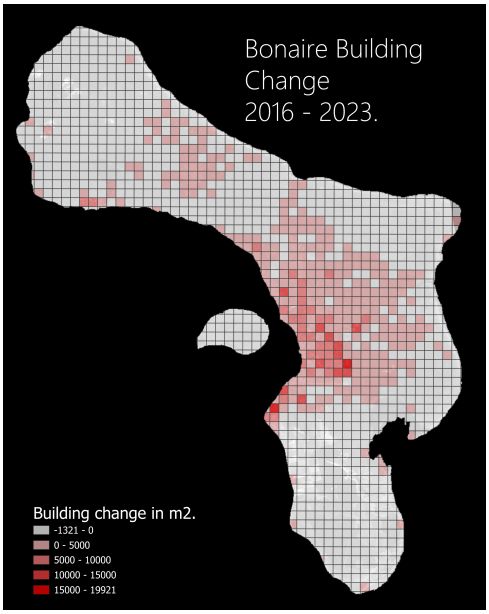


Figure 5.25: Change in detected building area across Bonaire between 2016 and 2023, aggregated to a 500 m grid. Positive values indicate an increase in detected building area and negative values indicate a decrease.

5.2.3. Validation of building detection

Building-detection performance was assessed separately for Aruba and Bonaire using manually identified reference buildings from the available high-resolution imagery. For Aruba, the 2018 Open Buildings detections were compared with the 2018 DLV aerial imagery seen in Figure 5.26, while for Bonaire the 2023 Open Buildings detections were compared with high-resolution imagery from winter 2023 seen in Figure 5.27.



Figure 5.26: High-resolution 2018 DLV aerial imagery of Aruba showing the manually identified reference buildings used for validation of the Google Open Buildings detections. Red points indicate one manually identified reference building each..



Figure 5.27: High-resolution NLSA imagery of Bonaire from winter 2023, showing manually identified reference buildings used for validation of the Google Open Buildings detections. Red points represent manually identified buildings.

For Aruba, the assessment identified 230 true-positive detections, 4 false negatives, and 27 false-positive building polygons. These values correspond to a recall of 98.3%, a precision of 87.8%, and an F1-score of 92.7%. The high recall indicates that nearly all manually identified buildings were detected, while the lower precision reflects a smaller number of false-positive detections.

For Bonaire, the assessment identified 674 true-positive detections, 17 false negatives, and 116 false-positive building polygons. These values correspond to a recall of 97.5%, a precision of 83.9%, and an

F1-score of 90.2%.

Overall, building-detection performance was strong for both islands, with recall above 97% and F1-scores above 90%. Aruba showed slightly higher precision and F1-score than Bonaire, while recall was similarly high for both datasets. Because the two assessments were based on different high-resolution reference datasets and observation years, the results are interpreted separately rather than as one combined accuracy estimate.

Table 5.3: Building-detection accuracy for Aruba and Bonaire.

Island	TP	FN	FP	Recall (%)	Precision (%)	F1 (%)
Aruba	230	4	27	98.3	87.8	92.7
Bonaire	674	17	116	97.5	83.9	90.2

5.3. Vegetation detection and change

The vegetation-change analysis shows spatially variable changes in remotely detected vegetation across both islands. Because no independent vegetation-validation dataset was available, the results are interpreted as changes in detected vegetation extent rather than confirmed ecological gain or loss.

5.3.1. Aruba

The island-wide vegetation analysis for Aruba compares PlanetScope imagery acquired in summer 2016 and summer 2023. Using observations from the same season also reduces the potential influence of seasonal differences in vegetation conditions, although variation in rainfall and image-acquisition conditions between years may still affect the detected vegetation extent.

The island-wide vegetation results for Aruba show predominantly positive change in remotely detected vegetation between 2016 and 2023. The strongest increases are concentrated mainly across the central, eastern, and southeastern parts of the island. Several 500 m grid cells show increases above 100,000 m², with the largest values falling within the highest mapped class of approximately 200,000–250,000 m².

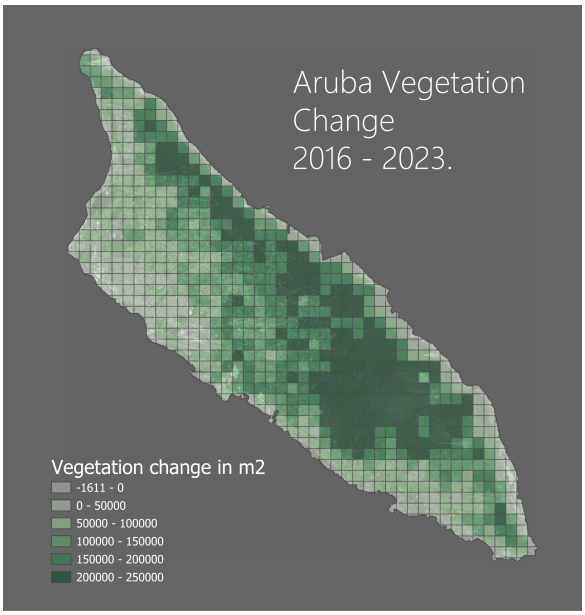


Figure 5.28: Change in detected vegetation area across Aruba between 2016 and 2023, aggregated to a 500 m grid. Positive values indicate an increase in detected vegetation area and negative values indicate a decrease.

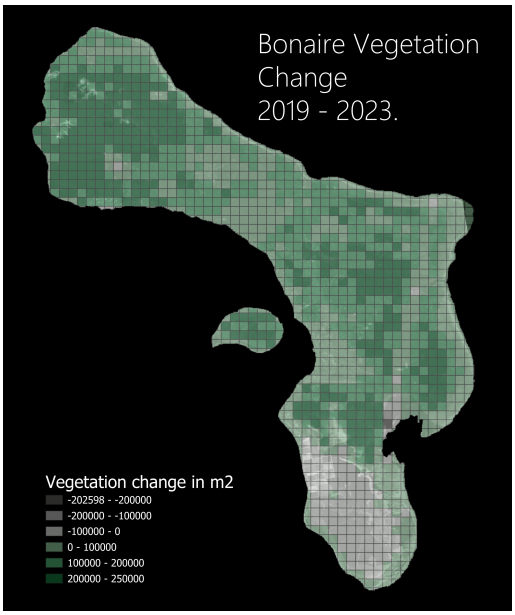


Figure 5.29: Change in detected vegetation area across Bonaire between 2019 and 2023, aggregated to a 500 m grid. Positive values indicate an increase in detected vegetation area and negative values indicate a decrease.

The developed western coastal strip generally shows smaller increases than the interior and southeastern parts of Aruba. Negative values occur in fewer locations and indicate areas where less vegetation was

detected in 2023 than in 2016. Overall, the island-wide pattern indicates a predominantly positive change in detected vegetation area, although the magnitude of change varies substantially across Aruba.

5.3.2. Bonaire

As with Aruba, the island-wide vegetation analysis for Bonaire was based on summer observations, comparing PlanetScope imagery from 2019 and 2023. The spatial pattern of detected vegetation change is more mixed than on Aruba. Large parts of northern and central Bonaire show positive change, including several grid cells with increases above 100,000 m². At the same time, negative values occur across parts of southern and south-central Bonaire, indicating areas where less vegetation was detected in 2023 than in 2019.

Overall, Bonaire shows a combination of positive and negative changes in detected vegetation area rather than one dominant island-wide pattern. The strongest positive changes occur mainly in the northern and central parts of the island, while the largest negative changes are concentrated farther south.

Because no independent vegetation-validation dataset was available, these results are interpreted as changes in remotely detected vegetation extent rather than independently confirmed ecological vegetation gain or loss.

5.4. Combined spatial results

The shoreline, detected building, and remotely detected vegetation results were combined to compare the different forms of coastal change occurring within each of the six study sections. Table 5.2 summarises the main section-scale indicators used in this comparison.

Positive building and vegetation values indicate a net increase in detected area between 2016 and 2023. For shoreline change, positive values indicate mean seaward displacement and negative values indicate mean landward displacement. The vegetation values represent the section-scale 2016–2023 comparison for both islands.

The combined results show that the three indicators do not follow one common pattern across the six sections. Some sections combine increasing detected building area and vegetation with landward shoreline displacement, while others show little building change together with positive vegetation change and either landward or seaward shoreline displacement.

Table 5.4: Summary of coastal setting, mean shoreline displacement, detected building change, and remotely detected vegetation change across the six coastal study sections between 2016 and 2023.

Island	Section	Coastal setting	Summer shoreline (m)	Winter shoreline (m)	Building change (m^2)	Vegetation change (m^2)
Aruba	Section 1	Sandy beach coast	-4.72	-8.36	+15,027	+16,370
Aruba	Section 2	Mangrove-influenced coast	+0.11	+4.32	+11,037	+65,110
Aruba	Section 3	Rocky exposed coast	-0.25	-11.14	0	+26,525
Bonaire	Section 1	Rocky limestone coast	+3.91	-4.48	+20,072	+9,241
Bonaire	Section 2	Rocky limestone coast	-6.16	+0.88	+8,588	+16,978
Bonaire	Section 3	Rocky exposed coast	+4.96	+6.12	+31	+85,402

5.4.1. Aruba

The three Aruba sections show contrasting combinations of detected building change, remotely detected vegetation change, and shoreline displacement across different coastal settings. Sections 1 and 2 both show increases in detected building area, but differ in their shoreline behaviour and coastal characteristics. Section 1 is predominantly characterised by sandy beaches and coastal development, while Section 2 contains mangrove-influenced coastal environments. Section 3 differs from both, consisting mainly of a rocky and more exposed coastline with limited development. These differences provide context for interpreting the spatial patterns observed across the three indicators.

Section 1 recorded an increase of approximately 15,027 m² in detected building area and 16,370 m² in remotely detected vegetation between 2016 and 2023. Mean shoreline displacement was landward in

both seasonal datasets, with -4.72 m in summer and -8.36 m in winter. The integrated map shown in Figure 5.30 shows a strongly developed coastal setting, with buildings located close to the shoreline and vegetation change occurring farther inland and between developed areas. As shown in the shoreline analysis, this section also contains some of the more pronounced localised shoreline fluctuations observed in Aruba, particularly around the curved beach areas. The combination of substantial detected building growth and local shoreline variability makes this section particularly interesting for further investigation. However, the occurrence of these changes within the same section does not demonstrate that shoreline displacement is a consequence of development, as both may be influenced by other environmental and coastal processes.

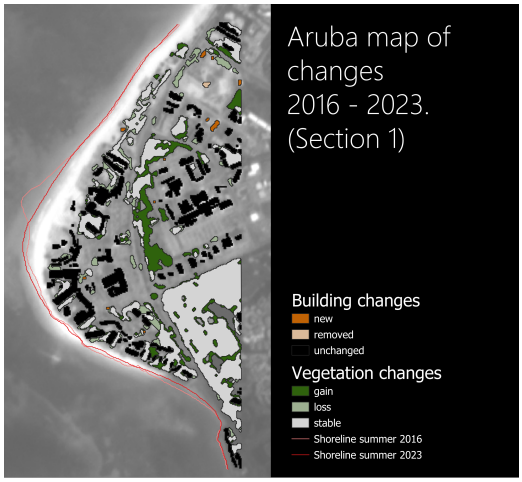


Figure 5.30: Integrated spatial change map for Aruba Section 1, showing detected building change, vegetation change, and the initial and final shoreline positions.

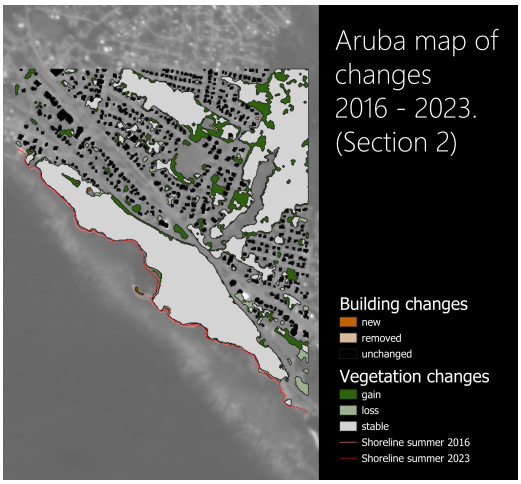


Figure 5.31: Integrated spatial change map for Aruba Section 2, showing detected building change, vegetation change, and the initial and final shoreline positions.

Section 2 showed an increase of approximately 11,037 m² in detected building area and the largest vegetation increase of the three Aruba sections, at approximately 65,110 m². Mean shoreline displacement was slightly seaward in both seasons, with +0.11 m in summer and +4.32 m in winter. The integrated map shown in Figure 5.31 indicates that building change is concentrated within the developed part of the section, while vegetation change occurs across a broader area. The mangrove-influenced coastal setting differs from the sandy beaches of Section 1, as vegetation forms part of the coastal boundary in several locations. This is relevant to the shoreline analysis, where the detected boundary may be influenced by the presence of mangroves, shallow water, and small coastal features. Consequently, some of the pronounced localised shoreline variations identified in this section may reflect differences in shoreline detection rather than equivalent physical changes in coastal morphology.

Section 3 differs from Sections 1 and 2 because there was no net change in detected building area between 2016 and 2023. Remotely detected vegetation increased by approximately 26,525 m², while mean shoreline displacement was -0.25 m in summer and -11.14 m in winter. This section is characterised by a predominantly rocky and exposed coastline, where the coastal geometry is more strongly constrained by resistant geological material than along sandy beaches. The relatively consistent shoreline positions observed in the summer dataset are therefore compatible with the coastal characteristics of this section. However, the larger negative mean displacement in winter indicates differences between the seasonal observations. As this coastline is also exposed to breaking waves, part of the detected shoreline variability may be influenced by wave foam, which can affect the identification of the land–water boundary in satellite imagery. This potential source of uncertainty is examined further in Chapter 6. The integrated results are therefore characterised mainly by vegetation change and differences in detected shoreline position, without a corresponding net increase in detected building area. The integrated spatial change map for this section is provided in Figure B.1 in Appendix B.

Overall, the Aruba sections do not show one consistent relationship between development, vegetation change, and shoreline displacement. Sections 1 and 2 both show increases in detected building area, but

differ in the direction of their mean shoreline displacement. Meanwhile, the largely undeveloped rocky Section 3 also shows negative mean shoreline displacement, despite the absence of detected building growth. The contrasting coastal settings help place these differences in context, although they do not independently explain the observed changes. In particular, the combination of coastal development and pronounced local shoreline variability in Section 1 highlights an area where more detailed investigation of coastal processes and human influences could be valuable.

5.4.2. Bonaire

The three Bonaire sections also show contrasting combinations of detected building change, remotely detected vegetation change, and shoreline displacement. Sections 1 and 2 are both characterised mainly by rocky limestone coastlines but differ in their development patterns. Section 1 represents an established developed coastal area, while Section 2 contains areas where development is less extensive. Section 3 consists of a more exposed rocky coastline with very limited development. These differences in coastal characteristics and development intensity provide context for comparing the observed changes across the three sections.

Section 1 recorded an increase of approximately 20,072 m² in detected building area, the largest increase among all six study sections, alongside an increase of 9,241 m² in remotely detected vegetation. This indicates that substantial additional building area was detected within an already developed coastal environment. Mean shoreline displacement differed between seasons, with +3.91 m in summer and -4.48 m in winter. The integrated spatial change map in Figure 5.32 shows the distribution of building and vegetation changes in relation to the shoreline, illustrating how further development has occurred within an already established coastal area. Despite the considerable increase in detected building area, the shoreline positions remained relatively consistent along most of the section. The rocky limestone coastal setting may contribute to this relatively stable configuration, although localised deviations were also identified, particularly around the coastal basin discussed in the shoreline analysis. The results therefore show that substantial detected building growth can occur alongside relatively limited mean shoreline displacement, without necessarily indicating a direct relationship between the two.

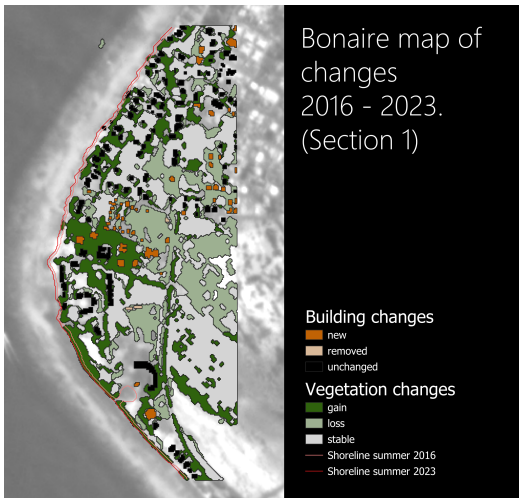


Figure 5.32: Integrated spatial change map for Bonaire Section 1, showing detected building change, vegetation change, and the initial and final shoreline positions.

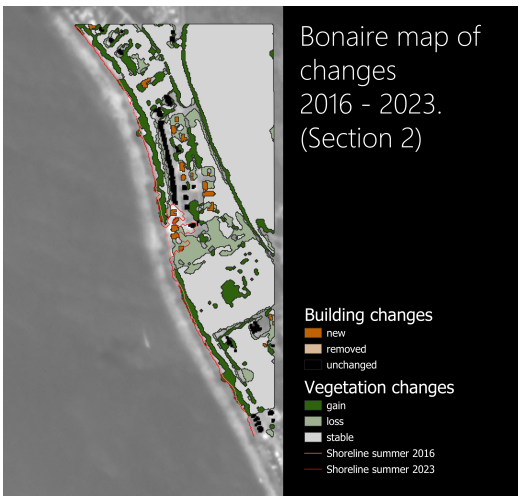


Figure 5.33: Integrated spatial change map for Bonaire Section 2, showing detected building change, vegetation change, and the initial and final shoreline positions.

Section 2 showed a smaller increase of approximately 8,588 m² in detected building area and 16,978 m² in remotely detected vegetation. Compared with Section 1, the integrated spatial change map in Figure 5.33 shows a different development pattern, with building changes occurring within a coastal area that is less extensively developed. While Section 1 shows considerable additional building area within an already established developed environment, Section 2 illustrates development occurring in a less built-up coastal setting. Mean shoreline displacement was -6.16 m in summer and +0.88 m in winter, indicating different displacement directions between the two seasonal datasets. Although the section is also characterised by a rocky limestone coastline, the shoreline analysis identified several

pronounced localised deviations, some of which were associated with cloud contamination and the incorrect detection of built-up surfaces as part of the shoreline. These differences indicate that the measured shoreline displacement should be considered alongside extraction uncertainties rather than interpreted solely as physical coastal change or as a consequence of development.

Section 3 showed almost no detected building change, with only approximately 31 m^2 of net increase in detected building area. In contrast, remotely detected vegetation increased by approximately 85,402 m^2, the largest vegetation increase among all six study sections. Mean shoreline displacement was seaward in both seasonal datasets, with +4.96 m in summer and +6.12 m in winter. Similar to Aruba Section 3, this section consists predominantly of a rocky and exposed coastline. The relatively consistent shoreline configuration observed throughout the study period is therefore compatible with the resistant coastal characteristics of the area. However, the repeated small-scale fluctuations in the shoreline displacement profiles may also partly reflect differences in wave conditions and the presence of foam from breaking waves, which can interfere with the automated shoreline extraction. This possible influence is discussed further in Chapter 6. The integrated results show that substantial increases in remotely detected vegetation can occur in areas with very limited building development and relatively small mean shoreline displacement. The integrated spatial change map is provided in Figure B.2 in Appendix B.

Overall, the Bonaire sections illustrate how different forms of coastal change occur across areas with contrasting development patterns and coastal characteristics. Sections 1 and 2 both experienced increases in detected building area but differed in their initial development intensity and the magnitude of subsequent building change. Section 1 showed substantial additional building area within an already developed coastal environment, while Section 2 showed a smaller increase within a less extensively developed setting. In contrast, Section 3 remained largely undeveloped, with almost no detected building change but the largest increase in remotely detected vegetation. Despite these differences, no consistent relationship between development intensity and shoreline displacement is apparent across the three sections.

Across all six study sections, the combined results show that detected building change, remotely detected vegetation change, and shoreline displacement do not follow one common spatial pattern. Aruba and Bonaire show some similarities, particularly in their rocky and exposed Section 3 coastlines, where limited building development and relatively consistent shoreline configurations are observed. However, differences are also apparent. Aruba Section 1, characterised by sandy beaches and substantial coastal development, shows pronounced localised shoreline fluctuations alongside considerable detected building growth, whereas the developed limestone coastal sections of Bonaire generally show smaller shoreline variations along most of their length. The mean shoreline displacement results also differ between the islands, with Aruba showing predominantly negative mean displacement, while Bonaire displays more mixed behaviour, including differences between seasonal observations. Vegetation increased in all six sections, although the largest detected increase occurred in Bonaire Section 3, while Aruba Section 2 showed the largest increase on Aruba. These contrasts suggest that coastal setting provides important context for interpreting the results, but that development intensity, vegetation change, and shoreline displacement cannot be directly linked based on the observed spatial patterns alone. Furthermore, some of the larger shoreline deviations were associated with extraction uncertainties rather than confirmed physical coastal change. The combined results therefore highlight the importance of considering both coastal characteristics and data limitations when comparing the different study sections, as discussed further in Chapter 6.

6

Discussion

The results demonstrate that shoreline change, detected building change, and remotely detected vegetation change vary both between Aruba and Bonaire and between the individual coastal sections. No single relationship between shoreline movement and the other indicators is apparent across all six sections. Instead, each section represents a different combination of coastal morphology, development, vegetation change, and shoreline behaviour.

This chapter discusses the interpretation and implications of the main findings, followed by the limitations associated with the available data, the applied methods, and the integrated spatial comparison.

6.1. Interpretation of the main findings

6.1.1. Shoreline change and coastal characteristics

The shoreline results demonstrate considerable spatial variability both between and within the selected coastal sections of Aruba and Bonaire. Although some sections show consistent mean displacement directions across the seasonal datasets, others differ between summer and winter. Local shoreline variations are also often substantially larger than the section-wide means. This indicates that coastal change cannot be characterised adequately by one displacement value for an entire section.

The differences are particularly relevant when considering coastal type. Aruba Section 1, which consists mainly of developed sandy beaches, shows pronounced local variations in shoreline geometry. In contrast, the more exposed rocky sections on both islands generally display relatively consistent shoreline configurations along much of their length. However, apparent displacement is still present, particularly in the winter observations for Aruba Section 3. Since rocky coastlines are more strongly constrained by resistant geological material, this variability should not automatically be interpreted as physical erosion or accretion.

One possible explanation is the influence of wave exposure on NDWI-based shoreline detection. The windward sides of Aruba and Bonaire are more directly exposed to energetic waves, resulting in increased breaking-wave activity and whitewater close to the coastline. Angelini et al. (2024) note that NDWI-based water classification can fail in the presence of foam because whitewater has a different spectral response from open water. Consequently, part of the apparent shoreline variability along exposed coastlines may reflect changing wave and foam conditions between image acquisitions rather than equivalent movement of the physical rock boundary.

The localised deviations identified in Aruba Section 2 and Bonaire Sections 1 and 2 further demonstrate that differences in the detection of small coastal features, built surfaces, or cloud-contaminated areas can strongly influence the extracted shoreline geometry. In Aruba Section 2, for example, a small coastal feature was included in some extracted shorelines but not others. Such differences should not automatically be interpreted as physical movement of the coastline.

The contrasting summer and winter mean displacement values also show that the apparent direction

and magnitude of shoreline change can depend on the observations used. This is particularly evident in Bonaire Sections 1 and 2, where the mean displacement direction differs between seasons. These differences reinforce the need to interpret the shoreline results in relation to acquisition conditions and positional uncertainty.

6.1.2. Development, vegetation, and their spatial relationships

The building results show that increases in detected building area were concentrated mainly in sections that were already relatively developed. Sections 1 and 2 on both islands generally contain a greater concentration of constructed assets close to the coast, whereas Section 3 on both islands is substantially less developed.

Vegetation does not follow the same spatial pattern as development. Remotely detected vegetation increased in all six coastal sections, with the largest increases occurring in Aruba Section 2 and Bonaire Section 3. At the island scale, Aruba showed predominantly positive detected vegetation change, while Bonaire showed a more mixed spatial pattern.

These results show why vegetation, development, and shoreline displacement should not be interpreted as interchangeable indicators of the same coastal process. A section can simultaneously contain increasing detected building area, increasing vegetation, and landward shoreline displacement. Conversely, relatively undeveloped sections may also show apparent shoreline variability.

Aruba Section 1 provides an example of substantial detected building growth occurring alongside pronounced localised shoreline variability on a sandy coast. However, the occurrence of these changes within the same section does not demonstrate that development caused the observed shoreline displacement. Similarly, Bonaire Section 1 contains the largest detected building increase among all six sections but does not show a consistent landward shoreline response between seasons.

The comparison therefore indicates that building development, vegetation, and shoreline displacement vary differently between coastal sections. None of the indicators consistently explains the others. Their value lies in showing how different forms of coastal change overlap spatially under contrasting coastal settings, rather than identifying a single controlling relationship.

6.2. Implications for coastal monitoring and management

The results demonstrate the value of considering several indicators when monitoring coastal change in Aruba and Bonaire. Shoreline displacement alone does not describe the wider environmental and development context in which coastal change occurs. By examining shoreline position alongside detected building development, vegetation change, coastal type, and exposure, the analysis provides a more comprehensive spatial overview of the selected coastal sections.

The differences between sandy, rocky, and mangrove-influenced coastlines indicate that shoreline monitoring should account for local coastal characteristics. These environments differ in their physical behaviour and in the way their boundaries are represented in satellite imagery. Consequently, shoreline-change results are most informative when interpreted together with coastal morphology, image quality, and positional uncertainty.

The study also illustrates the importance of examining coastal change at different spatial scales. Section-wide mean displacement provides a useful overview but may conceal localised variation or extraction artefacts. Detailed shoreline profiles and spatial maps therefore provide important additional information when identifying areas where the detected coastline differs substantially between observations.

From a coastal management perspective, the integrated analysis may help identify locations where several forms of change occur within the same coastal area. For example, shoreline displacement occurring near existing development or changes in vegetation may indicate locations where more detailed investigation would be valuable. However, these spatial relationships do not establish that the detected changes are causally related or that the locations are necessarily at greater risk.

The vegetation results similarly require careful interpretation. Although vegetation can contribute to sediment retention and coastal stability, changes in remotely detected vegetation extent do not

directly represent changes in ecological condition or coastal protection. This is particularly relevant in mangrove-influenced environments, where ecological functioning also depends on factors such as tidal exchange, salinity, sedimentation, and vegetation structure.

The findings can therefore support the identification of areas for additional monitoring or field-based assessment. Their main practical contribution lies in revealing spatial contrasts and co-occurrences rather than prescribing specific coastal management interventions or providing a direct assessment of coastal vulnerability.

6.3. Limitations of the study

6.3.1. Data availability, image quality, and spatial resolution

A major limitation of the study concerns the trade-off between spatial resolution, temporal coverage, geographical coverage, and data accessibility. The highest-resolution datasets were generally not the datasets with the most useful temporal record.

For Bonaire, approximately 30 cm optical imagery was available, while Aruba had access to very-high-resolution aerial imagery from 2018. These datasets provided considerably greater spatial detail than the approximately 3 m PlanetScope imagery used for the main analysis. However, their limited temporal coverage prevented their use for consistent multiyear change detection.

PlanetScope was therefore selected because it provided more suitable temporal coverage for shoreline and vegetation analysis. Google Open Buildings similarly provided annual building detections across the 2016–2023 study period. This choice represents a compromise between spatial detail and temporal consistency. Data accessibility also remains relevant because PlanetScope is a commercial dataset, potentially limiting the transferability of the workflow to users without equivalent access.

The approximately 3 m PlanetScope resolution places a limit on the scale at which coastal change can be interpreted. Narrow beaches, irregular rocky edges, small vegetation patches, and foam zones may occupy only one or several pixels. Pixels close to the coastline can therefore contain mixed spectral information from water, sand, vegetation, rock, or whitewater.

Image quality also varied between observations. Cloud cover, shadows, haze, wave foam, and changing water conditions can affect the extraction of shoreline and vegetation boundaries. An example occurs in the Bonaire summer 2021 imagery, where cloud contamination locally interfered with shoreline classification. As illustrated in Figure 6.1, the automatically extracted boundary followed parts of the cloud-contaminated area rather than the physical land–water boundary.

This demonstrates that automated extraction does not eliminate the need for quality control. Higher-resolution imagery may reduce some mixed-pixel effects, but it would not remove uncertainty associated with clouds, wave foam, water levels, georeferencing, or shoreline definition.

6.3.2. Shoreline extraction and temporal comparison

The shoreline methodology introduces uncertainty because the extracted shoreline represents an instantaneous land–water boundary rather than a fixed geomorphological coastline. Changes in its detected position may therefore reflect physical morphological change, different water levels or wave conditions, and errors in automated extraction.

This is particularly important when measured displacement approaches the positional uncertainty of the extraction. As reported in Section 5.1.3, the accuracy assessment was based on 603 manually interpreted reference points. The RMSE ranged from 6.29 m to 10.79 m across the Aruba sections and from 4.62 m to 6.22 m across the Bonaire sections. Several section-wide mean displacements are of a similar magnitude to these errors and should therefore not be treated as precise measurements of erosion or accretion.

The validation results also demonstrate that extraction accuracy varies between coastal settings. Aruba Section 2 showed the largest positional error, while the detailed analyses of Bonaire Sections 1 and 2 revealed cases where coastal basins, cloud contamination, or built surfaces produced erroneous shoreline boundaries. These examples show that some localised deviations reflect classification inconsistencies rather than equivalent physical changes.



Figure 6.1: Example of cloud contamination affecting the automatically extracted shoreline in the Bonaire summer 2021 imagery. The red line represents the automatically detected boundary. Bright cloud pixels over the water locally produce an erroneous contour that does not correspond to the physical shoreline.

The distinction between an instantaneous waterline and a geomorphological shoreline is particularly relevant for rocky coastlines. Freund (2025) demonstrated that satellite-derived coastal-boundary algorithms can be adapted to detect cliff lines rather than conventional waterlines. Although this approach was not applied in the present study, it illustrates why the most relevant morphological boundary may differ from the boundary extracted using NDWI.

Temporal comparison introduces an additional limitation. Although the images were grouped into summer and winter observations, these categories do not guarantee comparable water levels or hydrodynamic conditions. Torres and Tsimplis (2012) show that the Caribbean Sea experiences a seasonal sea-level cycle, with annual harmonic amplitudes of approximately 2–9 cm. Even relatively small vertical changes may produce noticeable horizontal displacement of the waterline on gently sloping beaches.

The differences between seasonal shoreline results may therefore reflect a combination of morphological change, hydrodynamic variability, and extraction uncertainty. The shoreline measurements should consequently be interpreted together with the spatial profiles, image conditions, and validation results rather than as exact measurements of long-term coastline movement.

6.3.3. Building and vegetation indicators

The Google Open Buildings Temporal dataset provided consistent annual building detections for the study period. However, these represent modelled building geometries rather than confirmed cadastral observations. Apparent differences between years may therefore result from both genuine development and variation in model performance.

Preliminary machine-learning tests using high-resolution imagery for Bonaire demonstrated that individual buildings could be detected in greater spatial detail, as shown in Figure 6.2. However, missed detections, false positives, and insufficient temporal coverage limited the suitability of this approach for the present study.

The Open Buildings validation results support its use for identifying broader spatial development



Figure 6.2: Preliminary results for building detection using machine learning with 30 cm resolution data for Bonaire.

patterns, with recall above 97% for both islands. Nevertheless, false-positive detections remained present, meaning that individual building polygons should be interpreted with caution.

Another limitation concerns the use of building footprint area as an indicator of development. This represents the horizontal extent of buildings but does not capture vertical development. In Aruba's tourism areas, for example, multi-storey hotels may represent considerably greater development intensity than low-rise buildings with similar footprints. Building area should therefore not be interpreted as a complete measure of development intensity or the value of exposed assets.

The vegetation analysis introduces different limitations. Continuous NDVI values were converted into binary classifications of vegetated and non-vegetated surfaces. Although useful for estimating vegetation extent, this approach does not distinguish between sparse and dense vegetation or directly represent vegetation condition.

The use of image-specific classification thresholds also means that changes in detected vegetation area may partly reflect differences in spectral conditions between observations. This is especially relevant where vegetation responds to rainfall, drought, salinity, or seasonal conditions.

Consequently, the positive changes in detected vegetation area reported for all six sections do not necessarily demonstrate ecological improvement or increased coastal buffering. Because no independent vegetation-validation dataset was available, the findings should remain interpreted as changes in remotely detected vegetation extent.

6.3.4. Scope of the integrated analysis

The integrated comparison was based on six selected coastal sections representing contrasting coastal environments rather than a statistically representative sample of the entire coastlines of Aruba and Bonaire. Consequently, the identified relationships cannot automatically be generalised to all coastal areas on either island.

External exposure was also treated primarily as a contextual descriptor based on coastal orientation and published information on prevailing wind and wave conditions. The study did not quantitatively reconstruct local wave climates, sediment transport, or water levels for each section. The contribution of these physical processes to observed shoreline displacement could therefore not be isolated.

Furthermore, the integrated analysis identified spatial co-occurrences rather than testing statistical correlations or causal relationships. Detected building growth near shoreline displacement does not

establish that development caused the displacement. Similarly, detected vegetation change cannot independently explain differences in shoreline behaviour.

Taken together, these limitations indicate that the methodology is most suitable for comparing spatial patterns across contrasting coastal settings. The strength of the approach lies in examining shoreline change, development, vegetation, and coastal characteristics within the same spatial framework while retaining the uncertainty and meaning of each indicator. It therefore supports the identification of spatial contrasts and co-occurrences without reducing them to a single vulnerability score or implying causal relationships that were not tested.

7

Conclusion and recommendations

7.1. Conclusion

This study investigated how spatial patterns of coastal change vary in relation to external coastal exposure, development, vegetation, and coastal characteristics in selected sections of Aruba and Bonaire. By combining shoreline, building, and vegetation observations within the same spatial framework, the study demonstrates that coastal change is spatially heterogeneous and that no single indicator adequately describes the patterns observed across the analysed coastal sections.

Regarding the first sub-question, Aruba and Bonaire contain contrasting coastal types. Aruba includes sandy and strongly developed leeward coastal areas and a sheltered mangrove-influenced section as well as more exposed rocky sections, while Bonaire contains contrasting leeward and windward coastal settings, including rocky limestone coastlines and more vegetated or less developed sections. The analysed sections therefore represent substantially different morphological and exposure conditions that provide the context for interpreting the remotely sensed indicators.

Regarding shoreline change, the results show considerable spatial variation both between and within the coastal sections. Aruba Section 1 had mean changes of -4.72 m in summer and -8.36 m in winter, while Section 2 showed +0.11 m and +4.32 m, respectively. Section 3 showed a relatively small summer mean of -0.25 m but a stronger winter mean of -11.14 m. The detailed profiles additionally revealed local changes substantially larger than these section averages.

Bonaire showed a different overall pattern. Section 1 changed direction between the two seasonal datasets, with a mean seaward displacement of +3.91 m in summer and a mean landward displacement of -4.48 m in winter. Section 2 also differed between seasons, with mean landward displacement of -6.16 m in summer and slight mean seaward displacement of +0.88 m in winter. Section 3 showed mean seaward displacement in both seasons, at +4.96 m and +6.12 m.

These mean values should, however, be interpreted together with the positional uncertainty of the shoreline extraction. The positional accuracy assessment, based on 603 manually interpreted reference points, showed that extraction accuracy varied between the selected coastal sections. Several section-wide displacements are similar in magnitude to the corresponding RMSE values, meaning that the smaller changes cannot be treated as precise measurements of physical erosion or accretion. The exposed Section 3 coastlines showed relatively consistent shoreline configurations along much of their length, although localised differences and apparent displacement were still present despite their more rocky character. Wave-generated foam may influence NDWI classification in such environments, while clouds and other image-quality problems can also generate erroneous boundaries. The detailed results additionally identified inconsistencies in the extraction of small coastal features and built surfaces. The shoreline results therefore demonstrate the sensitivity of satellite-derived shorelines to acquisition and coastal conditions.

Regarding detected building change, increases in detected building area were concentrated mainly in the already developed parts of the islands. Within the analysed sections, Aruba Sections 1 and 2 gained

approximately 15,027 m^2 and 11,037 m^2 of detected building area between 2016 and 2023, while Section 3 showed no net change. On Bonaire, Section 1 recorded approximately 20,072 m^2 of increase, Section 2 approximately 8,588 m^2, and Section 3 only approximately 31 m^2. Bonaire Section 1 therefore showed the largest increase in detected building area among all six sections.

Regarding vegetation, all six coastal sections showed a positive net change in remotely detected vegetation area between 2016 and 2023. The magnitude varied substantially. Aruba Section 2 recorded the largest vegetation increase on Aruba, at approximately 65,110 m^2, while Bonaire Section 3 recorded the largest increase among all six sections, at approximately 85,402 m^2. At the island scale, Aruba showed predominantly positive detected vegetation change, whereas Bonaire displayed a more mixed spatial pattern. These changes should be interpreted as changes in remotely detected vegetation rather than independently confirmed ecological improvement, since no independent vegetation validation was available and the binary NDVI classification is sensitive to image and environmental conditions.

Regarding the final sub-question, no single relationship between shoreline movement, development, and vegetation was identified across all sections. Highly developed sections did not consistently show the largest shoreline change, while relatively undeveloped Section 3 areas still showed substantial apparent shoreline variability. Vegetation increases also occurred under different combinations of development and shoreline behaviour. For example, Aruba Section 1 combined substantial detected building growth with pronounced localised shoreline variability, whereas Bonaire Section 1 recorded the largest increase in detected building area without consistently showing mean landward shoreline displacement. The indicators therefore describe overlapping but distinct dimensions of coastal condition.

The main research question can consequently be answered by concluding that spatial patterns of coastal change vary between sections characterised by different combinations of coastal morphology, exposure, development, and vegetation rather than following one common spatial pattern. The results demonstrate the importance of analysing these indicators together and at a local spatial scale, while also showing that their spatial relationships cannot be interpreted as evidence of direct causality.

Overall, the study is best interpreted as a comparative multi-indicator assessment of coastal change. The combined shoreline, building, vegetation, and coastal-setting information makes it possible to identify spatial contrasts and co-occurrences between sections, but it does not establish causal relationships or produce a numerical measure of coastal vulnerability. The reliability of the interpretation also depends strongly on the spatial resolution, positional accuracy, temporal consistency, and acquisition conditions of the underlying datasets. The approach is therefore most suitable for supporting comparative coastal monitoring and identifying locations where more detailed investigation may be valuable.

7.2. Recommendations

Future work should improve the shoreline analysis by selecting satellite observations according to comparable hydrodynamic conditions rather than relying primarily on fixed summer and winter categories. Where possible, image acquisition dates should be matched to tidal conditions, seasonal sea level, and wave conditions. This would reduce apparent shoreline displacement caused by differences in water level or coastal state between observations.

Additional quality control should also be introduced for cloud and wave-foam contamination. Cloud masks could be applied before shoreline extraction, while approaches that explicitly classify whitewater could improve results on exposed coastlines. Images producing unusually large or irregular shoreline changes should additionally be checked against the original satellite imagery before being included in the temporal analysis. Automated identification of anomalous shoreline geometries could further support this process.

Future monitoring would also benefit from combining temporally consistent satellite imagery with periodic very-high-resolution observations. The repeated imagery can provide the time series required to identify change, while high-resolution imagery can be used for accuracy assessment and detailed visual interpretation of narrow beaches, rocky coastlines, vegetation patches, and individual buildings. Independent reference observations acquired close to the satellite acquisition dates would further strengthen shoreline positional validation.

Future research could also investigate alternative coastal-boundary indicators for different coastal

settings. The instantaneous land–water boundary used in this study does not necessarily correspond to the most relevant geomorphological feature along rocky or cliffed coastlines. Approaches such as cliff-line detection could therefore be evaluated where appropriate, provided that their accuracy is assessed against suitable reference data.

Development analysis could be extended from building footprint area to a three-dimensional indicator by incorporating building height. This would provide a more representative measure of the vertical dimension of development in areas dominated by multi-storey construction, particularly the tourism areas of Aruba. Any temporal use of building height should, however, rely on height estimates that are consistent between observation years.

Vegetation analysis could similarly be expanded from vegetation extent to vegetation condition. Continuous NDVI values or additional vegetation indices could be analysed alongside classified vegetation area to distinguish changes in vegetation condition or density from complete vegetation gain or loss. Independent reference data would also strengthen future vegetation analyses by allowing the remotely detected classifications to be evaluated directly. This would be particularly valuable for mangrove environments, where vegetation may remain present despite changes in ecological condition.

Furthermore, extending the temporal record would help distinguish persistent trends from short-term variability. More frequent observations, combined with wave, water-level, and meteorological information, would allow localised features such as the small coastal feature in Aruba Section 2 to be investigated in greater detail and would help determine whether apparent changes reflect physical morphological change, differences in shoreline extraction, or a combination of both.

For the integrated analysis, future work could also introduce more formal spatial comparison methods while keeping the individual indicators separate. For example, distances between shoreline-change zones, detected building change, and vegetation change could be quantified to test whether apparent spatial co-occurrences are systematic. Extending the analysis to more coastal sections and incorporating additional information on local hydrodynamic conditions could further strengthen comparisons between coastal settings. This would strengthen the interpretation without requiring the indicators to be combined into a single vulnerability index or assuming causal relationships that have not been established.

Future studies should also report positional uncertainty alongside shoreline-change statistics so that small displacement values can be distinguished from changes that clearly exceed the expected extraction error.

References

Acosta, A., Ercole, S., Stanisci, A., Pillar, V. D. P., & Blasi, C. (2007). Coastal vegetation zonation and dune morphology in some mediterranean ecosystems. *Journal of Coastal Research*, *23*(6), 1518–1524.

Alexander, C. S. (1961). The marine terraces of aruba, bonaire, and curaçao, netherlands antilles. *Annals of the Association of American Geographers*, *51*(1), 102–123.

Angelini, R., Angelats, E., Luzi, G., Masiero, A., Simarro, G., & Ribas, F. (2024). Development of methods for satellite shoreline detection and monitoring of megacusp undulations. *Remote Sensing*, *16*(23), 4553. https://doi.org/10.3390/rs16234553

Apostolopoulos, D., & Nikolakopoulos, K. (2021). A review and meta-analysis of remote sensing data, gis methods, materials and indices used for monitoring the coastline evolution over the last twenty years. *European Journal of Remote Sensing*, *54*(1), 240–265. https://doi.org/10.1080/22797254.2021.1904293

Asensi, A., & Diez-Garretas, B. (2017). Coastal vegetation. In J. Loidi (Ed.), *The vegetation of the iberian peninsula* (pp. 397–432). Springer International Publishing. https://doi.org/10.1007/978-3-319-54867-8_8

Bosboom, J., & Stive, M. J. F. (2023). *Coastal dynamics* (Version 1.2). TU Delft Open. https://doi.org/10.5074/T.2021.001

Chauveau, D., Boyden, P., Desfromont, F., Scardino, G., Scicchitano, G., Mijts, E., Bejarano, S., Dean, S., Cerrone, C., & Rovere, A. (2026). Unraveling the spatial variability of fossil coral reef morphology on aruba and the implications for paleo sea level estimates. *Journal of Geophysical Research: Earth Surface*, *131*, e2025JF008384. https://doi.org/10.1029/2025JF008384

Cole, S., & Razak, V. M. (2003). *A framework for sustainable tourism in aruba* (Conference draft). National Tourism Council of Aruba.

Departamento Meteorologico Aruba. (n.d.). *Climate data aruba*. Retrieved August 26, 2026, from https://www.meteo.aw/climate.php

Eicher, H. K. (2023). *Evaluating coral ecosystem health in aruba: The development and future of aruba's coral reefs* [Master's thesis, Utrecht University].

Engel, M., Brückner, H., Messenzehl, K., Frenzel, P., May, S. M., Scheffers, A., Scheffers, S., Wennrich, V., & Kelletat, D. (2012). Shoreline changes and high-energy wave impacts at the leeward coast of bonaire (netherlands antilles). *Earth, Planets and Space*, *64*, 905–921. https://doi.org/10.5047/eps.2011.08.011

Frade, P. R., Bongaerts, P., Baldwin, C. C., Trembanis, A. C., Bak, R. P. M., & Vermeij, M. J. A. (2019). Bonaire and curaçao. In Y. Loya, K. A. Puglise, & T. C. L. Bridge (Eds.), *Mesophotic coral ecosystems* (pp. 149–162). Springer.

Freund, J. (2025, August). *Creating cliffsat: Adapting a satellite-derived shoreline algorithm for monitoring coastal cliff erosion* [Master's thesis]. Delft University of Technology.

García-Rubio, G., Huntley, D. A., & Russell, P. E. (2015). Evaluating shoreline identification using optical satellite images. *Marine Geology*, *359*, 96–105.

Giardino, A., de Vroeg, H., van Maren, B., & Nederhoff, K. (2018). *Coastal erosion and fine sediment management study for the area between surfside and cudarebe (aruba)* (tech. rep. No. 11200913-000-ZKS-0003). Deltares. Delft, The Netherlands.

Gijsman, R., Engel, S., van der Wal, D., van Zee, R., Johnson, J., van der Geest, M., Wijnberg, K., & Horstman, E. (2026). The exchange of water and sediment across a microtidal caribbean mangrove forest. *Estuarine, Coastal and Shelf Science*, *338*, 109933. https://doi.org/10.1016/j.ecss.2026.109933

Hamid, A. I. A., Din, A. H. M., Yusof, N., Abdullah, N. M., Omar, A. H., & Khanan, M. F. A. (2019). Coastal vulnerability index development: A review. *The International Archives of the Photogrammetry, Remote Sensing and Spatial Information Sciences*, *XLII-4/W16*, 229–235. https://doi.org/10.5194/isprs-archives-XLII-4-W16-229-2019

Harris, D. L., Rovere, A., Casella, E., Power, H., Canavesio, R., Collin, A., Pomeroy, A., Webster, J. M., & Parravicini, V. (2018). Coral reef structural complexity provides important coastal protection

from waves under rising sea levels. *Science Advances*, *4*, eaao4350. https://doi.org/10.1126/sciadv.aao4350

Hermans, T. D. G., Hartman, H. J. S., van den Burg, S. W. K., de Rooij, B., & Verweij, P. J. F. M. (2026). Leverage points for transformative change towards nature inclusivity on bonaire and aruba. *People and Nature*, *8*, 181–196. https://doi.org/10.1002/pan3.70210

Hippolyte, J.-C., & Mann, P. (2011). Neogene–quaternary tectonic evolution of the leeward antilles islands (aruba, bonaire, curaçao) from fault kinematic analysis. *Marine and Petroleum Geology*, *28*, 259–277. https://doi.org/10.1016/j.marpetgeo.2009.06.010

Jurgens, S. S., Mijts, E., & Van Rompaey, A. (2024). Are there limits to growth of tourism on the caribbean islands? case-study aruba. *Frontiers in Sustainable Tourism*, *3*, 1292383. https://doi.org/10.3389/frsut.2024.1292383

Kohsiek, L. H. M., Hulsbergen, C. H., & Terwindt, J. H. J. (1987). Beach erosion along the west coast of aruba, netherlands antilles. *Journal of Coastal Research*, *3*(1), 37–53.

Lewsey, C., Cid, G., & Kruse, E. (2004). Assessing climate change impacts on coastal infrastructure in the eastern caribbean. *Marine Policy*, *28*(5), 393–409. https://doi.org/10.1016/j.marpol.2003.10.016

Maiti, S., & Bhattacharya, A. K. (2009). Shoreline change analysis and its application to prediction: A remote sensing and akestatistics based approach. *Marine Geology*, *257*, 11–23. https://doi.org/10.1016/j.margeo.2008.10.006

Massetti, E. (2025). *Sea-level rise and climate adaptation in aruba* (IMF Selected Issues Paper No. SIP/2025/157). International Monetary Fund. Washington, DC.

McCarthy, M. J., Colna, K. E., El-Mezayen, M. M., Laureano-Rosario, A. E., Mendez-Lazaro, P., Otis, D. B., Toro-Farmer, G., Vega-Rodriguez, M., & Muller-Karger, F. E. (2017). Satellite remote sensing for coastal management: A review of successful applications. *Environmental Management*, *60*, 323–339. https://doi.org/10.1007/s00267-017-0880-x

Ng, K., Borges, P., Phillips, M. R., Medeiros, A., & Calado, H. (2019). An integrated coastal vulnerability approach to small islands: The azores case. *Science of the Total Environment*, *690*, 1218–1227. https://doi.org/10.1016/j.scitotenv.2019.07.013

Pantusa, D., D'Alessandro, F., Frega, F., Francone, A., & Tomasicchio, G. R. (2022). Improvement of a coastal vulnerability index and its application along the calabria coastline, italy. *Scientific Reports*, *12*, 21959. https://doi.org/10.1038/s41598-022-26374-w

Petrişor, A.-I., Hamma, W., Nguyen, H. D., Randazzo, G., Muzirafuti, A., Stan, M.-I., Tran, V. T., Aştefănoaiei, R., Bui, Q.-T., Vintilă, D.-F., Truong, Q. H., Lixăndroiu, C., Ţenea, D.-D., Sîrodoev, I., & Ianoş, I. (2020). Degradation of coastlines under the pressure of urbanization and tourism: Evidence on the change of land systems from europe, asia and africa. *Land*, *9*(8), 275. https://doi.org/10.3390/land9080275

Rechtbank Den Haag. (2026, January). Nederlandse staat beschermt inwoners bonaire onvoldoende tegen klimaatverandering [Judgment of 28 January 2026, ECLI:NL:RBDHA:2026:1344].

Rodgers, J. C. I., Murrah, A. W., & Cooke, W. H. (2009). The impact of hurricane katrina on the coastal vegetation of the weeks bay reserve, alabama from ndvi data. *Estuaries and Coasts*, *32*, 496–507. https://doi.org/10.1007/s12237-009-9138-z

Roukounis, C. N., & Tsihrintzis, V. A. (2022). Indices of coastal vulnerability to climate change: A review. *Environmental Processes*, *9*, 29. https://doi.org/10.1007/s40710-022-00577-9

Royal Netherlands Meteorological Institute. (n.d.). *Hurricanes in the caribbean netherlands*. https://www.knmi.nl/kennis-en-datacentrum/achtergrond/orkanen-in-caribisch-nederland

Royal Netherlands Meteorological Institute. (2017). *Climate change on the caribbean islands*. Retrieved August 26, 2026, from https://www.knmi.nl/over-het-knmi/nieuws/klimaatverandering-op-de-caribische-eilanden

Royal Netherlands Meteorological Institute. (2024). *The state of our climate 2023: Caribbean netherlands*. KNMI.

Ruiz de Alegria-Arzaburu, A., Mariño-Tapia, I., Enriquez, C., Silva, R., & González-Leija, M. (2013). The role of fringing coral reefs on beach morphodynamics. *Geomorphology*, *198*, 69–83. https://doi.org/10.1016/j.geomorph.2013.05.013

Scardino, G., Rovere, A., Barile, C., Nandasena, N. A. K., Chauveau, D., Dahm, M., Boyden, P., Bejarano, S., Casella, E., Kelly, H., Mijts, E., & Scicchitano, G. (2025). Coastal boulders emplaced by extreme wave events impacting the abc islands (aruba, bonaire, curaçao; leeward antilles, caribbean). *Quaternary Science Reviews*, *349*, 109136. https://doi.org/10.1016/j.quascirev.2024.109136

Schmutz, P. P., Potter, A. E., & Modlin, J., E. Arnold. (2017). Aruba, bonaire, and curaçao. In C. D. Allen (Ed.), *Landscapes and landforms of the lesser antilles* (pp. 293–318). Springer International Publishing. https://doi.org/10.1007/978-3-319-55787-8_18

Sirko, W., Brempong, E. A., Marcos, J. T. C., Annkah, A., Korme, A., Hassen, M. A., Sapkota, K., Shekel, T., Diack, A., Nevo, S., Hickey, J., & Quinn, J. A. (2023). High-resolution building and road detection from sentinel-2 [arXiv preprint]. https://doi.org/10.48550/arXiv.2310.11622

Torres, R., & Tsimplis, M. Seasonal sea level cycle in the caribbean sea [EGU2012-3304-1, EGU General Assembly 2012]. In: In *Geophysical research abstracts*. *14*. EGU2012-3304-1, EGU General Assembly 2012. 2012.

Torresan, S., Critto, A., Rizzi, J., & Marcomini, A. (2012). Assessment of coastal vulnerability to climate change hazards at the regional scale: The case study of the north adriatic sea. *Natural Hazards and Earth System Sciences*, *12*, 2347–2368. https://doi.org/10.5194/nhess-12-2347-2012

van Duyl, F. C., Post, V. E. A., van Breukelen, B. M., Bense, V., Visser, P. M., Meesters, E. H., Koeniger, P., & Vermeij, M. J. A. (2024). Composition and distribution of the near-shore waters bordering the coral reefs of aruba, bonaire, and curaçao in the southern caribbean. *Marine Pollution Bulletin*, *209*, 117297. https://doi.org/10.1016/j.marpolbul.2024.117297

Vitousek, S., Buscombe, D., Vos, K., Barnard, P. L., Ritchie, A. C., & Warrick, J. A. (2023). The future of coastal monitoring through satellite remote sensing. *Cambridge Prisms: Coastal Futures*, *1*, e10. https://doi.org/10.1017/cft.2022.4

Xu, X., Xu, S., Jin, L., & Song, E. (2011). Characteristic analysis of otsu threshold and its applications. *Pattern Recognition Letters*, *32*, 956–961. https://doi.org/10.1016/j.patrec.2011.01.021

Xu, X., Li, X., Chen, M., Li, X., Duan, X., Zhu, G., Feng, Z., & Ma, Z. (2016). Land-ocean-human interactions in intensively developing coastal zone: Demonstration of case studies. *Ocean & Coastal Management*, *133*, 28–36. https://doi.org/10.1016/j.ocecoaman.2016.09.006

Yao, Z., Chen, J., Jiang, C., Liang, H., Wu, Z., Deng, B., Long, Y., & Bian, C. (2024). Experimental analysis of the changes in coral sand beach profiles under regular wave conditions. *Journal of Marine Science and Engineering*, *12*(2), 287. https://doi.org/10.3390/jmse12020287

Zambrano Cortes, D. G. (2012). *An ecological-economic model of the tropical dry forest on the island of bonaire* [Master's thesis, Vrije Universiteit Amsterdam].

A

Supplementary shoreline change results

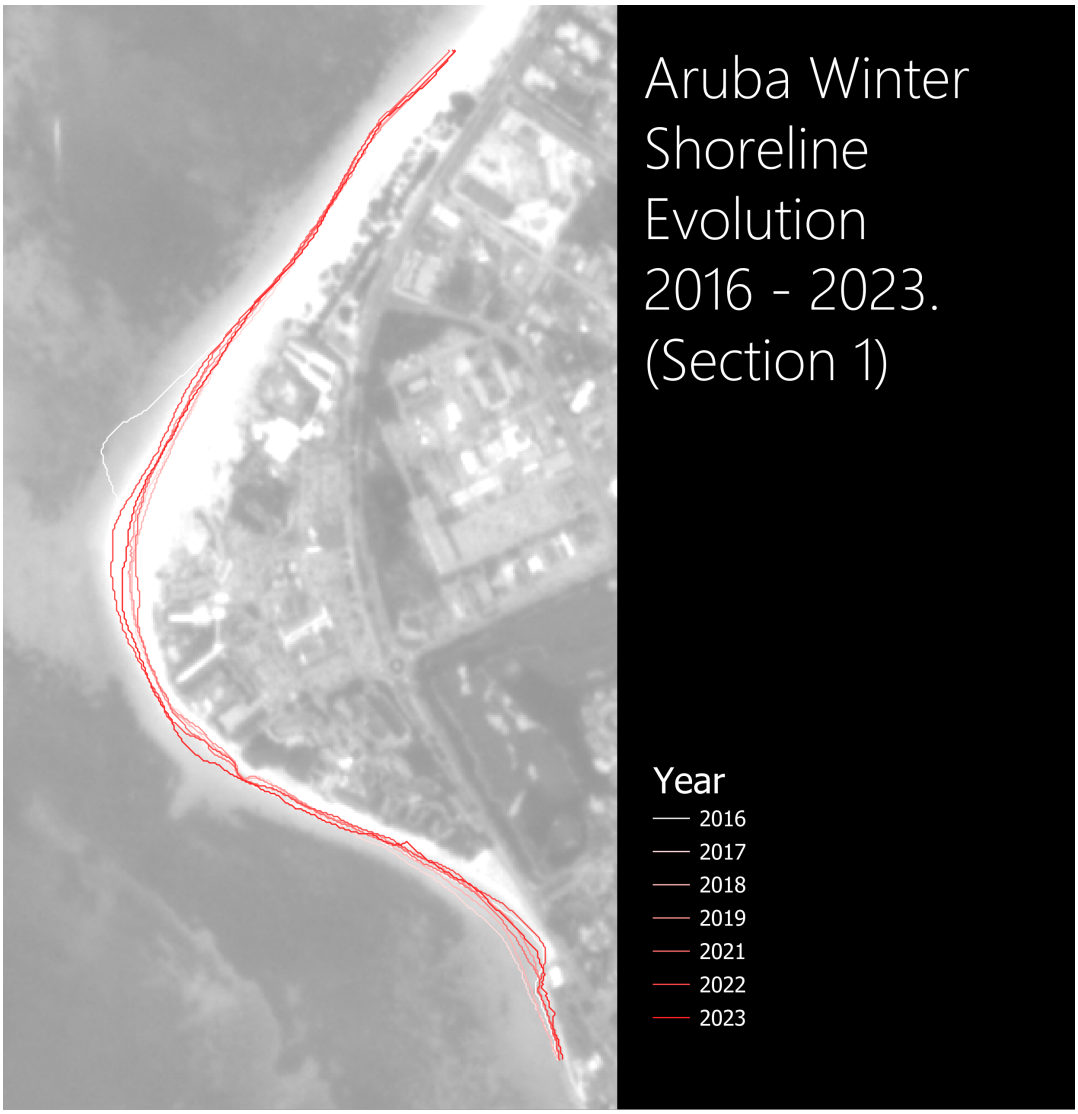


Figure A.1: Extracted winter shoreline positions for Aruba Section 1 between 2016 and 2023.

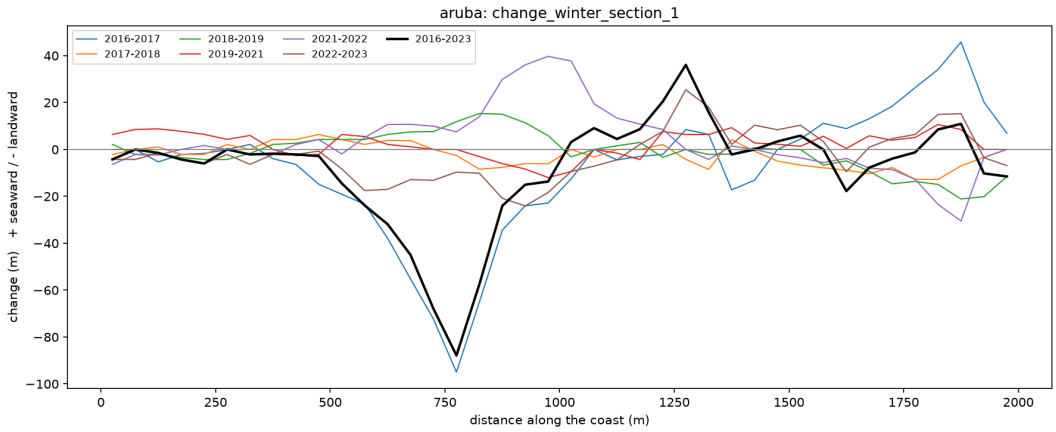


Figure A.2: Winter shoreline change along Aruba Section 1. Coloured lines represent change between successive available observations and the black line represents net change between 2016 and 2023. Positive values indicate seaward displacement and negative values indicate landward displacement.

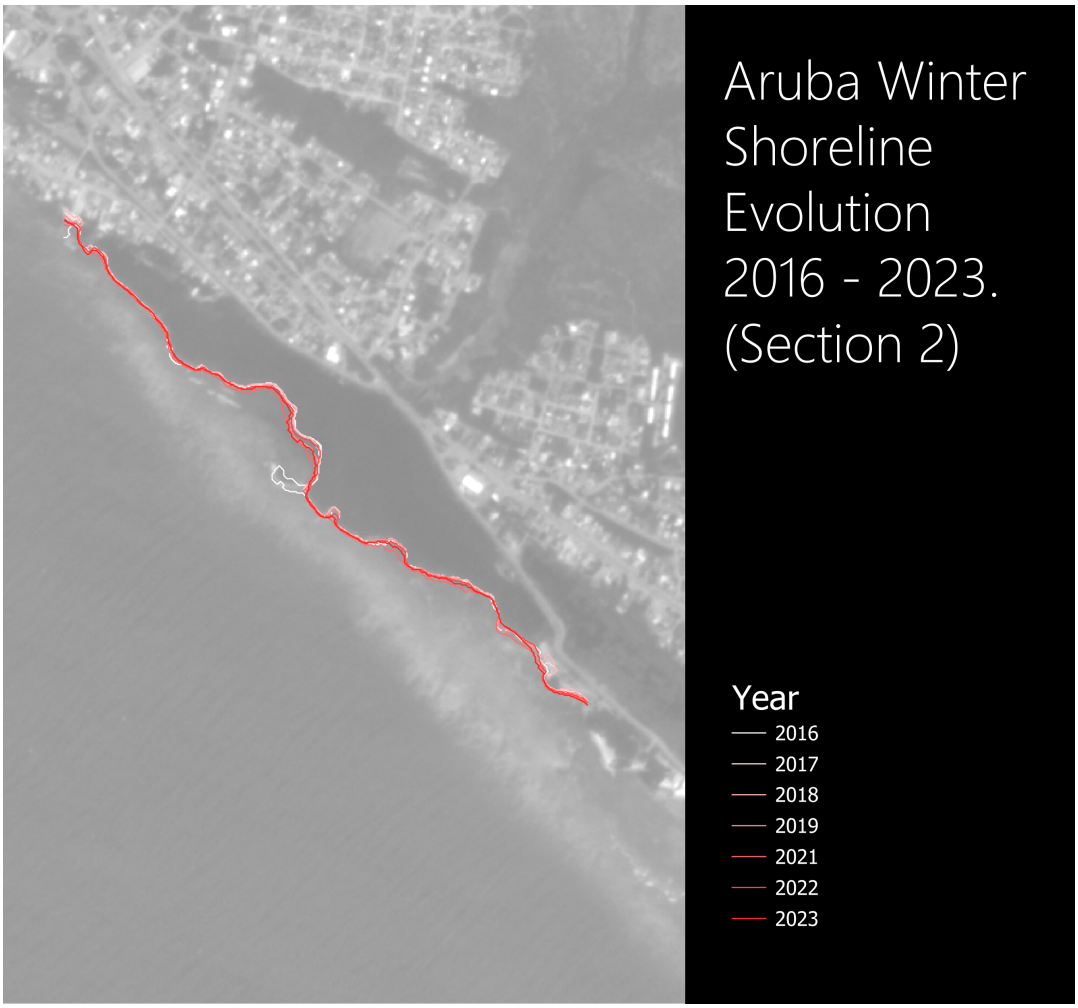


Figure A.3: Extracted winter shoreline positions for Aruba Section 2 between 2016 and 2023.

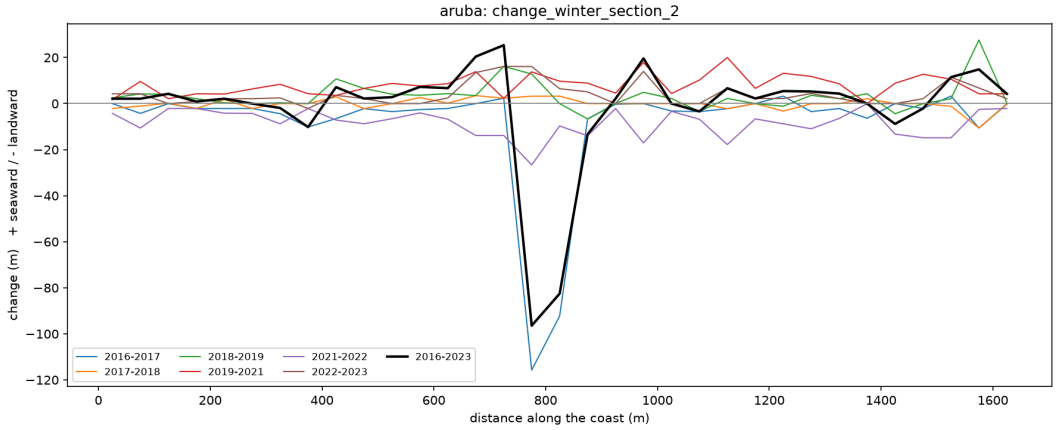


Figure A.4: Winter shoreline change along Aruba Section 2. Coloured lines represent change between successive available observations and the black line represents net change between 2016 and 2023. Positive values indicate seaward displacement and negative values indicate landward displacement.

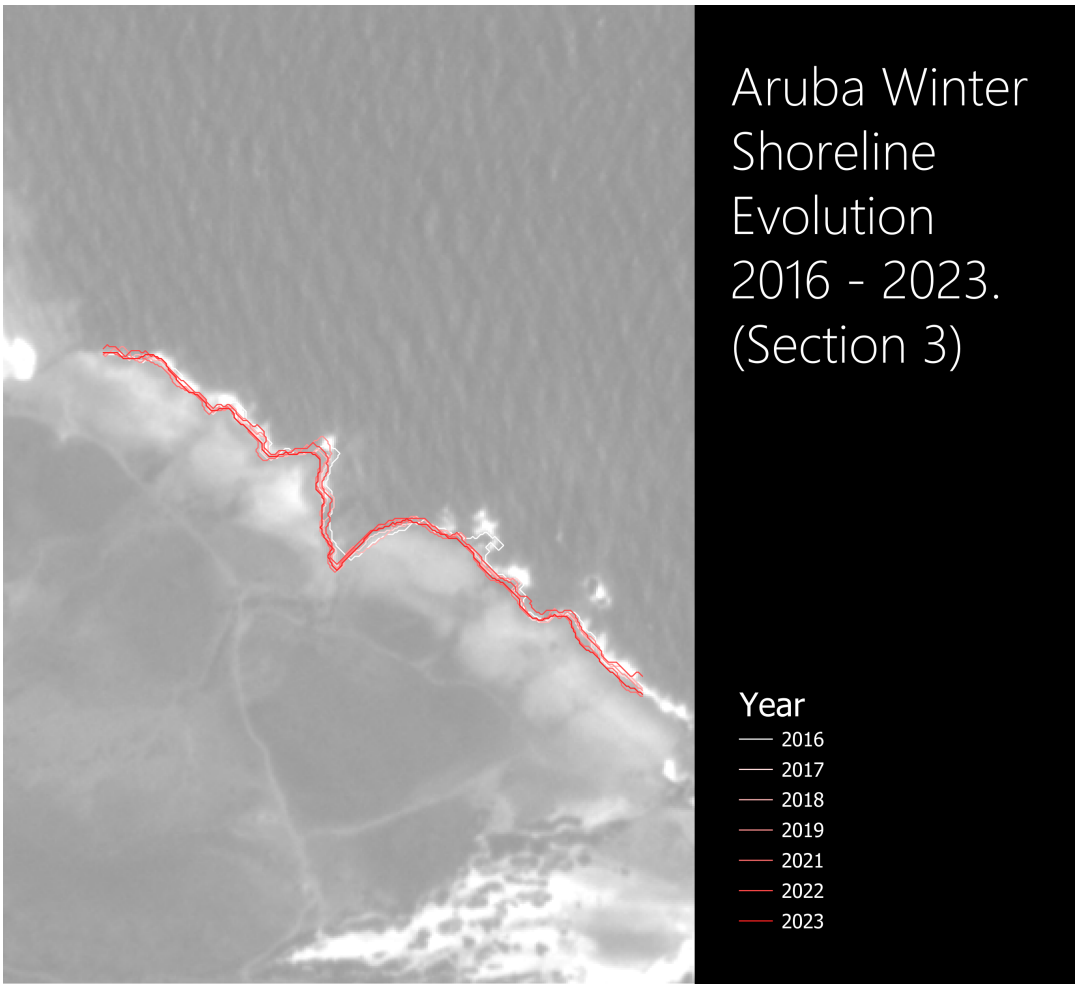


Figure A.5: Extracted winter shoreline positions for Aruba Section 3 between 2016 and 2023.

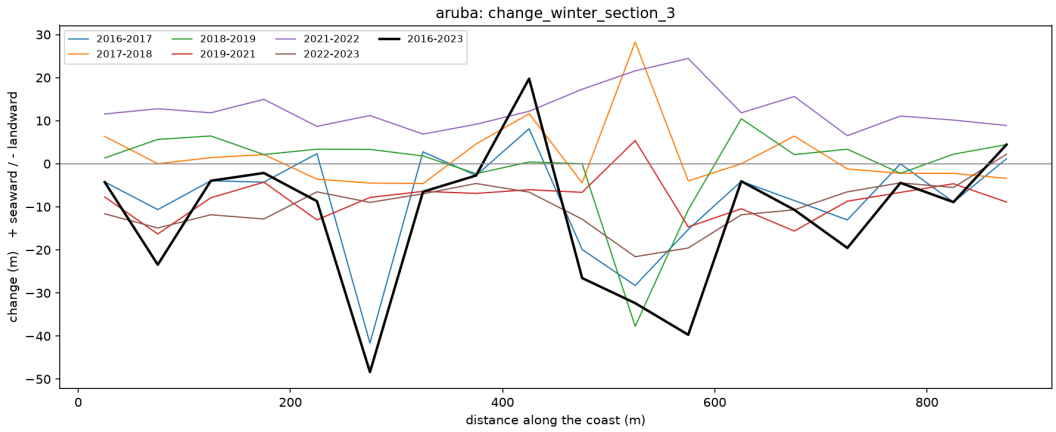


Figure A.6: Winter shoreline change along Aruba Section 3. Coloured lines represent change between successive available observations and the black line represents net change between 2016 and 2023. Positive values indicate seaward displacement and negative values indicate landward displacement.

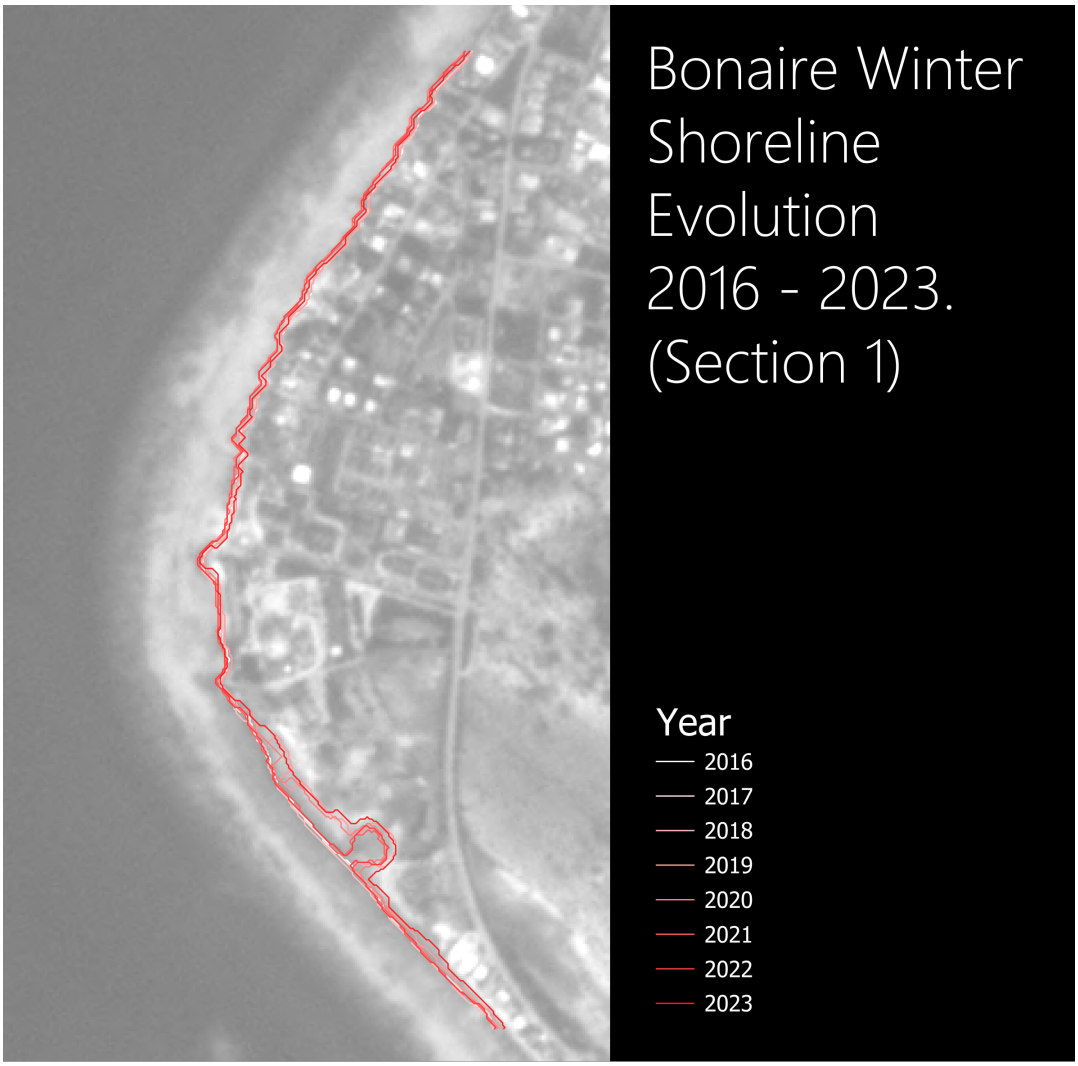


Figure A.7: Extracted winter shoreline positions for Bonaire Section 1 between 2016 and 2023.

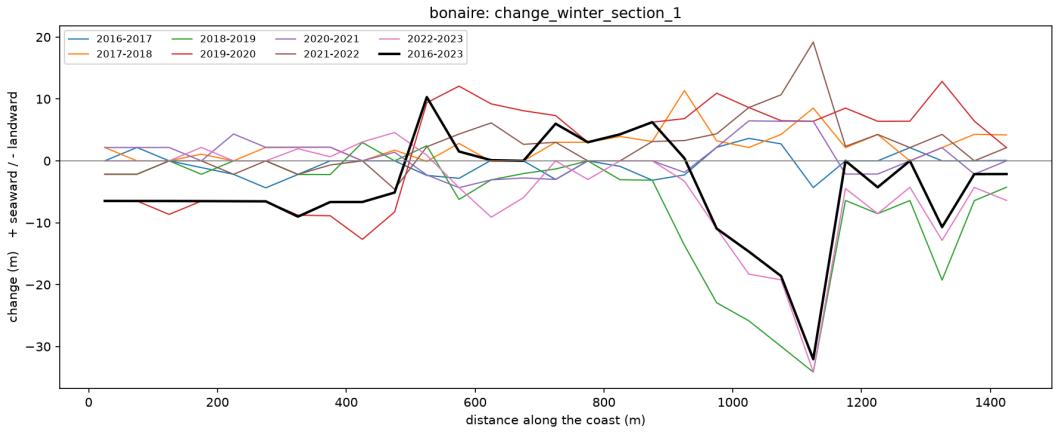


Figure A.8: Winter shoreline change along Bonaire Section 1. Coloured lines represent change between successive available observations and the black line represents net change between 2016 and 2023. Positive values indicate seaward displacement and negative values indicate landward displacement.

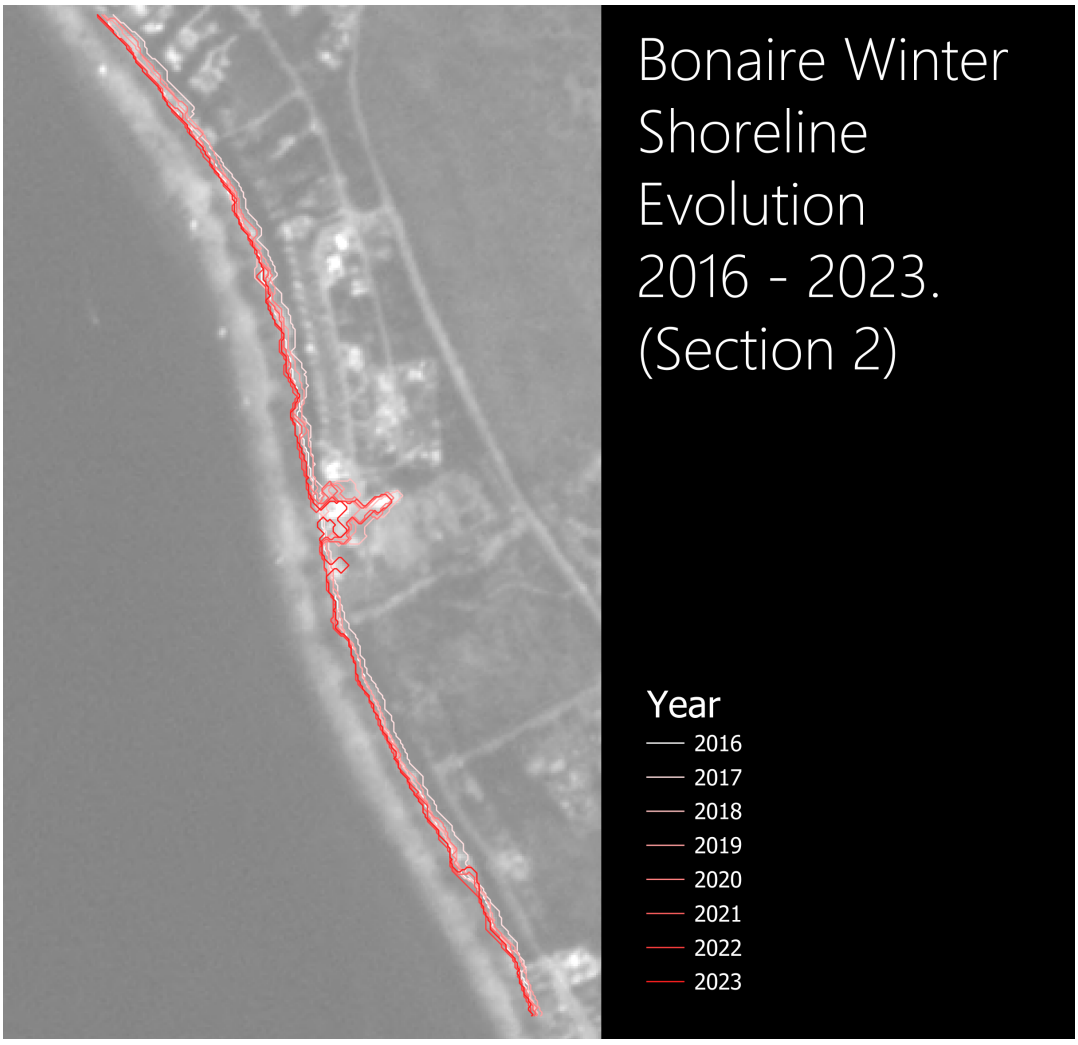


Figure A.9: Extracted winter shoreline positions for Bonaire Section 2 between 2016 and 2023.

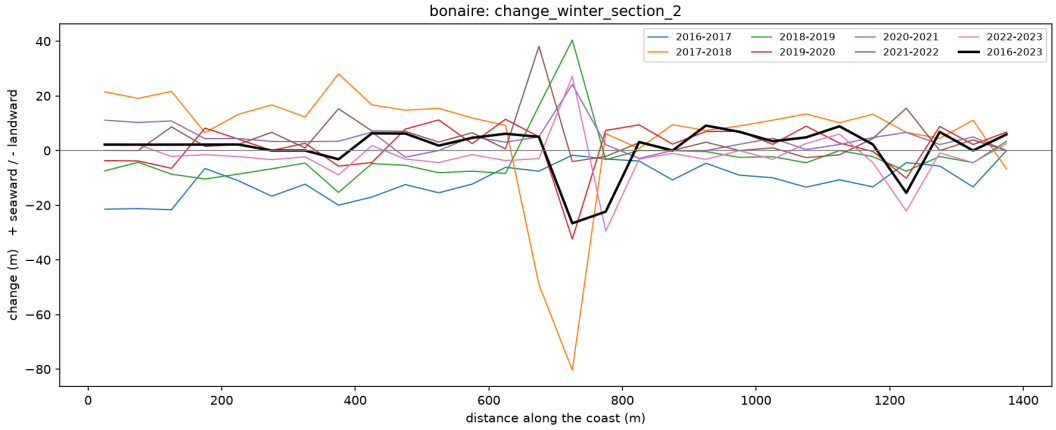


Figure A.10: Winter shoreline change along Bonaire Section 2. Coloured lines represent change between successive available observations and the black line represents net change between 2016 and 2023. Positive values indicate seaward displacement and negative values indicate landward displacement.

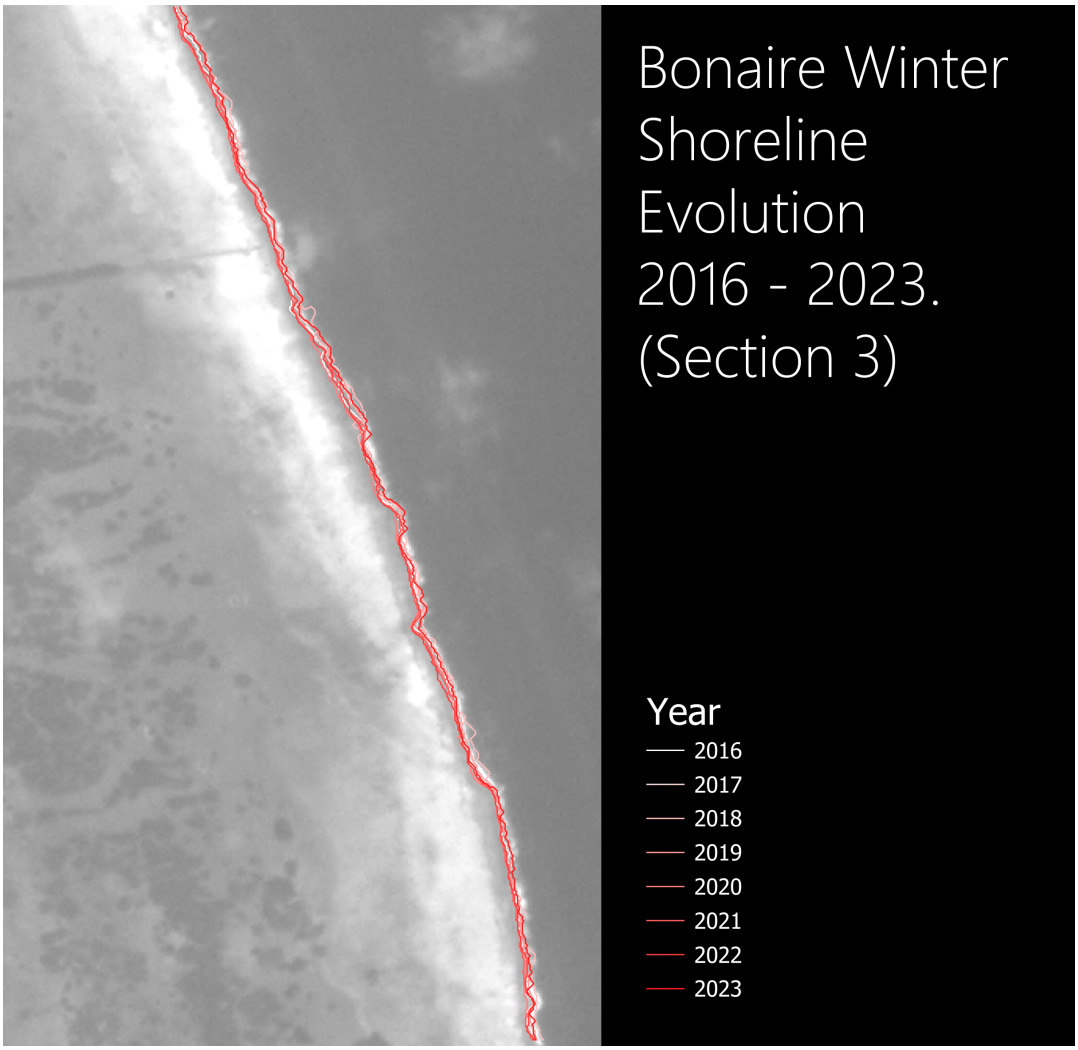


Figure A.11: Extracted winter shoreline positions for Bonaire Section 3 between 2016 and 2023.

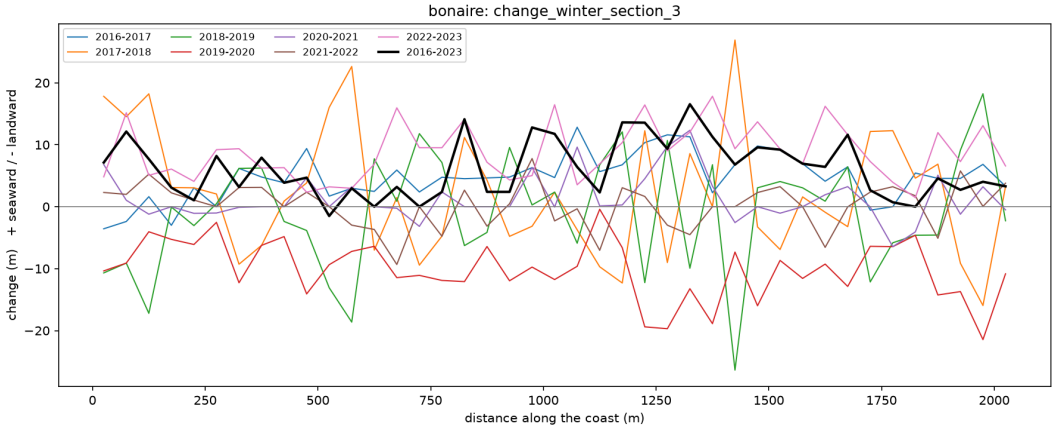


Figure A.12: Winter shoreline change along Bonaire Section 3. Coloured lines represent change between successive available observations and the black line represents net change between 2016 and 2023. Positive values indicate seaward displacement and negative values indicate landward displacement.

B

Supplementary integrated spatial results.

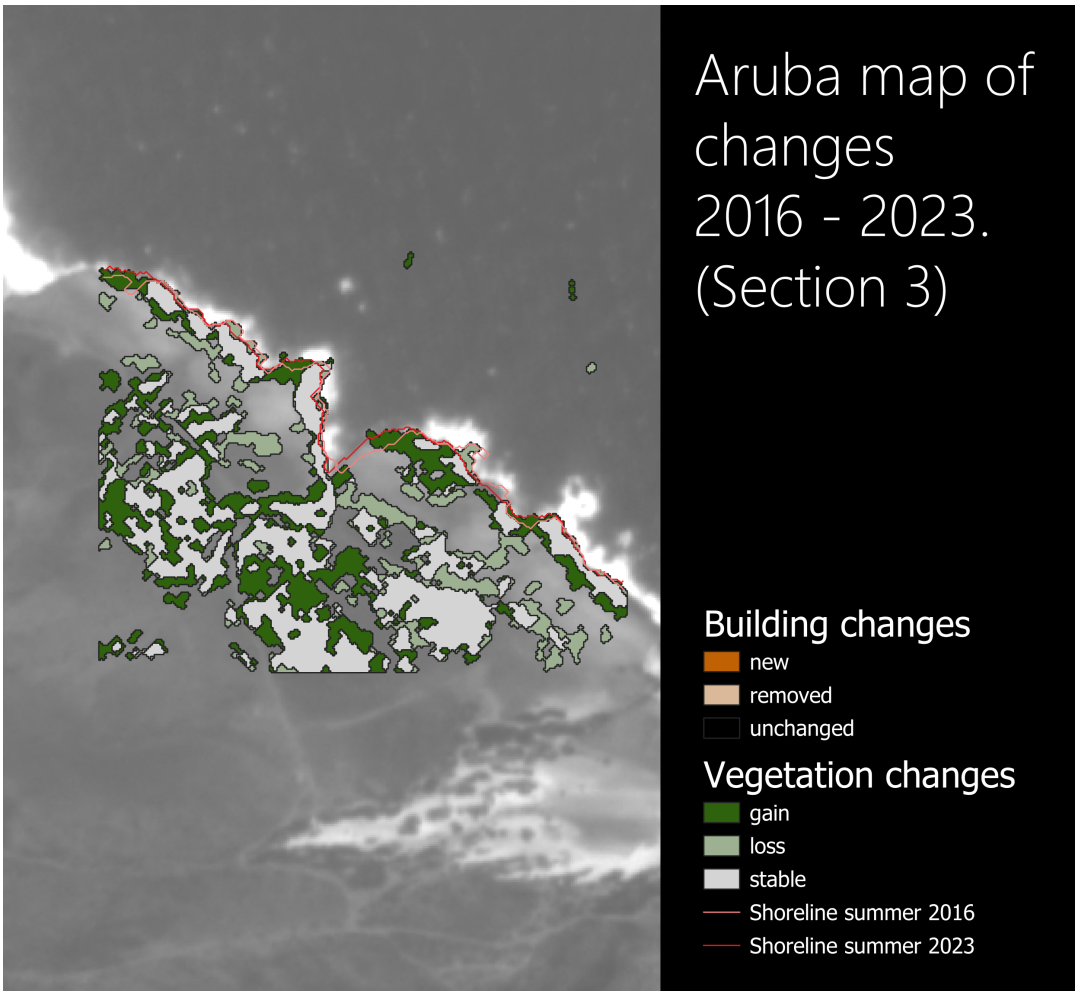


Figure B.1: Integrated spatial change map for Aruba Section 3, showing detected building change, vegetation change, and the initial and final shoreline positions.

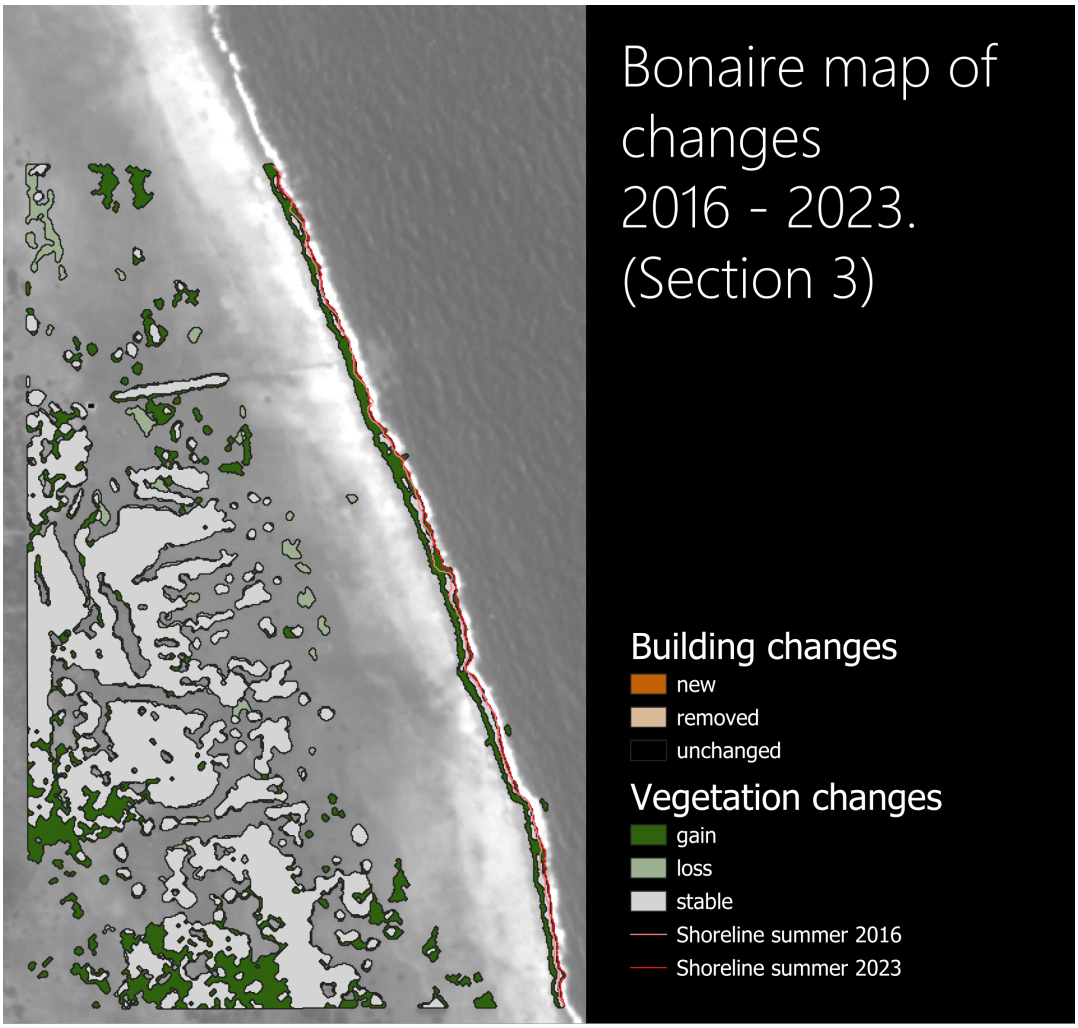


Figure B.2: Integrated spatial change map for Bonaire Section 3, showing detected building change, vegetation change, and the initial and final shoreline positions.

C

Google Earth Engine building extraction script

The following Google Earth Engine JavaScript code was used to extract and export building polygons for Aruba and Bonaire. Building presence was classified using a threshold of 0.5, and the resulting raster masks were vectorised at a spatial scale of 4 m. The exported GeoJSON datasets were subsequently used for the building-change analysis.

```
// Google Open Buildings: Aruba and Bonaire
// Yearly temporal building polygons and v3 footprints

var temporal = ee.ImageCollection(
  'GOOGLE/Research/open-buildings-temporal/v1'
);

var polygonsV3 = ee.FeatureCollection(
  'GOOGLE/Research/open-buildings/v3/polygons'
);

// Island bounding boxes
var regions = {
  Aruba: ee.Geometry.Rectangle(
    [-70.07, 12.40, -69.85, 12.64]
  ),
  Bonaire: ee.Geometry.Rectangle(
    [-68.45, 12.00, -68.18, 12.33]
  )
};

var START_YEAR = 2016;
var PRESENCE_THRESHOLD = 0.5;
var SCALE = 4;
var DRIVE_FOLDER = 'OpenBuildings_ABC';

// Extract building polygons for a given year
function buildingsForYear(region, year) {
  var img = temporal
    .filterBounds(region)
    .filterDate(
      year + '-01-01',
      (year + 1) + '-01-01'
    )
    .mosaic();

  var mask = img.select('building_presence')
    .gt(PRESENCE_THRESHOLD)
    .selfMask()
    .rename('building');

  var vectors = mask
    .addBands(img.select('building_height'))
    .reduceToVectors({
      geometry: region,
      scale: SCALE,
      crs: 'EPSG:4326',
      geometryType: 'polygon',
```

```
      eightConnected: false,
      labelProperty: 'building',
      reducer: ee.Reducer.mean(),
      maxPixels: 1e10,
      tileScale: 4
    });

  return vectors.map(function(f) {
    return ee.Feature(f.geometry(), {
      year: year,
      height_m: f.get('mean'),
      area_m2: f.geometry().area(1)
    });
  });
}

// Export yearly polygons and v3 footprints
Object.keys(regions).forEach(function(name) {
  var region = regions[name];

  Map.addLayer(
    region,
    {color: 'red'},
    name + ' AOI',
    false
  );

  var years = temporal
    .filterBounds(region)
    .aggregate_array('system:time_start')
    .map(function(t) {
      return ee.Date(t).get('year');
    })
    .distinct()
    .sort();

  years.evaluate(function(yrs) {
    print(name + ' - available years:', yrs);

    yrs.filter(function(y) {
      return y >= START_YEAR;
    }).forEach(function(y) {
      Export.table.toDrive({
        collection: buildingsForYear(region, y),
        description: name + '_buildings_' + y,
        folder: DRIVE_FOLDER,
        fileNamePrefix: name + '_buildings_' + y,
        fileFormat: 'GeoJSON'
      });
    });
  });

  // Export latest v3 building footprints
  var v3 = polygonsV3.filterBounds(region);

  print(name + ' - v3 polygon count:', v3.size());

  Map.addLayer(
    v3,
    {color: 'yellow'},
    name + ' v3 footprints',
    false
  );

  Export.table.toDrive({
    collection: v3,
    description: name + '_buildings_v3_latest',
    folder: DRIVE_FOLDER,
    fileNamePrefix: name + '_buildings_v3_latest',
    fileFormat: 'GeoJSON'
  });
});

// Preview latest Aruba building presence
var latestPreview = temporal
  .filterBounds(regions.Aruba)
  .sort('system:time_start', false)
  .first();

Map.centerObject(regions.Aruba, 11);

Map.addLayer(
  ee.Image(latestPreview).select('building_presence'),
  {
```

```
    min: 0,
    max: 1,
    palette: ['black', 'orange']
  },
  'Latest presence (Aruba)',
  false
);
```